Integrated Science and Implementation of Geologic CO_2 Storage in Abu Dhabi: Characterization, Containment, Migration and Monitoring

An MIT Proposal

in collaboration with
ADCO-Petroleum Institute-Masdar Institute-Stanford University

Ruben Juanes
Bradford Hager
Nafi Toksöz
Yves Bernabé
Brian Evans
Michael Fehler
Thomas Herring
Alison Malcolm
Dennis McLaughlin
Karl Berteussen (Petroleum Institute)
Thomas Steuber (Petroleum Institute)
Hosni Guedira (Masdar Institute)
Mohamed Sassi (Masdar Institute)

August 30, 2010

I. INTRODUCTION AND MOTIVATION

This collaborative research proposal from the Massachusetts Institute of Technology (MIT) responds to an Abu Dhabi initiative of economic growth, diversification, creation of clean technology, and sustainable development. The United Arab Emirates (UAE), as a result of its fast social and economic growth, has one of the highest carbon footprints per capita in the world. The Abu Dhabi government has established an ambitious plan to capture CO_2 from a wide range of large carbon emitting industrial plants, and transport it through pipelines to inject it for enhanced oil recovery and/or subsurface storage in geological formations. This is one way in which the UAE and, especially, Abu Dhabi, is taking steps towards reducing greenhouse gas emissions and, ultimately, achieving carbon neutrality. Indeed, carbon capture and storage (CCS) has emerged as a critical enabling technology for the continued use of fossil fuels in a carbon constrained world [*MIT*, 2007]. Deployment of CCS in Abu Dhabi will position Abu Dhabi as a leader in clean hydrocarbon energy.

Although the main purpose of CO_2 capture in the UAE is to lower its carbon footprint, the immediate use of captured CO_2 is for enhanced oil recovery (EOR). Traditionally, in UAE, the associated natural gas that is produced with oil, has been separated and reused for injection into oil reservoirs to maintain their pressure and increase oil production. Currently, all local power plants use natural gas, but the increasing demand for electricity has led to the consideration of the use of alternative gases for enhanced oil recovery, preserving natural gas for electricity production and other industrial uses in the growing UAE economy. Carbon dioxide is an attractive alternative, due to its high miscibility with oil under reservoir conditions. This makes the oil swell, lowering its density, lowering its viscosity, increasing its mobility, allowing for enhanced production of the reservoir oil. This attractive combination of CO_2 emission reduction and economic incentive has already resulted in an ambitious project to capture and inject CO_2 for enhanced oil recovery.

However, deployment of CCS at large scale must rely on storing CO_2 beyond its use for EOR. On one hand, even under aggressive growth of CO_2-based EOR, the volumes are likely to be far from those required to contribute significantly toward Abu Dhabi's goal of carbon neutrality. Moreover, not all the injected CO_2 stays underground in this process and a large portion of it—which increases over time—comes back to the surface with the produced oil and needs to be separated and recycled into the system. This limits the effectiveness of EOR as a carbon mitigation technology. As a result, other options for longer-term storage of CO_2 in subsurface formations (e.g. saline aquifers, and depleted oil and gas reservoirs) are required. Since there are no depleted oil and gas reservoirs in Abu Dhabi—and there will not be in the immediate future—deep saline aquifers have been identified as the target of choice for subsurface CO_2 injection and storage (Figure 1).
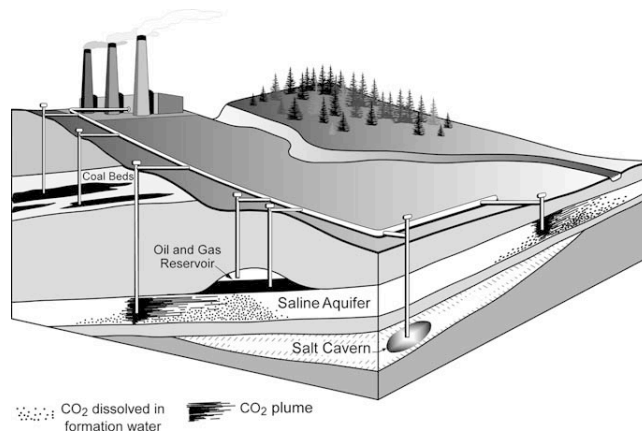
Figure 1: Schematic of different options for geologic storage of CO2, including depleted oil and gas reservoirs, unminable coal beds, and deep saline aquifers. Saline aquifers are the prime candidates for CO2 sequestration due to their large capacity and widespread occurrence (modified from *Bachu*, 2003).

CCS in deep saline aquifers offers several advantages, including their large capacity and widespread occurrence. If the CCS program is properly designed, implemented and monitored, large quantities of CO2 ($\sim$10's to 100's million tons per year) can be effectively sequestered in local aquifers, minimizing pipeline construction and transportation costs. CO2 storage in deep aquifers poses, in turn, a set of serious challenges. Much less data is usually available in aquifers than in hydrocarbon-bearing reservoirs. Effective assessment of storage security must involve, therefore, significant effort in the initial characterization and sustained effort in monitoring. The geology of productive reservoirs and conductive aquifers is dominated by carbonate rock, and less is known about CO2 injection in carbonates than in clastic reservoirs. The challenges of large injection volumes, scarce geologic and geophysical data, uncertainty in the chemical/geomechanical behavior of carbonates, and the need for monitoring are indeed the key drivers for this proposal.

This proposal evaluates the science and implementation of CO2 storage in deep saline aquifers in the UAE, and it addresses what we believe are the critical issues for successful deployment of CCS. The focus is on model-based monitoring. Many monitoring techniques exist, each with a specific strength and all, in principle, have a role to play. Model-based monitoring provides a unifying framework to integrate the data from the different techniques, and to assess their added value to CCS projects in specific aquifers.

Abu Dhabi is uniquely positioned to take a leadership role in the area of carbon mitigation. For CCS to become a reality, however, several elements (capture, transport, EOR, aquifer storage) need to coalesce. This proposal contributes chiefly to anchoring our understanding of the aquifer storage component, and to establishing a roadmap for the deployment of large-scale geologic CO2 storage in the UAE. This proposal is synergetic with a recently submitted proposal by Stanford University, which is focused on the simulation of trapping mechanisms. It is designed as a collaborative proposal and, by virtue of close collaboration with ADCO, the Petroleum Institute and the Masdar Institute, along with the proposed knowledge-transfer activities, we expect that the lessons learned in the project will expand Abu Dhabi's workforce trained in the science, technology and policy of CCS.

Scope of the Project

The proposal addresses key aspects related to the characterization, containment, migration and monitoring of the injected CO2. It is organized in four thrusts:

1. *Site Characterization.* This first task builds on the characterization efforts currently ongoing, and led by the Petroleum Institute. In this task, we propose to work closely with the Petroleum Institute to review all existing information (geologic, geophysical, geomechanical, and rock/fluid properties), identify critical additional data, and make recommendations for any additional data that ought to be collected. This task will delineate reservoir architecture, and evaluate and rank potential target formations.

2. *Geomechanical Modeling and Caprock Integrity.* This thrust involves inter-related theoretical and experimental research tasks. One of the central aspects is the development of computational models for the simulation of coupled flow and geomechanics. This task, which builds on previous joint work with Stanford, will focus on the study of the state of stress at depth, caprock integrity and fault activation upon CO2 injection, with application to individual selected formations. We will complement the theoretical developments with chemomechanics laboratory experiments that will test the interplay between CO2 dissolution, rock strength, flow properties, and compaction for actual carbonate reservoir rock and caprock. The experiments will inform the computational models and will lead to an integrated assessment of caprock integrity, which will identify not only the potential for leakage risk, but also which leakage pathway is most likely (e.g., well leakage, sandy caprock, fractured caprock, or active fault).

3. *Capacity Estimates and Risk Assessment of CO2 Injection.* Demonstrating that CCS is a safe and effective technology when deployed at large scale (~10's-100's Mt/yr) requires assessing the long-term fate of the injected CO2. In this thrust, we will develop *analytical* models of pressure dissipation and CO2 migration at the geologic basin scale, including structural trapping, capillary trapping, and dissolution trapping. Analytical models provide ultra-fast forward simulation, which in turn allows for exhaustive sampling of uncertainty (Monte Carlo simulation)—an approach that is synergetic with the numerical simulation developments of the Stanford group. The analytical models will be extended to include reactive modeling (dissolution of carbonates).

4. *Comprehensive Monitoring Program.* A comprehensive quantitative understanding of the reservoir is required both prior to and during the injection of CO2. We will develop a set of predictive models that describe flow and geomechanical processes within the reservoir as well as connections between measurements and reservoir states. By combining model predictions and measurements we will be in a position to generate predictions that are physically realistic and also consistent with field data. . The UAE CCS project requires multiple kinds of observations, each sensitive to different physical and chemical properties acting over different spatial and temporal scales. These include: 1) Fluid pressures, fluxes, and composition in injection and monitoring wells; 2) Active seismic monitoring; 3) Passive seismic monitoring; 4) Measurements related to induced seismicity; 5) Geodetic

measurements, including data from GPS stations and InSAR surveys; 6) Microgravity measurements; 7) Electrical resistance tomography; and 8) Geochemical and surface monitoring of CO2. The procedure linking observations and models will be an ensemble *data assimilation* algorithm that will use the models to generate a set of possible system descriptions, all consistent with observations. This makes it possible to provide a cost-benefit analysis of the importance of different data types, as well as to design robust operating and monitoring strategies that can work well over a range of conditions.

The project is designed to have a 4-year duration (Jan 1, 2011 – Dec 31, 2014). Most of the work will be completed by mid-2014, in accordance with the timeline proposed by ADCO. This is essential to guarantee the aggressive timeline for CCS deployment in the UAE.

Strategy for Collaboration with Other Institutions

The goal of this proposal is to catalyze a *comprehensive program* of geologic carbon dioxide storage in the UAE. Success of this research effort will rely heavily on proper communication and transfer of knowledge of the lessons learned throughout the project. This proposal is focused on the scientific research, and only includes partial data acquisition and field instrumentation (for instance, we have budgeted for the acquisition of InSAR data and the purchase and deployment of GPS stations, but will rely on ADCO/PI for seismic surveys and installation of seismic networks). Therefore, it is critical for the timely success of the project that an engineering team in Abu Dhabi be dedicated to knowledge transfer and implementation of the scientific outcomes in the field.

We anticipate that the project will build on the strong collaboration with the other institutions involved in the program, and our recommendation is that they include the following elements:
1. *MIT-ADCO*. Detailed and extensive science/knowledge transfer will be instrumental. Required data collection (e.g., running seismic, deployment of seismic network, coring, etc.) may be identified by MIT and executed and deployed by ADCO. As noted above, it is critical that an engineering team at ADCO be dedicated to this project, and that members of this team will visit MIT on a regular basis.
2. *MIT-Petroleum Institute (PI)*. Collaboration will be essential for geological, geophysical, rock/fluid data sharing, and knowledge of the subsurface reservoirs. PI's involvement will be instrumental for site characterization and selection, development of geomodels, and implementation of monitoring in the field. We propose that PI faculty and researchers will visit MIT, especially during the early stages of the project. As part of the project, we are proposing an annual two-day workshop to be held at MIT or Abu Dhabi. This would be an excellent opportunity for PI students to interact with MIT faculty. Some of the MIT faculty also teach a short course on CCS during the summer, which PI students could attend.
3. *MIT-Masdar Institute of Science and Technology*. A cooperative agreement already exists between MIT and Masdar Institute. The MIT Technology and Development Program's MIT-Abu Dhabi program currently provides the framework for research collaboration and educational initiatives. This project will extend the relationship

between MIT and Masdar Institute through research collaboration outside the scope of the current cooperative agreement. The opportunities for student involvement mentioned above (annual project workshop, and CCS short course) would of course apply to Masdar Institute students as well.

4. *MIT-Stanford*. The Stanford and MIT research proposals are designed to be *synergetic*, not overlapping. There is a long history of collaboration between some of the research team members. In particular, close collaboration is anticipated to take place in the areas of: (1) geomechanics; (2) CO_2 migration at the basin scale; (3) Data sharing from multiphase flow experiments (Stanford) and chemo-mechanical experiments (MIT).

We also make the following recommendations to foster collaboration and integration:
1. *Annual two-day conference* to be held at MIT or at Abu Dhabi, involving all the parties. The first day would be devoted to presentation of scientific results, and the second day would be reserved for focused business meetings and planning of future activities.
2. *Project oversight by a common Steering Committee*. This committee will be charged with the oversight and guidance of the project at the highest level. It will include representation from all institutions, and embody overarching expertise in subsurface science, CCS technology, clean energy systems, and research and education initiatives.

Management Plan

The organizational chart of the project is shown in Figure I.1 below. The principal investigator (Prof. Ruben Juanes) and co-principal investigators (Prof. Bradford Hager and Prof. Nafi Toksoz) will serve as Project Directors. They will lead oversee progress of the different research tasks and promote communication among the senior personnel and other researchers, to ensure cross-fertilization and the execution of an integrated project. They will name an Executive Director, who will be in charge of financial and operational matters, and putting in place the mechanisms for both internal communication (bi-weekly meetings and seminars) and external communication with the other parties in this collaborative project. An expert in the field will lead each of the four thrusts: Dr. Michael Fehler (Task 1), Prof. Bradford Hager (Task 2), Prof. Ruben Juanes (Task 3), and Prof. Dennis McLaughlin (Task 4). They will be responsible for overseeing and integrating the research under their task, and communicating progress with the Executive Director and the Project Directors.

The entire project will be overseen by the Steering Committee, which in annual reviews will provide feedback on conducted research and offer guidelines for forthcoming activities. Their input will be instrumental for achieving integration of the project results with the specific needs in Abu Dhabi and promoting effective knowledge transfer of the research results, both at a technological and educational level.
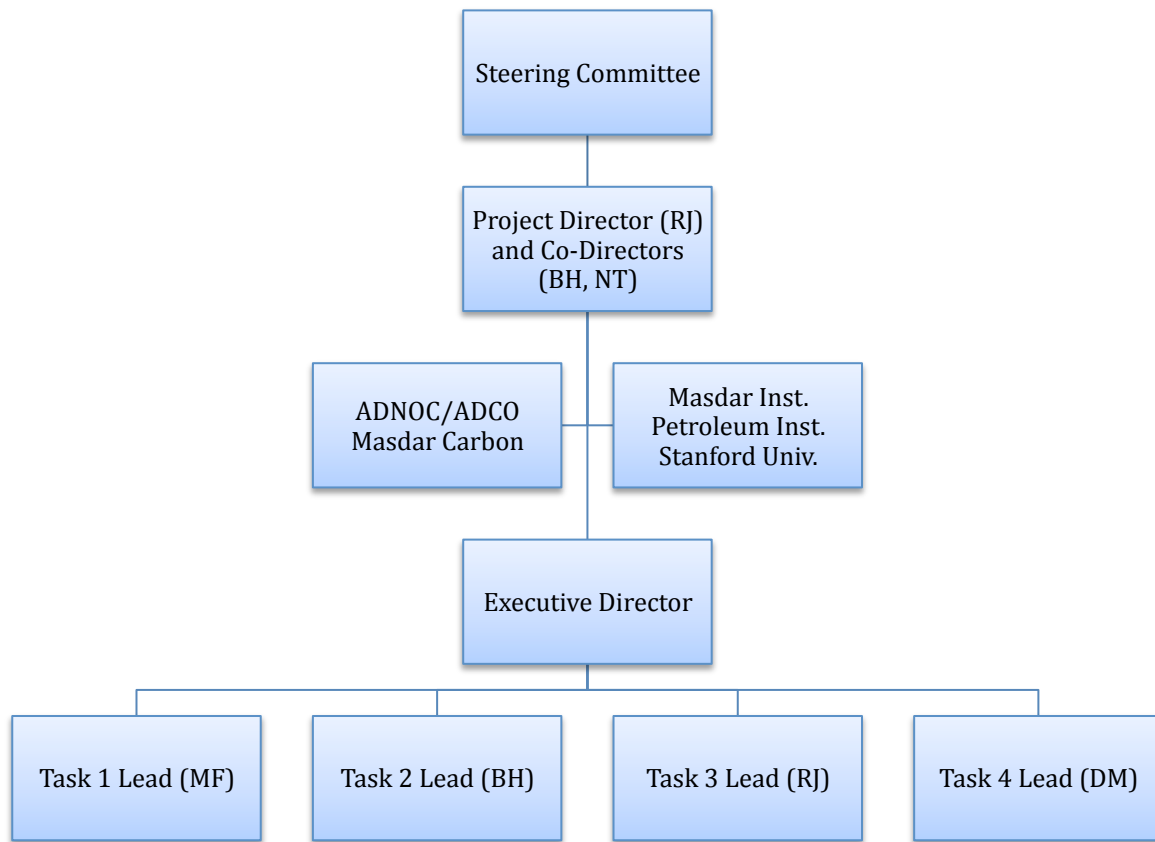
Figure I.1: Project organization chart.

Roles of Senior Personnel

Prof. Ruben Juanes will serve as the project director and Principal Investigator. He will lead the research on Task 3.1 (capacity estimation and risk assessment) and Task 3.2 (flow modeling), and co-lead Task 2.1 (coupled flow and geomechanics). He will work closely with the co-Principal Investigators to coordinate overall progress and establish effective knowledge transfer among MIT, ADCO, PI and Masdar.

Prof. Bradford Hager will serve as project co-Principal Investigator. He will co-lead Task 2.1 (coupled flow and geomechanics), lead Task 4.2 (pressure monitoring at wells) and Task 4.6 (geodetic monitoring with InSAR and GPS), co-lead Task 4.7 (microgravity and gravity gradiometry), and lead Task 4.8 (electrical resistance tomography). He will work closely with the Principal Investigator on the organization and management of the project.

Prof. Nafi Toksöz will serve as project co-Principal Investigator. He will have major involvement in Task 1 (site characterization), and will lead Task 4.5 (induced seismicity) and Task 4.9.1 (isotopic monitoring).

Prof. Yves Bernabé will have major involvement in Task 2.2 (laboratory studies of geomechanics and mineral trapping).

Prof. Brian Evans will lead Task 2.2 (laboratory studies of geomechanics and mineral trapping).

Dr. Michael Fehler will lead Task 1 (site characterization), co-lead Tasks 4.3 and 4.4 (active and passive seismic), and have major involvement in Task 4.5 (induced seismicity).

Prof. Thomas Herring will co-lead Task 4.6 (geodetic monitoring with InSAR and GPS) and Task 4.7 (microgravity and gravity gradiometry).

Prof. Alison Malcolm will have significant involvement in Task 1 (site characterization) and co-lead Task 4.3 (active seismic) and Task 4.4 (passive seismic).

Prof. Dennis McLaughlin will lead Task 4.1 (data assimilation and monitoring design), and serve as the focal point for integration of the model-based monitoring effort.

Prof. Karl Berteussen, from Petroleum Institute, will be heavily involved in Task 1 (site characterization), Task 2.1 (coupled flow and geomechanics), and Task 4.6 (geodetic monitoring with InSAR and GPS), especially with regard to application and implementation of the technology in the field in the UAE.

Prof. Thomas Steuber, from Petroleum Institute, will be heavily involved in Task 1 (site characterization), especially for integration of geologic and geophysical data into static geomodels, site selection, and field implementation.

Prof. Hosni Guedira, from Masdar Institute, will have major involvement in Task 4.6 (geodetic monitoring with InSAR and GPS), especially for the deployment and maintenance of the GPS network in the field.

Prof. Mohamed Sassi, from Masdar Institute, will have a major involvement in Task 2.2 (laboratory experiments of geomechanics and mineral trapping), Task 3.2 (flow modeling), and Task 4.9.2 (surface monitoring through diode laser absorption sensors).

II. RESEARCH TASKS

1. Site Characterization

The Petroleum Institute (PI) has been charged with collecting and organizing data that will lead to site selection. PI will also recommend one or more sites for consideration for further study. During site selection, it is essential that there is sufficient information to conduct further work to estimate the storage capacity of the proposed reservoir, to evaluate the capability of the target reservoir to successfully sequester CO2, and to develop an appropriate monitoring program. The suitability of any site will vary with site geology, tectonic regime, depth of burial, surface characteristics, likely trapping mechanisms, and anticipated leakage pathways. The work we propose in this MIT-led project is dependent on having an exhaustive characterization of the site or sites that are under consideration for CO2 sequestration. Since many aspects of initial site characterization will be based on available data for associated petroleum reservoirs, additional data may be required to further characterize the proposed CO2 storage reservoir.

Figure 1.1 is a regional geological map of the United Arab Emirates. There is very little outcrop of the rocks that form the reservoirs and their seals, except in the northeastern region, near the border with Oman. Most of the surface is Quaternary sand, similar to the region in westernmost Oman, where we have been monitoring surface deformation and seismicity induced by hydrocarbon production.
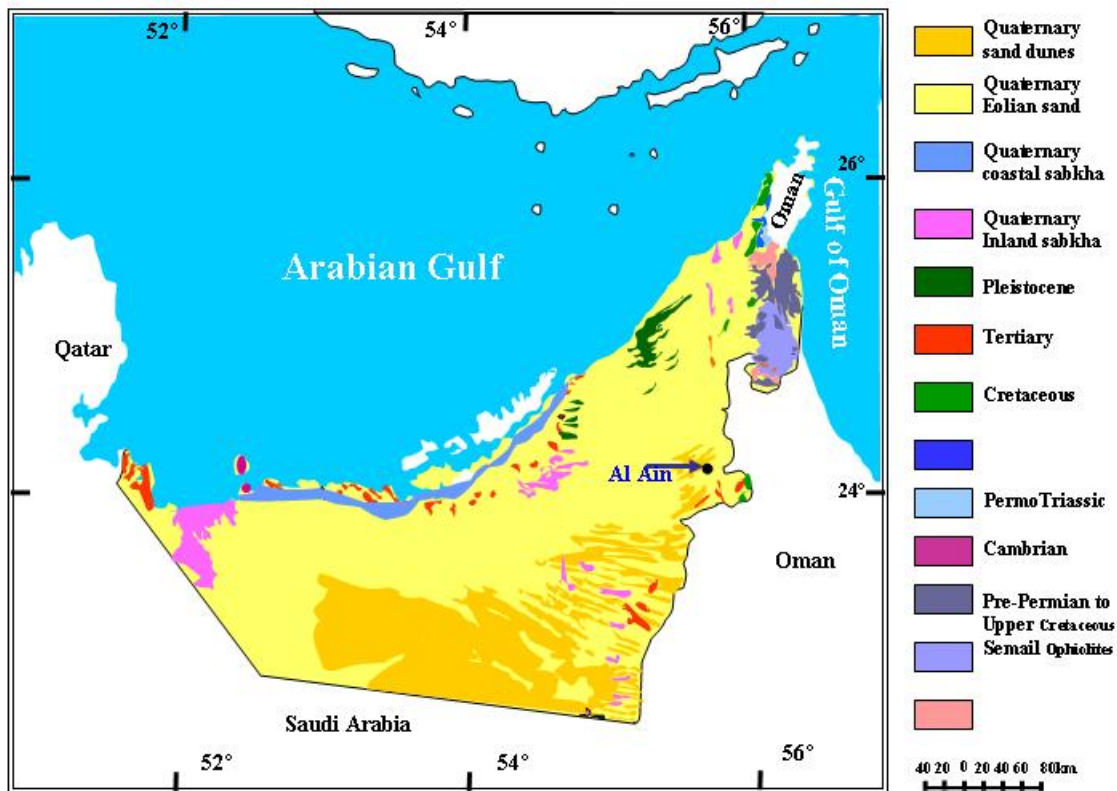

8

Figure 1.1. Regional geological map of the United Arab Emirates (from http://www.angelfire.com/az3/mohgameil/emirates.html). Figure 1.2 shows the locations of the major petroleum fields within the United Arab Emirates. The major seals for petroleum reservoirs are anhydrates and shales.   The saline aquifers that are the candidate reservoirs for sequestered CO2 are carbonates.
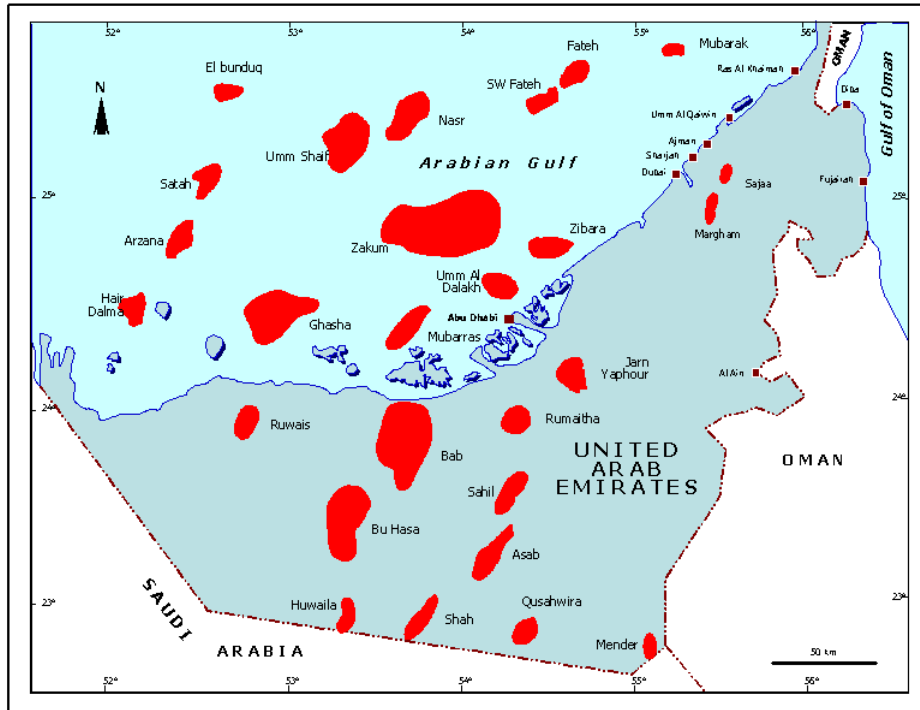

Figure 1.2. Map showing locations of oil and gas fields in the United Arab Emirates. From http://www.angelfire.com/az3/mohgameil/emirates.html.

To proceed with the work we propose, we need a significant amount of information about the site(s) selected for study. We anticipate that this information will either be provided to us by PI or that raw data will be available for us to make our own assessment of required reservoir characteristics. As more information is available, we will be able to assess the suitability of each site, the capacity of the reservoir and the feasibility of conducting the types of measurements that we propose for monitoring of the injections. Existing information that we will review includes:

(1) Geologic information including descriptions of the geologic units above and within the reservoir, locations of mapped faults, and information about the regional tectonics including the regional stress field.

(2) Geophysical information including 3D seismic surveys, interpretations of processed results from the 3D surveys, and information about regional and local seismicity. Both raw and processed active seismic data will be needed to conduct a more detailed assessment of the continuity and thickness of the cap rock, existence of faults within the reservoir and caprock, and reservoir heterogeneity. Velocity models used for migration and any updated information about the velocity model,

9

particularly for the reservoir and caprock regions will be essential for conducting future seismic and geomechanical modeling. Sonic logs taken above and within the reservoir will be useful for calibrating seismic data and as complementary information for use in interpretation of other geological and geophysical data.

(3) Geomechanical information that can be used to infer the state of stress within the reservoir and caprock. This information may be obtained from borehole data such as breakouts inferred from caliper and televiewer logs, minifrac results, or information about fracture anisotropy within the reservoir, and mud loss events. Any data from boreholes needs to have associated wellbore location information.

(4) Rock/Fluid Properties. Information will be needed about properties of both reservoir and cap rocks. Both geological descriptions and results of geophysical measurements will be essential for evaluating the candidate sites.

(5) Locations and information about all existing wells will be needed to assist in the interpretation of the geophysical and geological data. Wellbore trajectories will be helpful for placing well information within a 3D model of the reservoir region. In addition, this information will help to determine which wellbores can be used in monitoring of injections into the reservoir. Information about well completions will help to better characterize the likelihood of existing wells as potential leakage pathways for injected CO_2.

Site characterization tasks include:

(a) Compiling all available data provided by PI for each proposed site, evaluating data quality, and making recommendations for new data that need to be collected. This will be done in collaboration with PI and other participants in this project. The goal will be to ensure that all background information is available for studies that need to be conducted to both characterize the reservoir and determine possible mechanisms for escape of CO_2.

(b) Discussion with PI about the merits of each proposed site. We will work with PI to evaluate available data and make preliminary assessment of storage capacity as well as discussing the challenges related to monitoring each site.

(c) Delineation of the reservoir architecture including known and inferred structures within the reservoir and caprock that will act as barriers or facilitators for migration of injected fluids. This will likely involve further analysis of active seismic data and evaluation of changes in the reservoir that have accompanied previous production from the reservoir. Additional data may need to be collected for better evaluation.

(d) Make recommendations for new data that need to be collected.

Evaluation and Ranking of Potential Target Formations
We will build upon the initial ranking performed by the PI. The most important criterion is leakage risk, which depends upon the integrity of the seal, and injectivity. Capacity is also important. Another factor is the depth of the reservoir. The deeper the reservoir, the less prone it is to leakage due to the thickness (and, perhaps, number) of potential barriers between the reservoir and the surface. However, the deeper the reservoir, the more expensive it is to compress the CO_2 to be stored in it. Also, the deeper the reservoir, the more difficult it is to obtain information about its behavior and, as a result, be certain that it

is not leaking. The source energy needed to monitor reservoir behavior with seismics increases as the depth to the reservoir increases, as does the error in analyzing the data induced by propagating through the caprock. The surface deformation and gravity signal for a given mass flux of CO2 scale roughly inversely to the depth cubed. In evaluating and ranking potential target formations, we will try to optimize the competing dependences on depth.

2. Geomechanical Processes and Caprock Integrity

The interaction between the pore fluids and the rock is an essential component in the assessment of CO2 storage in geologic formations. Thus geomechanical studies provide critical input data for reservoir design and management. The unique nature of this UAE CCS project requires a research program much more extensive than those typically done by service organizations. Injecting large volumes of carbon dioxide will create a pore-fluid that, at least initially, will disturb both the local mechanical and chemical equilibrium of pore fluid and the surrounding reservoir and cap rocks. The pressurization of the formation upon injection of supercritical CO2 will reduce the effective stress in the rock. This process can have several effects that need to be evaluated, including the displacement of brine, the activation of dormant faults that can then serve as leakage pathways, and the creation of fractures that may compromise the integrity of the caprock. In addition to understanding these mechanical effects, both the short- and long-term reliability and stability of the repository demands detailed knowledge of chemical effects associated with the disturbance in chemical equilibrium. The kinetics of the interactions between the fluid and minerals [2004], and the effects of the fluid/rock interactions on the mechanical and transport properties of the reservoir and cap rock [*Shukla et al.*, 2010] must be determined. In this second task we propose a combination of theoretical, computational, and laboratory work to evaluate chemo/geomechanical processes and seal integrity in the target deep aquifers identified in Task 1.

2.1 Development of Coupled Computational Models of Flow and Geomechanics (RJ, BH)

Reservoir geomechanics is concerned with the simultaneous study of the coupled fluid flow and the mechanical response of the reservoir. Quantification of the state of deformation and stress of the reservoir is essential for the correct prediction of a number of processes critical to geologic CO2 storage, including pressure evolution, surface subsidence, seal integrity, hydrofracturing, and induced seismicity.

2.1.1 Geomechanics background

Injection of CO2 into a saline aquifer changes the state of stress, both within and outside of the aquifer, affecting the stability of preexisting faults, the permeability of existing fractures, and potentially creating new fractures. The effects of injection depend on the existing (pre-injection) state of stress, the elastic moduli of the structures, and the fault

frictional properties. The effects are not always intuitively obvious and should be quantified using state-of-the-art geomechanical models.

The constitutive law for an isotropic poroelastic medium can be written

$$\sigma_{ij} = 2\mu\varepsilon_{ij} + \delta_{ij}\left(\lambda\varepsilon_{kk} + \zeta p + K\alpha_s T\right) \tag{2.1.1.1}$$

where σ_{ij} is the stress tensor, ε_{ij} is the strain tensor, p is the pore pressure, T is the temperature, μ is the shear modulus, λ is the drained, isothermal Lamé constant, K is the drained porous medium bulk modulus, and α_s is the cubical thermal expansion coefficient for the solid. The coefficient $\zeta = 1\text{-}K/K_s$, where K_s is approximately equal to the bulk modulus of the solid constituents [*Rice and Cleary*, 1976], is of order unity (typically 0.4 – 0.8).

Usually reservoirs are much wider than they are deep, so inflation due to an increase in p or T occurs approximately in a condition of uniaxial extensional strain, ε_{33}, under constant vertical stress, σ_{33}. Under these conditions, the changes in the horizontal compressive stresses are

$$\Delta\sigma_{11} = \Delta\sigma_{22} = \frac{(1-2\nu)}{(1-\nu)}\left(\xi\Delta p + K\alpha_s\Delta T\right) \tag{2.1.1.2}$$

where Poisson's ratio, $\nu = \dfrac{(1-2\nu)}{(1-\nu)}$, is typically in the range 0.2 – 0.3.

The various ways in which changes in pore fluid pressure can affect fault stability are sketched in Figure 2.1.1, which shows a reservoir intersected by a normal fault, as would be produced in a tectonic stress field where the maximum compressive stress is vertical and the minimum compressive stress is horizontal. Assume that CO2 is to be stored within the upper reservoir. Injection of CO2 increases the pore fluid pressure both within the plume and in an expanding halo in the aquifer, there is an increase in the horizontal compressive stress (red arrows). Such an increase in compressive stress would tend to suppress motion on small normal faults within the reservoir, as well as tending to suppress the opening of fractures. It would also act to clamp the normal fault where it intersects the reservoir, increasing its stability.

Vertical expansion of the reservoir layer would also induce stresses outside the reservoir itself that could affect the integrity of the cap rock and seals. The shear stresses on the normal fault above and to the left of the reservoir, where the tectonic shear stress and the injection-induced shear stress are parallel, would be increased, tending to destabilize this fault. On the other hand, the shear stresses on the normal fault below and to the left of the reservoir would be diminished, stabilizing this segment of the fault.

In addition to the stress changes sketched in the figure, there would be a rather complicated state of stress generated at the end of the reservoir due to the spatial variation in pore pressure and lithology. The reservoir would tend to curl, similar to a thermostat, introducing further perturbations in fault stability.
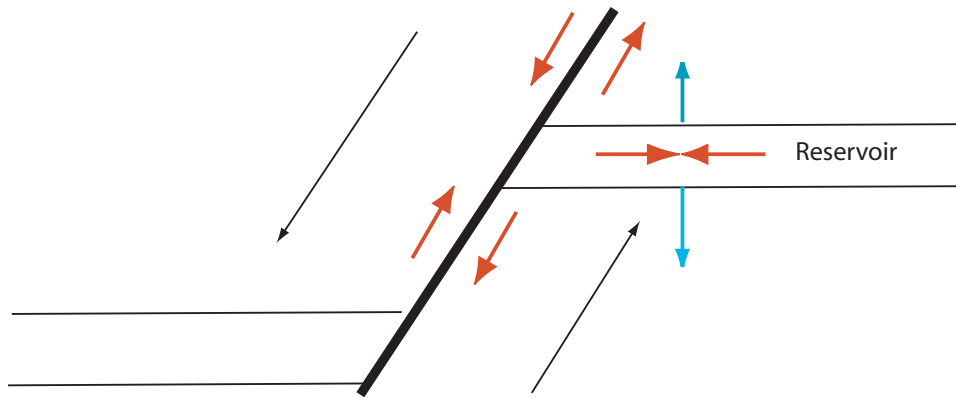

Figure 2.1.1.1: Schematic of strain (cyan arrows) and stress (red arrows) resulting from an increase in pore pressure in a reservoir offset by a normal fault (black arrows). The increase in horizontal compressive stress within the reservoir tends to inhibit additional normal fault slip within and on the fault segment just to the left of the reservoir. However, the vertical expansion of the reservoir induces shear stresses on the fault in orientations that tend to stabilize the fault below the reservoir, but tend to destabilize the fault above the reservoir. If fault slip should occur, additional changes in stress and fault stability would occur. Quantifying the change in fault stability requires a geomechanical model and an estimate of the preinjection state of stress.

Faults on the verge of slip are called "critically stressed." Faults are moved towards a critical stress state by increased pore pressure, decreased coefficient of friction, and destabilizing changes in the background stress. Faults and fractures that are oriented with respect to the principal stresses such that slip is facilitated can provide conduits for fluid flow [e.g., *Barton et al.*, 1995].

Morris et al. [2010] combined fluid flow simulations and a simple geomechanical model to investigate the fracture-induced permeability evident at the In Salah, Algeria, CO2 sequestration site. As discussed in detail in section 4.6, there is evidence from both surface deformation in the region of injection well KB-502, and breakthrough of CO2 from KB-502 into observation well KB-5, that injection of CO2 triggered slip on a favorably oriented fault, resulting in the opening of a high-permeability zone connecting KB-502 to KB-5. Figure 2.1.1.2 shows their calculation of the pore pressure increase that would be required to induce slip on faults of varying orientations (assuming a typical coefficient of friction of 0.6). Their geomechanical analysis predicts that Fault F12, which connects the injection well and the observation well, is unstable at a relatively low pore pressure increase. If this result had been available prior to injection, the breakthrough could have been anticipated.
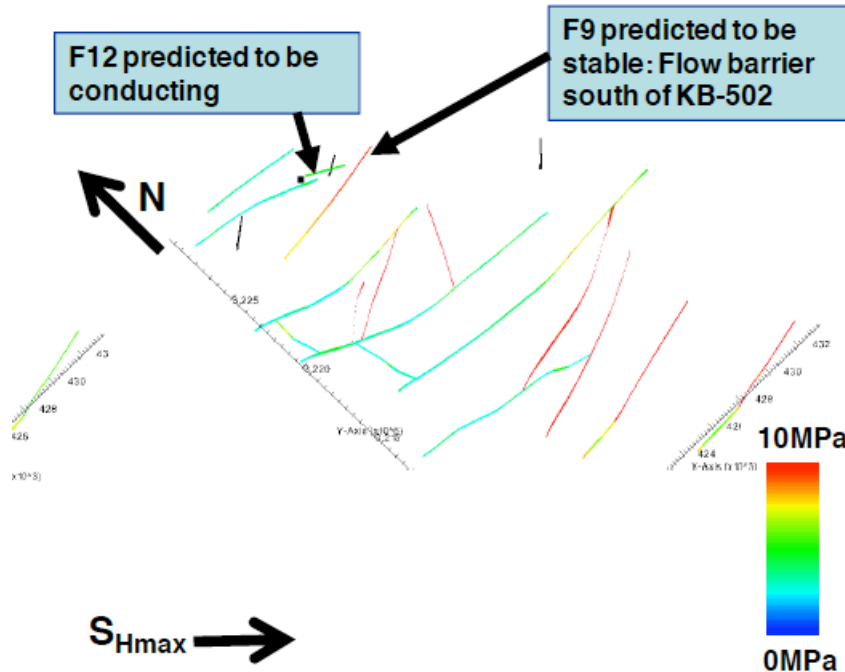
Figure 2.1.1.2 Critical stress analysis providing an overview of mechanical stability [after *Morris et al.*, 2010]. The estimate of the change in pore-pressure that will result in shear failure of faults, given the orientation of the maximum horizontal compressive stress and the faults, is given by the color bar. Fault F12, connecting injector well KB-502 (line to right) and monitoring well KB-5 (dot to left) is predicted to slip at relatively low pressure. Fault F9, to the right of KB-502 is predicted to be stable. CO2 breakthrough observed in KB-5 and the observed surface deformation validate these predictions.

2.1.2 Critical Issues in Coupling Geomechanics and Flow in CO2 Sequestration

Much work has been done in the area of coupled flow and geomechanics. Particularly relevant are the works of Settari [e.g., Settari and Mourits, 1998; Settari and Walters, 2001], Lewis [e.g., Lewis and Sukirman, 1993; Lewis and Schrefler, 1998], Armero [e.g., Armero and Simo, 1992; Armero, 1999], and Tran [e.g., Tran et al., 2004, 2005], among many others [e.g., Fredrich et al., 2000; Mainguy and Longuemare, 2002; Thomas et al., 2003; Dean et al., 2006; Jean et al., 2007]. In recent years, two computational issues have received particular attention. One issue is the development of appropriate discretization schemes that are capable of representing the displacement field while being mass conservative at the element level. Discretization schemes that satisfy both requirements include the mixed finite element method [Jha and Juanes, 2007] and a discretization that combines nodal finite elements for mechanics and finite volumes for flow [Dean et al., 2006; Kim et al., 2009].

The second computational issue is the coupling strategies for the solution of the flow and mechanics problems [Dean et al., 2006]. They range from one-way coupling [Fredrich et al., 2000] to loose or explicit coupling [Minkoff et al., 2003], iterative coupling [Settari and Walters, 2001; Thomas et al., 2003; Tran et al., 2002] and fully coupled approaches [Lewis and Schrefler, 1998].

While much work has already been done in the area of coupled flow and geomechanics, many aspects that are critical to CO2 sequestration remain poorly understood. In particular, it is important to significantly advance the reservoir mechanics science in the following areas:

1. Understanding surface deformation of faulted reservoirs (see Ferronato et al. [2008] for some recent work in this direction).
2. Elucidation of the poromechanics of faults – the influence of the full stress tensor and pressure increase on fault slip.
3. Assimilation of surface deformation data upon CO2 injection in a deep aquifer, as evidenced by InSAR and GPS data (Task 4.6).
4. Linking CO2 injection to microseismic events (Task 4.5), through a global model of fault slip, and use passive seismic data (Task 4.3) as part of the data assimilation framework (Task 4.1).

In this task, we will develop coupled models of flow and geomechanics of CO2 injection in deep geologic formations that will address the issues above. We will do so by coupling a flow code with the PyLith geomechanics code.

PyLith (http://www.geodynamics.org/cig/software/packages/short/pylith) is a finite element code for the simulation of static and dynamic large-scale geodeformation problems. Much of its development has been motivated by the modeling of tectonic stress in the Earth's crust, but its applicability extends to problems at any other scale, such as the reservoir scale. Some of the advantages of PyLith over other mechanical deformation simulation codes are the following:

1. It is an open source code, which can be modified for specific purposes.
2. It is written in a C++ modular environment, easier to maintain and extend.
3. It is written to take advantage of parallel computing, something that could be instrumental given our recent acquisition of a 100+-node cluster.
4. One of the fundamental advantages is that it allows localized deformation along discrete features, such as faults – this is an essential feature for the simulation of production-induced subsidence in faulted reservoirs, see Figure 1.
5. It is maintained by a well-established community (CIG), which offers regular updates and continued development.
6. It is well integrated with gridding/meshing codes, such as LaGriT (for tetrahedral meshes, https://lagrit.lanl.gov/) and CUBIT (for hexahedral meshes, http://cubit.sandia.gov/).

The implementation effort will focus on two areas:

1. Incorporate realistic material behavior, such as nonlinear elasticity, plasticity and viscoplasticity. Although we have experience in the implementation of implicit return-mapping algorithms for the solution of plastic deformation, we still need to evaluate carefully how this will be implemented in PyLith.
2. Incorporate the coupling with the flow equations. We will take full advantage of our previous work in this area (Jha and Juanes, 2007; Kim et al., 2009). We will use a single computational grid, in which the displacements are solved for at the element

15

nodes, and the pressures at the element centers, see Figure 2.1.1. This choice combines simplicity (single grid, no need for remapping computed quantities), stability (with a low-order approximation of the displacements), and local mass conservation.
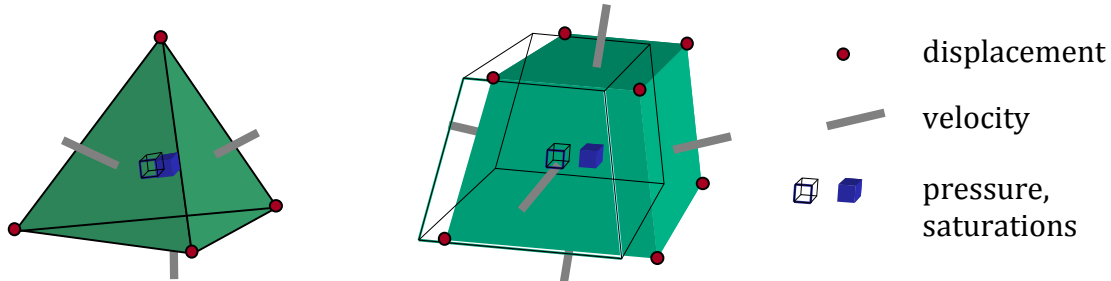

Figure 2.1.1: Discretization of the different variables on tetrahedral and hexahedral elements.

What is needed is to develop a module that computes fluid pressures and saturations. From an implementation standpoint, this requires the element-element connectivity and element based hydraulic properties (permeability, porosity, relative permeability, etc.). Conceptually, one solves the discrete equations of coupled flow and geomechanics, which lead, at every nonlinear iteration, to a system of equations of the form:

$$\begin{bmatrix} A & B \\ B^T & C \end{bmatrix} \begin{bmatrix} u \\ p \end{bmatrix} = \begin{bmatrix} g \\ f \end{bmatrix} \qquad (2.1.2.1)$$

where A is the stiffness matrix, B is the poromechanics coupling matrix, C is the conductance matrix, u is the vector of nodal displacements, p is the vector of element-centered pressures, g is the vector of nodal forces and f is the vector of fluid mass sources/sinks.

The key aspect of our proposed approach is the solution of Equation (2.1.2.1) by a sequential method, in which the mechanics and flow problems are solved separately (sequentially), rather than simultaneously. This approach has enormous advantages in terms of flexibility and implementation simplicity – only two separate simulators are needed and the coupling is done by re-defining the matrices and right-hand side vectors of the individual problems. We will use PyLith as the mechanics simulator, and Stanford's General Purpose Research Simulator (GPRS) as the flow simulator. Recently, we have investigated the deficiencies of traditional sequential solution methods, and have proposed a new operator split (the fixed mean-stress split), which is unconditionally stable and whose accuracy and efficiency does not degrade in the undrained limit (Kim et al., 2009).

Profs. Juanes and Hager will collaborate closely with Prof. Hamdi Tchelepi from Stanford on this task, to ensure that the work is synergetic, and not overlapping. The focus of the work at MIT will be on the theoretical developments and implementation of fluid flow through and along faults, and the coupling of pressure and deformation fields in the presence of

strain localization and slip surfaces. We believe this is a key ingredient for the assessment of CO2 storage security, which has so far received little attention.

2.1.3 Detailed Work Plan
The work proposed is divided into four areas, each with its own set of tasks distributed across the four years of performance of the project.

1. Initial Assessment of Caprock Integrity.
   Although our assessment of caprock integrity will change as more information and better techniques become available, even a very simple geomechanical model such as that used by Morris et al. [2010] has value in assessing fault stability. This requires a good description of fault geometries in the candidate reservoirs. A characterization of the actual variations in elastic modulus in the region of the candidate reservoirs would help to improve the accuracy of the calculation.
   a. (Year 1) Carry out a comparable analysis for candidate reservoirs as part of our integrated assessment of cap rock integrity. Assess the potential for leakage risk that will inform operation decisions and conclude what leakage pathway is the most likely (well leakage, sandy caprock, fractured caprock, active fault, etc.)

2. Theoretical and Computational Developments
   While we will rely heavily on our previous work in this area, several theoretical developments are required to extend our capabilities to simulate CO2 storage.
   a. (Year 1) Extend the fixed-stress split [Kim et al., 2009] to multiphase flow environments. In fact, work is already under way in collaboration with Prof. Tchelepi at Stanford, and Dr. Jihoon Kim currently at Lawrence Berkeley Lab.
   b. (Years 1-2) Develop a theoretical and computational framework for flow along discrete faults, first for single-phase flow and subsequently for multiphase flow. This will build on our own developments [Juanes et al., 2002; Molinero et al., 2002], as well as on those of the Stanford group [Karimi-Fard et al., 2003].
   c. (Years 2-3) Develop a theoretical and computational framework of the poromechanics of faults, including a yield criterion for fault slip and a corresponding prediction of hydraulic activation of dormant faults. The objective is to determine the risk, as a result of CO2 injection and subsequent changes of the state of stress at depth, of: (1) leakage through faults, and (2) induced seismicity.

3. Computer Code Implementation
   The distinct advantage of our iteratively coupled approach is that a single-unit (fully-coupled) geomechanics code is not needed. Instead, we can focus our work on the two modules—flow and mechanics—fairly independently.
   a. (Year 1) Implement an iteratively coupled strategy for single-phase flow and the PyLith elastic deformation module.
   b. (Years 1-2) Incorporate realistic material behavior in PyLith, such as nonlinear elasticity, plasticity or viscoplasticity.

c. (Year 2) Investigate scenarios of fault slip with nonlinear rheology in PyLith, without coupling to the flow field.
d. (Years 2-3) Implement coupled multiphase poromechanics, based on an iteratively coupled strategy linking the GPRS reservoir simulator and PyLith.
e. (Year 3) Enhance GPRS to include flow through faults, and allow for a time-dependent permeability of faults to accommodate for hydraulic fault activation.
f. (Years 3-4) Implement a coupled GPRS+PyLith code with fault slip and hydraulic fault activation.

4. Application to CO2 Injection in Abu Dhabi Reservoirs
   a. (Year 1) Gather data for the different potential reservoirs.
   b. (Years 1-2) Integrate different sources of data, construct fault-compliant grid and build reservoir models of the target aquifers at different scales and different resolutions.
   c. (Year 2) Evaluate different scenarios of CO2 injection with the single-phase flow and geomechanics code.
   d. (Years 2-3) Simulate test cases of fault slip, first with no coupling to flow, then with single-phase flow and, finally, with multiphase flow.
   e. (Year 4) Apply the multiphase flow and geomechanics code (GPRS+PyLith) to the selected aquifer(s), under realistic injection scenarios. The final objective is to perform predictions of: pressure evolution, changes in the state of stress, risk of leakage, capacity estimation, and surface deformation.

2.2 Laboratory Studies of Geomechanics and Mineral Trapping (BE, YB, MS)

2.2.1 Introduction and Motivation
Geomechanical studies provide critical input data for reservoir management. However, the unique nature of this UAE CCS project requires a research program much more extensive than those typically done by service organizations. Injecting large volumes of carbon dioxide will create a pore-fluid that, at least initially, will disturb both the local mechanical and chemical equilibrium of pore fluid and the surrounding reservoir and cap rocks. Understanding both the short- and long-term reliability and stability of the repository demands detailed knowledge of the kinetics of the interactions between the fluid and minerals [2004], and the effect of the fluid/rock interactions on the mechanical and transport properties of the reservoir and cap rock [*Shukla et al.*, 2010]. Thus, although conventional geomechanical tests of limestone samples with realistic pore fluids will be necessary to provide engineering data for the repository design, it is quite important to realize that long-term reliability of the repository will require substantial additional knowledge of kinetic rates of the chemo-mechanical processes expected to occur and of the effects of those processes on mechanical and transport properties.
Among the specific factors that might affect the mechanical strength of either the repository or the cap-rocks are increased tendency for cataclasis caused by introducing pore fluids of varying chemistry [*Karner et al.*, 2003; *Karner et al.*, 2008], the introduction of inelastic deformation at grain contacts via some solution-transfer processes [*Min et al.*,

2009], or changes in local pore fluid pressure that might destabilize existing faults [*Streit and Hillis*, 2004]. During sequestration, the natural groundwater will be displaced by the sequestered fluid, a mixture dominated by supercritical CO_2, but which will probably also include water and brine chemicals [e.g., *Pruess et al.*, 2003; *Egermann et al.*, 2005]. During fluid exchange, the formation will experience the flow of at least two immiscible fluids. The new fluids are likely to be out of equilibrium with the mineral components, and thus, rapid and dramatic changes in the geometry of the pore space will occur owing either to dissolution or precipitation of minerals. Whether the fluid is under- or over-saturated in carbonate minerals is thought to be most significantly affected by pH of the pore fluid [*Druckenmiller and Maroto-Valer*, 2005; *Pokrovsky et al.*, 2009; *Zevenhoven et al.*, 2006]. Thus, the transmissivity of the formation may either increase or decrease, depending on the chemistry of the fluid [*Egermann et al.*, 2005], the local flow rates, and the initial geometry of the pore space, [*Bernabé et al.*, 2003; *Elsworth and Yasuhara*, 2006; *Mok et al.*, 2002; *Polak et al.*, 2004].

Mechanical experiments conducted porous carbonates with no added pore fluid show that both the yield and the ultimate failure strength depend critically on mineral chemistry and pore geometry [*Baud et al.*, 2006; *Schubnel et al.*, 2005; *Wei et al.*, 2010; *Wong and Baud*, 2009; *Xu et al.*, 2009]. If the pore structure of either reservoir or cap rocks is altered by the flow of potentially reactive fluids, then significant weakening or strengthening may occur, changing the response of the reservoir to regional stresses. Depending on the failure mode that is induced, permeability may either increase or decrease [*Baud et al.*, 2000; *Milsch et al.*, 2003; *Xiao et al.*, 2003; *Yasuhara et al.*, 2006; *Zhu et al.*, 2009]. Tests at elevated pressures and temperatures with realistic pore fluids have not been done on repository rocks, but both CO_2 pressure and the salinity of the pore fluid are known to affect the compaction rate of ground calcite aggregates [*Liteanu and Spiers*, 2009]. The compaction rate of those granular aggregates was found to be a complex function of the partial pressure of carbon dioxide and salinity, and those authors were unable to unambiguously identify the mechanism of compaction. Importantly, several recent geochemical studies [*Druckenmiller and Maroto-Valer*, 2005; *Pokrovsky et al.*, 2009; *Zevenhoven et al.*, 2006] indicate that the dissolution kinetics of carbonate minerals in multi-component aqueous solutions depends most strongly on the circumneutral pH, rather than on the fugacity of single component. The new geochemical information suggests that experiments should be conducted with pore fluids of more carefully controlled chemistry, and that both stagnant and flowing fluids should used.

In addition to changes in permeability that may occur during sequestration and that might result from reactions of the rock with single-phase fluids, it is also important to understand the modes of mixing of both miscible and immiscible phases in the repository (as discussed above). Several complex regimes of fluid invasion may occur during density-driven mixing of CO_2/brine solutions within porous rocks [see *Gollub and Langer*, 1999, and others]. For example, transitions between invasion percolation and viscous fingering and between fingering and fracture have been investigated in porous media under ambient temperature and pressure conditions using computations or laboratory experiments [Boudreau et al., 2005; Jain and Juanes, 2009; Holtzman and Juanes, 2010]. The invasion behavior under those conditions is governed by two dimensionless parameters involving the relations between pore-scale disorder, viscous and capillary forces, and the deformability of the solid medium.

Knowledge of the variables governing invasion transitions is much less detailed when considering actual repository conditions of elevated temperature and pressure. However, several promising techniques have been developed recently to image the internal structure of rocks while at elevated pressures and temperatures. These techniques incorporate remote sensing techniques during geomechanics experiments, including seismic tomography [*Lei and Xue*, 2009; *Stanchits et al.*, 2003], the location of acoustic emissions [*Backers et al.*, 2005; *Fortin et al.*, 2009; *Hall*, 2009; *Lockner et al.*, 1991; *Stanchits et al.*, 2009], or inversion of electrical resistivity measurements. For example, Lei and Xue, [2009] were able to use seismic tomography to image the injection of CO_2 into a water-saturated sandstone under elevated confining pressure, at room temperature and 34°C. Spatial resolution in both the tomography techniques and acoustic emission location depends strongly on the number of ultrasonic sensors employed, the acoustic wave length, the size of the sample, and the signal processing techniques used for the inversion of the data [*Stanchits et al.*, 2003]. The spatial resolution of images made using acoustic waves will always be less than that obtained with x-ray tomography, but it is much more difficult to utilize the latter technique at elevated pressures, unless high-energy synchrotron radiation is available. Often ultrasonic signals are stacked to improve the signal to noise ratio, but when this procedure is used, the time interval between measurements is affected.

2.2.2 Experimental techniques
The goal of the mechanical tests would be to measure permeability, strength, and acoustic velocities during triaxial loading with stagnant and flowing fluids at repository conditions. Flow properties, mechanical properties, and reaction rates will be interdependent on one another, and kinetic studies will be necessary, especially when estimating the long-term viability of the reservoir. Detailed studies of the microstructure resulting from the tests will be done using optical microscopy, electron microprobe, and scanning and transmission electron microscopy. Among the important variables to be considered and controlled are mineralogy of the repository and cap- rocks, chemistry of the extant pore fluid, temperature of the formation and pore-fluids, the pressure of the extant and injected fluids, and flow rates during sequestration.
It will be particularly useful to include a reaction vessel to provide well-mixed fluids of controlled chemistry as part of the upstream pore-fluid system [*Druckenmiller and Maroto-Valer*, 2005; *Pokrovsky et al.*, 2009; *Zevenhoven et al.*, 2006]. With this addition, two types of experiments could be conducted, the first could involve constantly flowing fluids, the second would involve inserting a pore fluid with known chemistry, shutting the fluid in, and observing changes in the mechanical and transport properties. The latter class of experiments could then observe the approach to chemical equilibrium of the fluid and solid phases. One challenging aspect of these experiments is the corrosive nature of the brine/CO_2 mixtures, especially when these are heated. Consequently, the apparatus will need to be designed with this complexity in mind. Usually this requires construction of the pore fluid system with Hastelloy metal, which is particularly resistant to corrosion at high temperatures and pressures. Planning for the mechanical and mineral trapping studies can begin as soon as candidate formations are identified. Once the apparatus is ready, mechanical tests can be begun with proxy rocks that are thought to be representative of the likely repository site.

Any microstructural studies could be conducted in close collaboration with the core-scale laboratory experiments to be conducted at Stanford. The Stanford study will include CT scanning of limestone samples during imbibition and drainage of a multiphase pore fluid at room pressures. These experiments will provide critical insights into the geometry of the pore space and the nature of flow within the formation, but they will need complementary information gleaned from tests at repository conditions.

Measuring permeability: By simultaneously measuring permeability and acoustic velocities during continued triaxial mechanical loading at reservoir pressures and temperatures, we will gain insight into the way that rock structure responds to changing load conditions. Several methods are available to measure fluid flow in rock cores in the laboratory: steady-state Darcy flow, transient-pulse monitoring, sinusoidal oscillation methods [*Bernabe et al.*, 2006; *Faulkner and Rutter*, 1998; 2000; *Faulkner et al.*, 2002; *Fischer and Paterson*, 1992; *Kranz et al.*, 1990; *Ngwenya et al.*, 2001; *Ngwenya et al.*, 2003; *Song and Renner*, 2007], and less-common techniques, including measurements made with linearly increasing upstream head [*Song and Renner*, 2006a; b; 2008], tests with constant injection rate [*Song et al.*, 2004], and experiments utilizing complex-transients [*Boitnott*, 1997].

Each method has advantages and disadvantages, and all should be considered when designing an experimental program. For example, the standard Darcy flow method is appropriate when it is desirable to introduce a continuous supply of fluid of constant composition or when the permeability of the rock being measured is relatively high. Because only a minimal volume of fluid actually flows in and out of the sample, the oscillation technique has been used to great effect in measuring changes in permeability while rock samples are deforming at wide variety of temperature and pressures*: e.g. [Cox, 2002; Fischer and Paterson, 1989; 1992; Ngwenya et al., 2003; Ojala et al., 2004; Xiao and Evans, 2003; Xiao et al., 2006; Zhang et al., 1994a; Zhang et al., 1994b; Zhang et al., 2000]* and in rocks undergoing metamorphic reactions [*Milsch et al.*, 2003; *Zhang et al.*, 2000]*.*

For all the methods, correct experimental design is critical. For example, in the oscillating head technique, increasing the amplitude of the driving signal increases the signal to noise ratio of the downstream signal. But, the variation in the upstream fluid pressure must still be chosen to be a fraction of the initial fluid pressure so that variations in effective pressure do not begin to influence the sample permeability itself. In many instances, it is important to reduce the volume of the downstream reservoir as much as possible, especially if one is interested in measuring sample storativity [*Bernabe et al.*, 2006]. When permeability is the greater concern, reducing the downstream reservoir is also useful, but the measurement is less sensitive. The aspect ratio of the samples is another design parameter (large ratios of S/L are desirable for measurement of *k*), but, of course, spatial sampling issues are always important in any physical properties measurement.

Imaging flow during geomechanics experiments: The measurement of permeability of a rock with two immiscible fluid phases is very complex. Because of genuine restrictions in the understanding of the physics of this problem, careful design of an experimental program is quite important. Discrepancies between the results obtained using different measurement techniques of a single property, like permeability, might be expected owing to such factors as varying saturation values and differential storativity in the two phases, both of which might change during the course of a measurement.

2.2.3 Detailed Work plan

1. Conventional triaxial mechanical experiments of repository and cap rocks will be conducted at *in situ* conditions, including lithostatic pressure (confining pressure) of 10 to 50 MPa, pore fluid pressure of 10-30 MPa, and temperatures between room temperature and 150°C. The mechanical tests would be designed to measure both yield and ultimate strength of repository and cap rocks under various states of confinement in drained and undrained conditions. The initial tests would be done with stagnant fluids; separate suites of tests using both aqueous fluids and supercritical carbon dioxide would be conducted. For the carbonate rocks, several suites of tests would be done with aqueous fluids that were initially saturated or unsaturated with respect to the solid minerals. Salinity and mineral content of the aqueous fluids would be designed to mimic the natural fluids. Tests will be conducted at several constant loading-rates, but there should also be tests done with loads that are maintained constant at 60-90% of the ultimate failure strength. Triaxial mechanical experiments on silicate rocks at modest temperatures indicate that inelastic deformation, even if it is dominantly cataclastic in nature, can be rate dependent, an effect sometimes called static fatigue. Fatigue effects might be particularly important when fluids not in chemical equilibrium with the rock minerals are inserted.
2. Similar tests should be conducted with supercritical carbon dioxide at various states of saturation with respect to water and salts.
3. During the mechanical tests, we would conduct simultaneous measurements of permeability using an oscillating pore pressure technique [*Fischer and Paterson*, 1989; 1992; *Kranz and Blacic*, 1984]. The details of the measurement will be adjusted depending on the initial permeability of the repository rocks and the rate of deformation of the rock [*Bernabé et al.*, 2006]. It should be possible to measure acoustic wave velocities at various intervals during at least some of the experiments, but the number of these experiments will depend on time constraints.
4. Detailed microstructure studies using reflected and transmitted optical light microscopy, back-scattered electron microscopy, and nano-indentation will be done before and after deformation to characterize the failure mechanisms, to investigate scaling of mechanical properties, and to understand any reactions that are occurring.
5. To begin to constrain fault reactivation, we will do tests on sawcuts and natural fractures induced after mechanical failure. Such lab-scale experiments cannot duplicate the reactivation of large-scale faults, but they can be used to understand the relative effect of pore fluid composition, temperature, or loading rates on frictional slip.
6. Any evaluation of the reliability of either the repository and the caprocks will need include knowledge of the kinetics of the interaction of the pore fluids, both natural and sequestered, and of the rocks. Because the viability of the repository must be ensured for a length of time far beyond that available for laboratory tests, it will important to understand the effect of metamorphic reactions on the strength and transmissivity of both the cap rock and the carbonates. Thus, it will be important to conduct experiments that investigate the kinetics of the reactions and of the effect of the reactions on strength. The correct design of the experiments must account for the details of the chemistry of the in situ pore fluid and of the sequestered pore fluid, which may be a mixture of the initial pore fluid and super-critical CO_2. By measuring permeability during constant load experiments, it will be possible to measure changes

in transmissivity owing to reactions, especially in the cap rocks. The sequestered fluid will initially be out of equilibrium with the repository rocks, and rate at which the two equilibrate will depend on the flow rate and the geometry of the pore space as well as other traditional thermodynamic parameters. There will inevitably be limits on the flow rate and total volume of pore fluid that can be circulated in the experiments, but it is possible to observe substantial changes in fracture transmissivity in limestone samples even at room temperature. It will be important to measure the effect of increasing effective pressure on the rates of these changes.

7. Micro structural analyses will also be important for the fluid-flow experiments and techniques similar to those in task 3 will also be done on these samples.

8. In collaboration with Prof. Mohammed Sassi, of the Masdar Institute, we will install and develop an experimental investigation of the mixing and flow of fluids when super-critical carbon dioxide is injected into brine-saturated carbonate reservoir rocks. These experiments, which will use acoustic tomography to image the fluid mixing, will be quite complementary to the calculations and ambient-pressure experiments proposed by Profs. Sassi, Juanes, and Bernabé in another section of this proposal, and to the x-ray imaging studies to be conducted at Stanford University. Although the acoustic images will be of lower quality than the x-ray CT-scans, the acoustic images may be acquired while the reservoir rocks are loaded mechanically at reservoir conditions. Such a capability will be critical for investigating the transition from convective fingering to fracture transmission. These experiments are technically challenging and will require detailed instrumentation of rock samples of large dimension (10 cm diameter). In addition, we anticipate that analysis of the data will require extensive use of seismic tomography and geophysical inversion techniques. To this end, we will establish a collaborative team, including Prof. Sassi of the Masdar Institute, Prof. Alison Malcolm, a seismologist from the Earth Resources Laboratory at MIT, and Brian Evans, of the rock mechanics laboratory at MIT, and their students.

2.2.4 Education and training

Education and training are also important goals of this project, and we expect to establish close collaboration with MASDAR and PI personnel in all the proposed chemo-mechanical studies. We envision that experiments would be conducted both in Abu Dhabi and at MIT. This collaborative effort would be enabled by developing parallel capabilities in laboratory equipment at MASDAR/PI and at MIT. The laboratory apparatus would be constructed in consultation with NER, a company that has already provided equipment to PI, but the equipment would be tuned to the current research requirements. Such a path is recommended by the exigencies of the timeline of the project, the unique nature of the repository fluids, and by the desirability of establishing close cooperation between scientists and engineers in Abu Dhabi and the US. Because the research proposed here is different from and complementary to typical engineering plans commissioned by oil service companies, the project will provide MASDAR and PI personnel a springboard to establish unique expertise in the science and engineering of repository geomechanics.
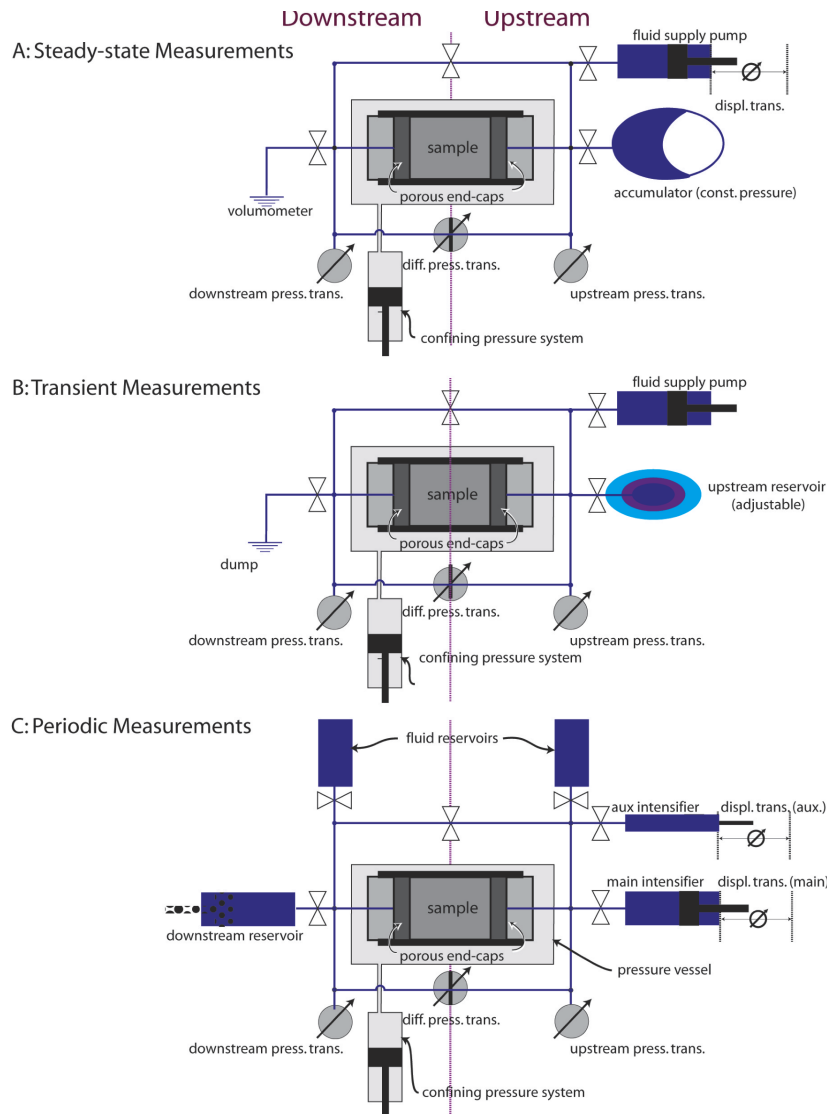
Figure 2.2.1: Simplified schematics for a) Steady-state Darcy flow measurements; b) Transient pulse decay technique; c) Periodic measurements including oscillation or complex transient methods. After *Trimmer* [1982]*; Bernabé* [1987]*; Fischer* [1992] *and Song and Renner* [2007]. Some parameters important for the experimental design are sensitivity of measurement of up- and down-stream pressures, ambient temperature stability, volume of up- and down-stream reservoirs, and stability of servo control of pressure generators.
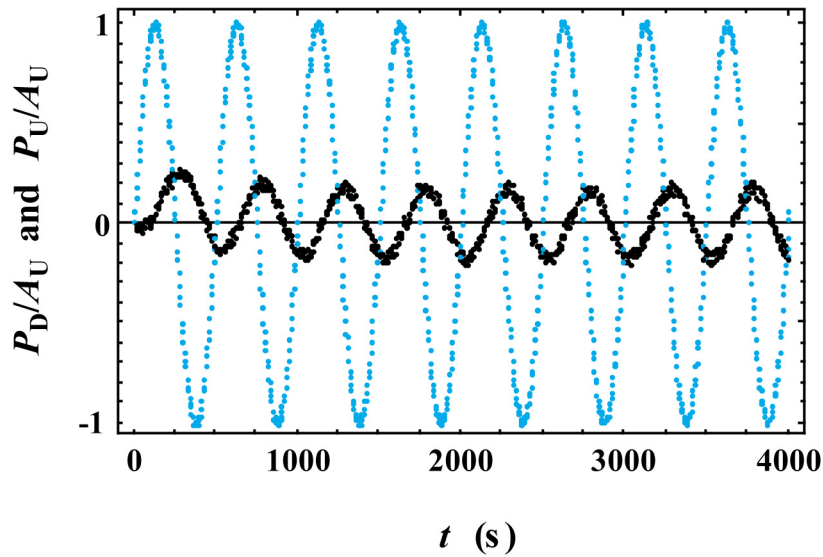
Figure 2.2.2: Simulated data for up- (blue dots) and down-stream (black dots) pressure measurements taken via the sinusoidal oscillation method, showing attenuation and phase delay between the two reservoirs, and the approach to steady-state in the down-stream measurement [Fig. 1 from *Bernabé et al.*, 2006]. For an example of actual data, see Fig. 3 of *Kranz et al.* [1990].

3. Capacity Estimates and Risk Assessment of Basin-scale CO2 Injection

The overall objective of this task is to develop tools for better understanding, modeling and risk assessment of CO2 permanence in geologic formations at the geologic basin scale. The main motivation for this proposal is that carbon capture and storage (CCS) will play an important role as a climate change mitigation technology only if it is deployed at a very large scale—possibly gigatonne per year injections over a period of decades. Continuous injection of this magnitude, even if distributed in space, will have an impact—and must be understood—at the scale of geologic basins. Specifically, the technical objectives of this task are:
1. To develop mathematical models of capacity and injectivity at the basin scale.
2. To apply quantitative risk assessment methodologies that will inform on CO2 permanence.
3. To apply the models to regional deep saline aquifers in Abu Dhabi.

Deep saline aquifers are attractive geological formations for the injection and long-term storage of CO2 [IPCC, 2005]. Even if injected as a supercritical fluid—dense gas—the CO2 is buoyant with respect to the formation brine. Several trapping mechanisms act to prevent the migration of the buoyant CO2 back to the surface, and these include [IPCC, 2005]:
(1) structural and stratigraphic trapping: the buoyant CO2 is kept underground by an impermeable cap rock, either in a closed, non-migrating system (static trapping), or in an open system where the CO2 migrates slowly (hydrodynamic trapping) [Bachu et al., 1994];
(2) capillary trapping: disconnection of the CO2 phase into an immobile (trapped) fraction

[Flett et al., 2004; Mo et al., 2005; Kumar et al., 2005; Juanes et al., 2006]; (3) solubility trapping: dissolution of the CO2 in the brine, possibly enhanced by gravity instabilities [Ennis-King and Paterson, 2005; Riaz et al., 2006]; and (4) mineral trapping: geochemical binding to the rock due to mineral precipitation [Gunter et al., 1997].

Much work has been devoted to modeling these mechanisms, mostly targeting the "local", single-point-of-injection scale. The greatest challenge for geological carbon, however, is the very large scale that must be achieved to have an impact on atmospheric CO2 emissions [IPCC, 2007]. Even if injection takes place at dozens of geographically-distributed sites, the storage of very large amounts of CO2 must be studied and modeled at the scale of geologic sedimentary basins (tens or hundreds of kilometers), as opposed to the pilot scale (hundreds of meters). In this task, we consider the basin-scale issues that are key to successfully sequestering large volumes of CO2: How can CO2 injection be conducted without inducing fractures that could channel CO2 toward the surface? How far will thin layers of mobile CO2 migrate? Where will displaced water exit the basin? Will dense CO2-saturated water sink? Robust modeling approaches are needed to answer these questions. In addition, the complex and imperfectly known processes as well as uncertain or unknown parameters call for quantitative risk assessment of CO2 sequestration at the basin scale.

3.1 Analytical Models of Flow Processes at the Basin Scale (RJ, DM)

A schematic of the basin-scale geologic setting for which flow models are developed is shown in Figure 3.1.1. The CO2 is injected in a deep formation that has natural groundwater flow. The injection wells (red) are placed forming a line-drive pattern. The distance between wells is of the order of hundreds of meters to a kilometer. Therefore, the CO2 plumes from the individual wells will interact early on in the life of the project. Under these conditions, the flow admits a model description on a vertical cross Section [Garven and Freeze, 1984a,b; Garven, 1995]. The conceptual line-drive model is clearly an approximation, but a useful one. It provides a geologic context for one-dimensional gravity-current models of CO2 migration [Vella and Huppert, 2006; Hesse et al., 2007, 2008; Juanes and MacMinn, 2008; Juanes et al., 2010].
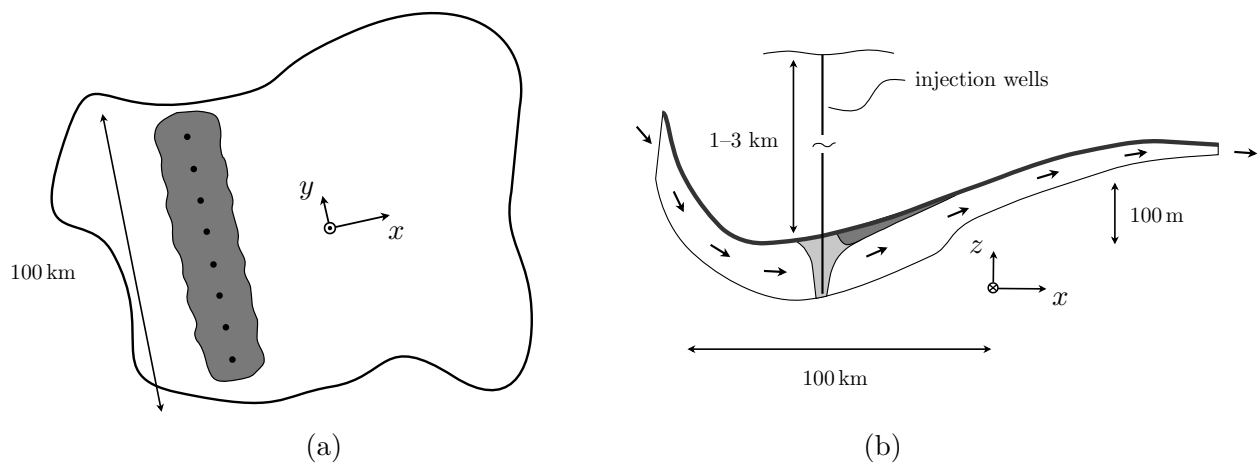

(a)

(b)

Figure 3.1.1: Injection of CO2 into a saline aquifer at the basin scale. (a) From a bird's-eye view, the plumes from the individual wells merge together as the CO2 spreads away from the well array (black dots). (b) In cross-section, the CO2 is shown in grey, the groundwater in white, and the caprock as a thick line. Arrows indicate the direction of groundwater flow. Typical horizontal and vertical scales are indicated. Note that the vertical scale of the aquifer is greatly exaggerated.

Due to buoyancy, the injected CO2 forms a gravity tongue, or gravity current. The high contrast in mobility between the injected CO2 and the initial brine exacerbates this gravity tongue, consequently decreasing the overall sweep of the aquifer. Once injection stops, the CO2 plume continues to migrate due its buoyancy and background regional groundwater flow. At the trailing edge of the plume, water displaces CO2, trapping it in residual form [Juanes et al., 2006].

We propose to develop *analytical* sharp-interface models of the evolution of CO2 plumes over the duration of injection (decades) and after injection (centuries). Our models will address the following fundamental questions: how far will the CO2 plume travel (that is, what is the footprint of the plume) and for how long does the CO2 remain mobile. Answers to these questions are essential in any first-order evaluation of the risk of a CO_2 storage project, and for obtaining capacity estimates at the basin scale.

Sharp-interface models of gravity currents in porous media have been studied for a long time [Barenblatt, 1996; Huppert and Woods, 1995; Kochina et al., 1983; Lyle et al., 2005], and they have been revived recently in the context of CO2 sequestration [Nordbotten et al., 2005; Hesse et al., 2007, 2008]. Recently, analytical solutions to the hyperbolic limit of sharp-interface models of gravity currents with capillary trapping have been presented by Hesse et al. [2008] to account for aquifer slope. In recent work [Juanes and MacMinn, 2008; Juanes et al., 2010], we have presented closed-form analytical solutions that account for plume shape during the injection period and regional groundwater flow.

In this task, we propose to extend this model to include all essential physics governing plume migration: (1) induced pressure gradients, (2) capillary trapping, (3) buoyancy, (4) regional groundwater flow, (5) aquifer slope, (6) dissolution into the brine (both due to diffusion from residual CO2 and convective mixing from mobile CO2), (7) loss through the confining unit, and (8) geochemical reactions. Our preliminary work suggests that analytical solutions can be obtained when all of these effects can be included (so far, dissolution and loss have not been accounted for in analytical models). These models will identify the key parameters governing ultimate migration distance. They will also allow us to evaluate, in a dynamic sense and at the basin scale, the transfer of trapping safety among the different trapping mechanisms, typically following the order structural trapping to capillary trapping to dissolution trapping to mineral trapping.

Application of models to regional deep aquifers in the UAE. We will apply the analytical solutions of CO2 plume migration and pressure evolution to specific geologic basins, to estimate: (1) the maximum footprint of the plume for a given CO2 storage scenario; (2) the

maximum injection rate that can be sustained during a certain injection period without fracturing the caprock or activating pre-existing faults.

A major uncertainty for analysis of basin transport and mechanical integrity relates to the role of faults (see Tasks 2.1 and 2.3). Our research will shed light into the activation of pre-existing faults, the formation of new fractures, and their hydraulic properties, especially with regard to multiphase flow. Vertical filtration of CO_2 through the caprock (either dissolved in brine or in its own separate phase) is not always detrimental. If the leakage is gradual and not catastrophic, and does not reach the drinking water aquifers, vertical loss of CO_2 into shallower formations is an effective mechanism to limit the lateral migration of CO_2.

Estimation of CO2 storage capacity and injectivity. We will apply the proposed models using data from specific geologic basins (Task 1); results will lead to more accurate capacity estimates, based on fluid flow dynamics, rather than *ad hoc* assumptions of an overall "efficiency factor" [Bachu et al., 2007; DOE-NETL, 2007]. In recent work, we have taken preliminary steps in this direction [Juanes et al., 2010; Szulczewski and Juanes, 2009], where we identified the efficiency factor for capillary trapping at the basin scale. Our research will give a new perspective on storage capacity and injectivity at the basin scale—a basin-specific estimation based on analytical fluid-dynamic models—with particular application to Abu Dhabi deep regional aquifers.

Risk assessment methodologies for uncertainty quantification. The ability of obtaining analytical solutions is essential, because it permits rapid sampling of the uncertainty in the input parameters, and thus more robust risk assessment. This principle has been used recently to perform uncertainty quantification of leakage through hundreds of wells across several geologic layers [Nordbotten et al., 2009]. For each geologic basin, we will break down the risk assessment methodology into four subtasks: (1) Sensitivity analysis on model parameters; (2) Determine probability distributions for parameters with greatest impact; (3) Uncertainty quantification; and (4) Estimates of risk of CO_2 leakage. These simplified, super-fast analytical forward models will also be instrumental for the design of monitoring techniques, as these models provide first-order estimates of pressure evolution and CO_2 plume footprint.

3.2 Comparison of Analytical Models with Reservoir Simulation Models (MS, RJ)

The concept of basin-scale modeling described in Task 3.1 is motivated by large-scale injection of CO_2, and the mathematical/analytical approach offers enormous advantages in terms of understanding the key aspects of the problem and providing ultrafast simulation models for robust uncertainty quantification. Yet, the proposed approach is not free of risks.

The first category of risks is that of limitations associated with the mathematical models to be developed—which are necessarily simplified to admit analytical solutions. The model neglects aquifer heterogeneity, which will often increase the migration distance of the CO_2

plume. The gravity tongue, however, is a persistent feature of the flow that is likely to dominate the picture, regardless of heterogeneity. Given the large distances involved, it is conceivable that the plume will sample a high fraction of the heterogeneity of the formation, so that effective representative parameters can be defined. The models will assume a sharp interface approximation. In reality, due to the finite size of the transition region between the CO_2 plume and the formation brine, the plume may become immobile before it reaches zero thickness—from this point of view, our estimates will be on the safe side. Therefore, we propose to mitigate this source of risk by comparing predictions from the simplified analytical models with those of numerical flow simulation models, either developed by the Stanford group, or using a commercial reservoir simulator such as GEM (by the Computer Modeling Group).

Another important source of modeling error (not just parameter uncertainty) is related to caprock processes, such as: location and conditions for activation of pre-existing faults, fracturing of the caprock, and how to incorporate leakage after caprock integrity is compromised. The caprock of aquifers will often have undulations, the geometry of which is poorly constrained without seismic surveys. This will lead to additional stratigraphic trapping, resulting in smaller migration distances. Another set of risks comes from the application of the models to individual basins. As it is true for virtually any mathematical model, the models developed here must be applied within reasonable bounds, and compromises must be made. It is likely that some formations will fall outside the range of applicability of the models. To overcome some of these risks associated with the interaction of the migrating plume with the host formation and the sealing caprock, we plan to inform the analytical models with the results from computational models of coupled flow and geomechanics, developed under Task 2.1, or evaluated using a commercial simulator such as GEM (by the Computer Modeling Group).

4. Comprehensive Monitoring Program

A comprehensive, quantitative understanding of the reservoir is required both prior to and during the injection of CO_2. A set of complete predictive models must be developed that describe flow and geomechanical processes within the reservoir as well as connections between measurements and reservoir states. By combining model predictions and measurements we will be in a position to generate predictions that are physically realistic and also consistent with field data. The ADCO CCS project requires multiple kinds of observations, each sensitive to different physical and chemical properties acting over different spatial and temporal scales. The procedure linking observations and models will be an ensemble *data assimilation* algorithm that will use the models to generate a set of possible system descriptions, all consistent with observations. This makes it possible to design robust operating and monitoring strategies that can work well over a range of conditions.

This section begins with a summary of our overall approach to monitoring, which relies on a site-specific data assimilation algorithm. Then it provides more detailed discussions of

the particular sensing technologies and measurement models that we believe should be considered for incorporation in the monitoring program.

4.1 Data Assimilation and Monitoring Design (DM)

4.1.1 Introduction

Mathematical modeling of the subsurface environment provides a useful way to assess candidate sites for carbon storage and to design effective carbon sequestration strategies. In particular, different sites and operating alternatives can be analyzed by varying the model inputs that characterize the target reservoir, as well as control variables, such as injection well locations, depths, and schedules. This is a classical application of modeling technology that relies strongly on having access to a physically realistic model. Here we consider two other important modeling applications that are particularly relevant to the UAE CCS project: i) using models to merge and interpret data (a process often called "data assimilation") and ii) using models and data together to design cost-effective real-time monitoring strategies. To understand how models relate to data assimilation and monitoring it is necessary to briefly consider why we should integrate modeling and data collection activities in a CCS monitoring program.

In the absence of a predictive model, monitoring is the only way to assess the performance of a carbon sequestration project. The disadvantage of a monitoring-only approach to performance assessment is that we are using the real world as a laboratory. If a sequestration strategy works well this is fine but, if it does not, the consequences could be undesirable and difficult to correct. That is why we use models (and small-scale lab and field experiments) to predict performance in advance. By trying out different alternatives in a controlled modeling experiment we can find designs that are likely to meet project specifications.

The subsurface models we use to identify promising sequestration strategies, however, are not perfect, since we do not have complete information on geological structure, flow properties, and other relevant environmental variables. If we had a perfect model and were completely confident in its predictions, there would be no need to monitor performance because we would know the outcome with certainty. The real-world needs of the UAE CSS project require a balance between the extremes of relying only on monitoring and relying only on modeling. We can construct models that give us useful information about the likely performance of a candidate reservoir but we also need to monitor since the model predictions are not, in fact, certain. The most realistic and scientifically defensible approach to performance assessment of CO2 sequestration is to integrate modeling and monitoring.

We will follow such an integrated approach here. First, we will develop data assimilation procedures (or work flows) that use models to combine measurements for performance assessment. Then we will expand these procedures to include a real-time monitoring design capability. Real-time design enables the CO2 monitoring program to evolve as new measurements become available, using models that are continually updated. In both cases

we will use models developed in other project tasks so that assumptions and results are consistent across the project. This integrated approach to monitoring and operations has a long and successful history in meteorology, where complex mathematical models are routinely used to merge (or assimilate) diverse measurements for forecasting and also to design "adaptive observation" programs.

Here, we will build on our experience with data assimilation and monitoring methods in meteorology, hydrology, and, most important, petroleum engineering [Moore and McLaughlin, 1978; Graham and McLaughlin, 1989; McLaughlin et al., 1993; McLaughlin, 2002; 2007; Zhou et al., 2006]. Over the past several years we have contributed to the growing field of real-time petroleum reservoir management by developing modeling, estimation, and control strategies to make best use of observations collected before and during secondary recovery operations [Jafarpour and McLaughlin, 2008, 2009, 2009a]. This work provides an excellent basis and starting point for a focused design of the monitoring program.

The following subsections briefly describe the concepts that we will use to develop a real-time modeling/monitoring program for this carbon sequestration project as well as the specific tasks we will undertake.

4.1.2 Approach

Bayesian estimation theory provides a useful framework for integrating models and measurements and for designing cost-effective monitoring programs [Jazwinski, 1970; Box and Tiao, 1973; Graham and McLaughlin; 1989; McLaughlin, 2007]. It recognizes that the key objective of monitoring is to reduce uncertainty about a specified set of output variables (y) that characterize the system of interest. An example relevant to sequestration is the cumulative CO_2 discharge at a specified control point integrated over a specified time interval. Models of the reservoir describe how such output variables depend on a vector of input variables (u). The inputs include uncertain structural, flow, mechanical, and transport properties as well as specified control variables such as CO_2 injection rates.

Observations of the system are available in the form of a measurement vector (z), which includes scattered borehole observations of structural and flow properties, pressure and CO_2 measurements at monitoring wells, and broader coverage seismic, surface deformation, and gravity measurements. The measurements can be taken at different times and locations and can have different resolution, coverage, and accuracy. Of particular interest for this project are the following types of measurements, all discussed in more detail in Sections 4.2 through 4.9:

- Fluid pressures, fluxes, and composition in injection and a limited number of monitoring wells;
- Active seismic measurements ranging from cross-well to VSP to 4-D surface seismics;
- Passive seismic measurements, including measurements that rely on induced seismicity;

- Geodetic measurements, including data from (existing or newly deployed) GPS stations and InSAR surveys;
- Time-lapse microgravity and/or gradiometry measurements;
- Electrical resistance tomography;
- Geochemical and surface monitoring of atmospheric CO2 concentrations.

These measurements represent a suite of possible sensing technologies that we intend to investigate for this particular application. Some of these may prove to be technically inappropriate or too expensive for the conditions at the UAE. An assessment of the most promising sensing technologies will be an ongoing task of our project, carried out as performance and cost data become available. Further details are dicussed below.

One of the key features of the Bayesian approach is the recognition that model predictions and measurements are both uncertain. This is expressed mathematically in terms of probability densities that describe the ranges of possible variable values. The basic idea can be conveyed by comparing classical deterministic and probabilistic descriptions of the variables of interest for CCS. Inputs and outputs are related as follows:

Deterministic system model   Probabilistic system model

$$y = g(u) \qquad\qquad p(y) = \int p(y\,|\,u)p(u)\,du \qquad\qquad (4.1.1)$$

The deterministic system model $g(\cdot)$ derives a predicted system output y from a specified input u. The actual output will generally differ from the prediction since the model is imperfect. The probabilistic model does not attempt to predict the true output, but instead characterizes the range of possible output values with the probability density $p(y)$. Since the uncertainty in y largely results from uncertainty in u, the input is characterized by a range of values through the input probability, $p(u)$. The connection between the input and output probabilities is defined by the conditional probability, $p(y\,|\,u)$, which is derived from the system model, $g(u)$, and probabilistic assumptions about model errors.

A similar set of deterministic and probabilistic descriptions applies to the measurements:

Deterministic measurement model   Probabilistic measurement model

$$z = h(u,\alpha) \qquad\qquad \boxed{} \qquad\qquad (4.1.2)$$

In this case the deterministic measurement model, $\boxed{}$, describes the measurement that we would expect to obtain with an input, u, and a particular sensor and monitoring strategy described by a vector of measurement design parameters α. In our application, this vector will include design parameters for each of the eight or nine sensing technologies considered. The design parameters for each technology include information about the accuracy, coverage, time, location, frequency, and resolution of each measurement. A particular sensing alternative can be removed from consideration by omitting it and its design parameters from the z and α vectors.

The actual measurement obtained in the field will generally differ from the deterministic prediction since the measurement model is imperfect. The probabilistic measurement model does not attempt to predict a single measured value, but instead characterizes the range of possible values with the conditional probability $p(z \mid y)$. This probability is derived from the deterministic system and measurement models, $g(u)$ and $\boxed{\times}$, and from probabilistic assumptions about measurement errors.

The Bayesian approach provides a quantitative way to account for the extra information that the measurements provide about the system outputs. This is accomplished through Bayes theorem, which describes the range of output values that we can expect if we observe a particular measurement, $z*$ with associated design parameters $\alpha*$:

$$p(y \mid z*,\alpha*) = \frac{p(z* \mid y,\alpha*)p(y)}{\int p(z* \mid y,\alpha*)p(y)dy} \qquad (4.1.3)$$

Since $z*$ and $\alpha*$ are known, the probability $p(z* \mid y,\alpha*)$ (also called the likelihood) is now only a function of the uncertain output, y. The conditional density, $p(y \mid z*,\alpha*)$, obtained from Bayes theorem gives an updated description of the likely range of possible output values if $z*$ is observed. This density forms the basis for Bayesian estimation methods. For example, it is common to adopt as an updated estimate of y the value that maximizes $p(y \mid z*,\alpha*)$. This estimate depends on the deterministic model through the prior probability and likelihood but it also depends on the measurement $z*$.

The additional information provided by the observation $z*$ can be assessed by comparing the prior probability, $p(y)$, and the updated probability, $p(y \mid z*)$. The concept is illustrated in Figure 4.1.1, which shows how the distribution of possible cumulative CO2 values changes after incorporation of a new set of field observations. Note how the updated probability narrows around the highest probability value. A convenient measure of the associated information gain is the relative entropy between the prior and updated probabilities:

$$d(z*,\alpha*) = \int p(y \mid z*,\alpha*) \ln \frac{p(y \mid z*,\alpha*)}{p(y)} dy \qquad (4.1.4)$$

This expression gives the value of a measurement, $z*$, that has already been collected. For real-time monitoring design we need to evaluate the information gain provided by a proposed additional measurement, z', which is generally characterized by a different set of associated design parameters α'. The value of z' is currently unknown (since it will be observed in the future) but the value of α' is specified since it defines the properties of the proposed measurement. In this case, we work with the possible range of z' values rather than a particular observed value. The expected information gain obtained by adding z' to an existing measurement $z*$ is the average gain taken over all possible z' values:

$$\overline{d(z^*,\alpha^*,z',\alpha')} = \int p(y \mid z^*,\alpha^*,z',\alpha')\ln\frac{p(y \mid z^*,\alpha^*,z',\alpha')}{p(y \mid z^*,\alpha^*)}\, p(z' \mid \alpha')dy\,dz' \qquad (4.1.5)$$

The unconditional measurement probability, $p(z')$, is obtained from:

$$\boxed{} \qquad (4.1.6)$$

The probability $p(z' \mid u)$ is derived from the deterministic system model $g(u)$, the deterministic measurement model $z' = h'(u,\alpha')$ for z', and probabilistic assumptions about the z' measurement errors.

Equation (4.1.5) (or similar expressions based on other performance measures) provides a quantitative way to assess the information gain provided by a new measurement with properties defined by the z' measurement model. By adjusting this model we can determine how information gain will vary as we change the measurement technologies used and the design paramaters included in the vector α.
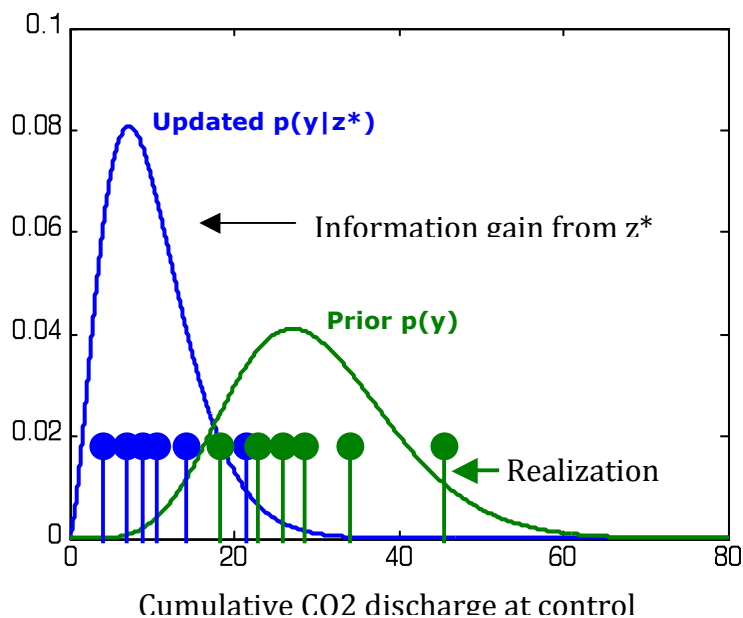
Figure 4.1.1: Typical set of prior (green) and updated (blue) probability distributions for a CO2 sequestration performance measure. Updated distribution incorporates new measurements and has reduced spread around a lower "most probable" value. Vertical lines indicate a few realizations that correspond to the two probability distributions. Each realization is obtained from a model simulation with a different set of inputs, corresponding to different geological structures and flow conditions. Ensemble methods use realizations to show display the range of possible outcomes and to describe probabilities.

A measurement strategy defined by a given α also has an associated cost $c(\alpha)$. The tradeoff between information gained and cost can be evaluated over a range of design options with a classical Pareto tradeoff curve [Steuer, 1986]. A hypothetical example is shown in Figure 4.1.2, which compares the information gain and cost associated with several proposed configurations for a new set of measurements (note the reversed cost axis). Designs below and to the left of the smooth curve are inferior (i.e. provide less information and/or are more expensive) to those on this curve. In a monitoring design program attention should be focused on strategies along the curve, which displays the tradeoff between information and cost.

Information cost tradeoffs can be used to decide whether to include promising new types of measurements (because they are likely to provide additional information for a reasonable cost) or whether to drop inappropriate candidate sensing technologies (because the information they are likely to provide does not justify the cost). Analytical techniques such as those described above are designed to provide useful information for decision-making. Ultimately, those responsible for the UAE CCS monitoring program need to decide how it should be managed. Actual monitoring decisions must rely on good judgment that considers a number of different information sources Bayesian analysis makes this process more quantitative and well informed.
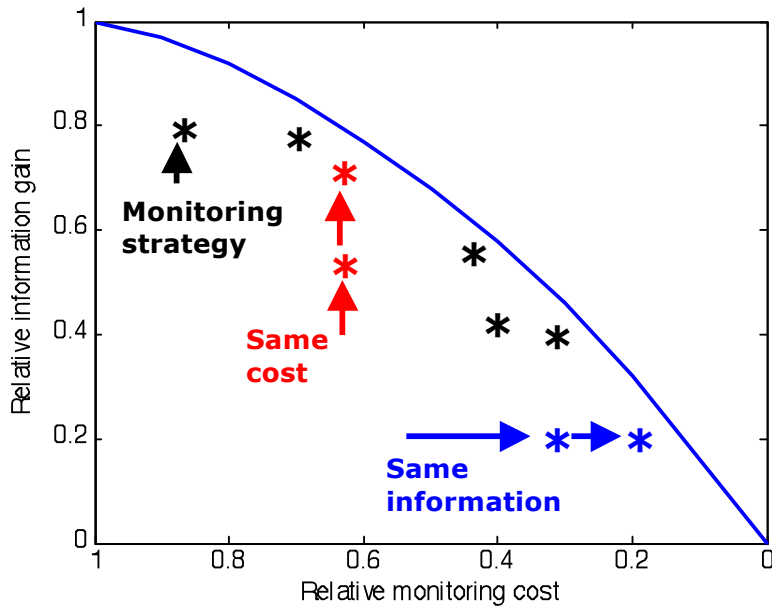
Figure 4.1.2: Information vs cost tradeoff for some representative monitoring strategies, indicated with asterisks and defined by design parameters in the vector α for each strategy. Strategies on (or near) the solid blue line give the most information gain for a given cost, or incur the least cost for a given information gain.

The Bayesian framework provides an elegant and quite general starting point for monitoring design. However, many issues need to be worked out to make it a practical tool

for carbon sequestration applications. These form the basis for our implementation plan, outlined in the next section. The important points to take from the Bayesian perspective are that i) it uses physically-based mathematical models to *integrate information* from many different data sources, and ii) it quantifies the information value of new measurements, providing a rigorous basis for monitoring design.

4.1.3 Application to CO2 Sequestration
The ideas summarized above are widely used in many fields, including petroleum engineering. We will adapt these Bayesian ideas to the special needs of the UAE CCS problem. This will be our major focus. Some of the distinctive issues to be considered for this carbon sequestration application include:

i) Uncertainties about geological structure, the flow and mechanical properties of the candidate reservoirs, and the field measurements used for updating are difficult to describe with classical input and measurement error probability densities.

ii) The output probability densities required in the Bayesian approach are difficult to derive unless overly restrictive and unrealistic assumptions (e.g. linear models and normally distributed inputs) are made. For practical applications these densities need to be replaced by more computationally manageable alternatives.

iii) The deterministic system and measurement models relevant to the CO2 sequestration application are generally high dimensional, nonlinear, and expensive to develop and use. This means that probabilistic data assimilation or monitoring design procedures must make very efficient use of all models, using a relatively small number of model simulations to generate realizations and assess sensitivities

There are a number of things that can be done to address these issues. The most important is to use an ensemble approach to approximate the probabilities required by the Bayesian framework [Arulampalam, 2002; Evensen, 2003;2004]. In practice, this means that probabilities are replaced by many realizations (i.e. geological structures, CO2 contours, etc.) that convey the range of possible conditions at the site. When measurements are incorporated the realizations are modified accordingly. This is illustrated in Figure 4.1.1, which shows, with vertical lines, a few prior and updated realizations that approximate prior and updated probability distributions.

An ensemble approach to the CO2 sequestration problem can work with geologically realistic realizations that "look like" real reservoirs. There is no need to restrict the approach to artificial realizations that conform to classical probability distributions. In addition, the ensemble approach replaces difficult-to-interpret multidimensional probability densities with informative images of possible reservoir structures, CO2 distributions, and sensor outputs. This is why ensemble methods are increasingly becoming the method of choice for analyzing complex geoscience problems. We have, for example, recently published several papers that describe how multiphase transport through channelized fluvial deposits can be analyzed with ensemble methods [Jafarpour and McLaughlin, 2008, 2009, 2009a].

Widely used ensemble estimation methods include Markov Chain Monte Carlo (MCMC) simulation, importance sampling (IS), and ensemble Kalman filtering (EnKF) [McLaughlin, 2007]. We believe that the ensemble Kalman filtering option is most appropriate for the UAE CO_2 sequestration application , primarily because i) it is feasible to use for high dimensional nonlinear problems, and ii) it can be set up and applied quickly [Evensen, 2003;2004]. These capabilities will enable us to focus on site application and interpretation of results rather than algorithm development.

A useful approach to the issue of model computational effort and efficiency is to replace a large and complex flow or transport by a smaller "reduced-order" model that is derived from the larger model. This reduced-order model is then used to generate the multiple realizations needed in the ensemble approach to data assimilation and monitoring design. Since the reduced-order model is "trained" with a full-size model set up for a specific site it incorporates local information and can often effectively reproduce the response of the full model at a fraction of the computational cost. We have been developing reduced-order versions of multiphase flow models for use in ensemble control strategies for secondary recovery. These models rely on advanced methods from control theory, electronics, and image processing. In all these fields, as in carbon sequestration, there are incentives to improve computational efficiency without sacrificing accuracy. The methods and insights developed in our ongoing secondary recovery work are directly relevant to this project.

Figure 4.1.3 illustrates the type of information available from a real-time subsurface transport monitoring design procedure based on Kalman filtering [Graham and McLaughlin, 1989]. This example compares plan views of true and estimated (most probable) solute plumes traveling downstream from a point. An adaptive monitoring network of several wells provides measurements for a Bayesian data assimilation procedure that relies on a flow and transport model. Methods similar to those outlined above are used to progressively add wells to the initial monitoring network. The monitoring network evolves in response to information provided by the data assimilation procedure, inserting more wells in the direction of plume movement, at locations where new information is most beneficial.
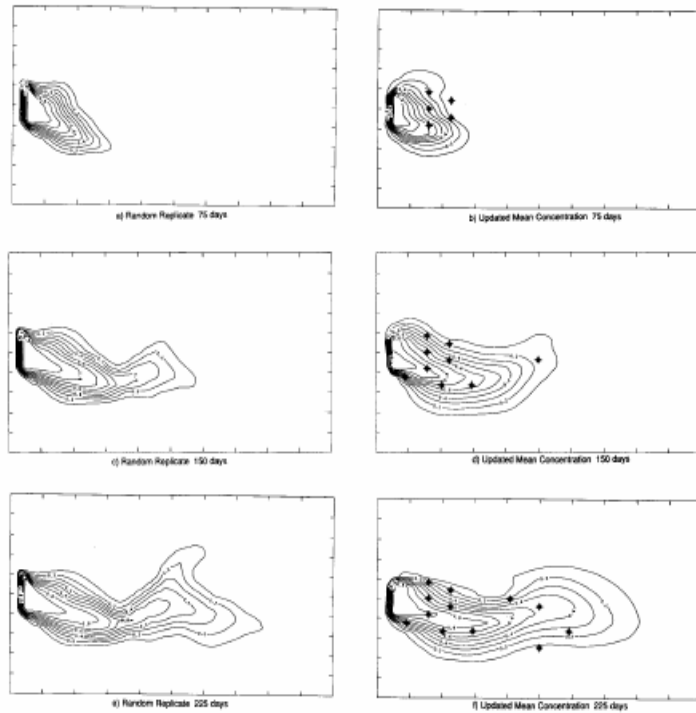
Figure 4.1.3: Temporal evolution of a subsurface plume monitored in real-time. Left side shows synthetically generated true plume at 75, 150, 225 days (top to bottom). Right side shows corresponding plume estimates derived from concentration and pressure observations at monitoring wells (indicated by crossed circles). New well locations added at each time are inserted in areas of maximum uncertainty. Note how initially symmetrical sampling network at 75 days expands towards the lower part of region as measurements indicate that the plume is moving below the centerline (from Graham and McLaughlin, 1989).

We have made a number of significant advances since this real-time monitoring design work was originally published. Extensions include provision for three-dimensional multiphase flow in channelized media and computational refinements that make it feasible to apply the ideas to very large problems. Here, we propose to combine the sound theoretical foundations of the Bayesian approach with the practical methods we have developed over the last few years. This project offers an exceptional opportunity to implement an informative and cost-effective monitoring strategy that will support successful operation of a state-of-the-art CCS system.

4.1.4 Tasks and Implementation Plan

Much of our effort will be devoted to customizing the data assimilation and monitoring design concepts outlined above to the special needs of this project. This is reflected in the task statements given below. These outline a progressive approach that relies on input from other project tasks and from other groups working on the UAE CO2 sequestration project. The research plan also provides updates and deliverables at frequent intervals.

Task 1: Assess monitoring needs

This task is designed to insure that our approach to the UAE CO2 sequestration data assimilation and monitoring design meets larger project needs and is relevant to site characteristics, operational objectives, and budget constraints. Task 1 will include a thorough review of site information and plans, operational guidelines, and proposed sensing technologies (including those described in Subsections 4.2-4.9). This will involve close coordination with project investigators working on both modeling and sensing. The results of this task will be summarized in a report that specifies monitoring objectives and constraints and indicates how these factors will be considered in the development of a data assimilation and monitoring design workflow.

Task 2: Develop and test data assimilation procedures
This task will formulate, develop, and test a site-specific data assimilation procedure. The procedure will be tested with available site data to insure that the proposed procedures provide a satisfactory site characterization relevant to the Abu Dhabi project objectives. Our approach will rely on ensemble methods that use reduced-order modeling to improve computational efficiency. The primary outputs of the procedure will be updated realizations that show possible present and future subsurface CO2 configurations compatible with measurements and with physical constraints derived from models of the site. These realizations can be displayed to guide operational decisions. They can also be used to construct probability densities and other measures relevant for performance assessment and monitoring design. Prior and updated realizations will be derived primarily with ensemble Kalman filters that rely on reduced-order models. Other more computationally expensive data assimilation methods, such as reduced-order importance sampling, will also be examined to provide a basis for comparison.

The emphasis in this task will be to integrate data assimilation into the workflow envisioned for the larger UAE project. The specific methods and models used and variables considered will be adjusted to insure that the data assimilation procedure is compatible with other project components. The results of this task will be summarized in a technical report designed to support project workflow development. Associated software will be provided, as needed, and the results of the data assimilation tests will be summarized.

Task 3: Develop and monitoring design procedures
This task will formulate, develop, and test a real-time monitoring design procedure that relies on the data assimilation procedure developed in Task 2. Monitoring performance measures will be derived in real-time from the latest realizations provided by the data assimilation procedure. These measures will indicate the relative benefit of a specified set of new measurements (for assessing both current and future conditions). The monitoring performance measures will rely on measurement models that describe the distinctive characteristics of observing systems and data collection procedures to be used at the UAE site.

The specific format of the monitoring design procedure will be worked out with potential users in order to insure that the information provided and the methods used to investigate monitoring alternatives are consistent with the overall project workflow. The procedure will be tested with available field data (or, when none is available, with synthetic model-

generated data). The results of this task will be summarized in a technical report designed to support project workflow development. Associated software will be provided, as needed, and the results of the monitoring design tests will be summarized.

Task 4: Evaluate and screen proposed sensing technologies
This is an ongoing task designed to determine which mix of sensing technologies is best suited for the UAE CCS application. The technologies to be considered will include those described in Sections 4.2 through 4.9 as well as any other promising options that may arise during the project. In the early stages of the project this task will include compilation of existing performance and cost data for each technology. The assessment will be periodically updated throughout the remainder of the project as new field test and simulation results become available. Each technology will be evaluated in terms of the information it provides about important performance variables as well as its implementation cost, using the methods developed in Task 3. Tradeoff curves such as the one illustrated in Figure 4.1.2 will be used to compare competing sensing alternatives, recognizing that different technologies provide qualitatively different types of information (i.e. multiple measures of information gain are required).

Task 5: Technology transfer
This task will focus on the practical implementation of data assimilation and monitoring design procedures developed at MIT. Much of the effort will be devoted to insuring that these procedures meet the broader needs of the UAE project and that they can be readily used by the appropriate staff members. The technology transfer will produce a written implementation report, web-based documentation, and a short course at the beginning of the task that will review methods and identify specific technology transfer needs.

4.2. Pressure variations in wells (BH)

Injecting CO2 into saline aquifers requires generating elevated pressures. The resulting pressure gradients drive a halo of brine at elevated pressure ahead of the CO2 front. The pressure required to inject CO2 increases in proportion to the injected flux of CO2 and is inversely proportional to the permeability. Measurements of flow rates, pressure variations, and temperature within the injection wells are essential in order to allow the useful modeling of the formation response. Measurements of fluid pressures within monitoring wells provide direct tests of the flow models. In addition, because the pressure in the brine increases far in advance of the CO2 front, monitoring pressure, in combination with flow models, provides early warning of any breakthrough of CO2. Measurement of fluid compositions is important for comparison to the predictions of the experiments described in 2.2.2. Finally, measurements of composition provide direct observations of breakthrough, as was observed at In Salah [e.g., *Ringrose et al.*, 2009].

If drilling of a substantial number of monitoring wells were required, such pressure measurements would be very expensive. If the reservoir has substantial variations in permeability, the risk that the location of a monitoring well is not representative, or even provides misleading information, is substantial. In addition, drilling new monitoring wells

risks degrading the seal integrity of the reservoir. Leaving existing wells accessible for measurements also presents the risk of leakage.

As discussed in 4.1, the expense and risk of direct measurement of pressure in monitoring wells should be considered in light of the uniqueness of the information that they would provide, relative to other monitoring techniques, as well as on how heterogeneous the reservoir is believed to be. The locations of additional monitoring wells should be chosen based on where the additional information provided is most diagnostic based on the current assessment of the uncertainty in the state of the model (e.g., Figure 4.1.3).

Detailed Work Plan
Work on this task will comprise a continuous low-level effort during the first 3 years, followed by a more intense effort in the final year, culminating in documentation of recommendations. Professor Hager will take responsibility for these tasks.

a) (Years 1-3) Extend our literature search on field results to date.
b) (Year 1) Collect information about existing wells that might be converted to monitoring wells.
c) (Years 1-3) Assure that the data assimilation procedure developed in 4.1 includes consideration of measurements of monitoring well pressure and fluid composition.
c) (Year 4) Address formally the resolving power of pressure and composition measurements in the context of other monitoring measurements.
d) (Year 4) Provide a cost-benefit analysis of these (possibly expensive) measurements.

4.3 Active Seismic (MF, AM)

4.3.1 4D Imaging

4.3.1.1 State of the Art
Active source approaches for change detection are usually implemented by collecting data at two different times, first before the change is considered to have occurred and second after the change is anticipated. The differences in the two datasets are quantified to infer the changes that have occurred in the Earth's subsurface. The two datasets are often processed independently to determine images of the subsurface properties at the two times. The differences in the resulting images are then calculated, through a combination of matching imaged reflectors that are assumed to be unchanged and adaptive subtraction of the images. Past studies using this method have been done for CO2 sequestration [*Lumley,* 2010*; Lumley et al.,* 2003], with some success.

For application to this project, we would require at least two high-quality data sets, one collected before the injection and one once the injection has been under way for some time. (Without these data, we will be limited to theoretical developments.) There are several options for the type of data that could be collected and processed, with corresponding changes in the amount of information that would be recovered. To determine the lateral extent of the reservoir and to have sensitivity to leakage over the largest area, full 3D

acquisition before and after injection should be undertaken. Test results could be obtained with 2D lines; however the reduction in dimension will significantly reduce both the extent and accuracy of the obtained results. Another option is to collect Vertical Seismic Profiling (VSP) data, which involves the use of borehole receivers that record seismic sources located on the surface. Analysis of VSP data gives some 3D information in the vicinity of the well containing the receivers and facilitates imaging below complicated overburden as well as increasing the frequency of the probing wavefield and thus the resolution of the images. Crosswell tomography further reduces the dependency of the resulting images on overburden structures and further increases the resolution (via the higher frequency content) of the recovered tomographic images, at the expense of a reduction in dimension to 2D and a narrowing of the study area to that between the two wells. The methodology we propose to develop is applicable to any of these data types; the sooner a decision is made in consultation with PI as to what type of data they will collect, the more we can tune our developments to a specific geometry. Part of our work will be to develop a quantitative approach for determining the value of the various types of data to answering the types of questions that are determined to be significant to assessing Carbon Sequestration. This will aid in answering the business aspect questions posed by the sequestration of $CO2$. Although we will undertake this work early in the proposed work timeline, we do not recommend that a decision be held until this work is complete as it is of fundamental importance to the rest of the study that high-quality data be available in a timely manner. One of the largest difficulties with the 'image and subtract' method of 4D processing is the difficulty in collecting truly repeatable data and thus the instabilities in subtracting the data. The lack of repeatability will be of particular importance in this case because the acquisition is expected to be over land. Although this proposal aims to develop methods for which repeatability is less of an issue, the best possible results will be obtained if care is taken to collect the data in a repeatable way. For example, in steam injection studies for heavy oil on land in Canada [*Byerley et al.,* 2009], permanently in place receivers and downhole explosive sources greatly improved the repeatability of the 4D data set.

The resolution of seismic imaging is a function of the wavelength of the waves that sample the region being imaged. With good acquisition aperture, and good illumination of the region of interest, the resolution of seismic migration imaging in the horizontal direction is generally taken to be a quarter of a wavelength. Vertical resolution is on the order of a wavelength. Since wavelength is inversely proportional to frequency, the higher the frequency, the smaller the wavelength. Since attenuation of seismic waves decreases the signal strength of high-frequency waves more rapidly with increasing propagating distance than those at lower frequency, imaging cannot be conducted at arbitrarily high frequencies. As an example, for targets at depths of 2 km, with velocities of 3 km/s, typical imaging frequencies for surface seismic (3D and 4D acquisitions) might be 50 Hz. This gives a wavelength of (wavelength = velocity/frequency) of 60 m so the horizontal resolution is of the order of 15 m if the region has good illumination (waves from many source/receiver pairs sampling each point in the region). Overlaying geological structure may limit illumination (basically the ranges of sources and receivers for which seismic waves sample the region of interest) and reduce the resolution (more discussion of this can be found in Fehler et al., 2005; Wu et al., 2005). Using methods that employ sensors in boreholes, like crosswell and VSP, can increase the resolution but the region of interrogation is confined to

be near the wellbores. Resolution of several borehole methods and the regions over which they sample is discussed by *Cheng* [2008]. Challenges in the repeatability of seismic measurements may limit the resolution of the detection of changes accompanying the injection and migration of CO2.

The main goal of seismic monitoring will be to detect changes in the reservoir and surrounding region that are caused by the injection and migration of CO2. The interpretation of these changes will require a model of how the physical changes *in situ* influence the measured seismic properties that we propose to measure. The model used for interpretation may be a fluid-substitution model like the widely-used Gassmann [1951] model or some variant of that model that is more appropriate for CO2 injections. A complete interpretation of the observed changes must be undertaken within the context of a geomechanical/fluid flow model, as is discussed elsewhere in this proposal.

We propose to investigate two different aspects of the CO2 sequestration problem as part of this project. First we will develop waveform inversion methods that are less sensitive to differences in the acquisition footprint than traditional methods. Second, we will develop a low-cost alarm system that can be used to alert to changes in the model and give a rough localization of these changes. These two aspects are discussed in the following sections.

4.3.1.2 Double-difference Elastic Tomography
Recently, *Denli and Huang* [2009] proposed a *Double Difference* elastic waveform tomography approach, which has its roots in the successful double-difference traveltime tomography approach used in earthquake studies [*Zhang and Thurber,* 2003]. The idea is that by subtracting the two acquired datasets rather than treating them separately, one isolates only the part of the data that results from changes in the medium properties. Subtracting the two datasets minimizes the impact of unknown structure that does not change on the resulting difference data. The difference dataset is then processed to find a perturbation of the initial model (found with the baseline data set) that is the change that is sought. The implementation of the method goes as follows: (1) condition the two datasets to correct for small differences in data acquisition parameters between the two datasets. This correction, which is extremely important and difficult to accomplish, can be implemented by spectral normalization or by finding a transfer function between portions of the two datasets that sample only suspected unperturbed portions of the Earth (the shallowest layers, for example). (2) The corrected dataset is subtracted from the initial dataset to obtain the difference in the Earth response between the times that the two datasets were collected. (3) The first dataset is imaged to find an initial, unperturbed model. (4) The difference dataset is imaged using the unperturbed model as a starting point and differences in this model are found. Denli and Huang [2009] proposed the double-difference method and implemented a simple waveform inversion scheme to test the method. We have already begun to collaborate with Denli and Huang to refine all four steps of the method, beginning from the refinement of the algorithm to improve steps (3) and (4). We would propose to spend the first 1-2 years of this project continuing to improve and refine this algorithm to improve the robustness to errors in the initial velocity model, resolution across different frequencies, and the efficiency of computation. This work can be done with synthetic data sets, generated at MIT, as well as with ultrasonic

tomographic data collected in the lab. However, the next stage of the work in which these ideas are applied to data collected by PI in Abu Dhabi will be easier if synthetic models of the actual reservoir can be obtained from PI. We will work with Prof Juanes to include realistic CO2 structures in the reservoir, based on the reservoir characterization of target Abu Dhabi reservoirs performed by the Petroleum Institute (Task 1). The third and fourth year of the project will be devoted to the application of these techniques to the field data set(s) as well as to the interpretation of the results, jointly with the results of other parts of this project, and the transfer of technology to researchers at Masdar and PI. This methodology is appropriate for VSP, surface seismic or crosswell tomography.

4.3.1.3 Detailed Work Plan
Year 1: We have already begun to develop the method. During the first year, we will continue to improve the method and test it on simulated data. Improvements will be to include a *total variation* constraint that will allow improved determination of locations where there are strong discontinuities in the changes in the reservoir. We will also investigate the application of a conjugate gradient solver to give a more robust solution to the tomography problem.

Year 2: Continued development and improvements to the tomography method. More tests with simulated data and some data from a CO2 injection that we will obtain from our collaborator at Los Alamos National Laboratory. We will begin to look at the issue of data conditioning approaches to minimize the influence of slight changes in the acquisition of multiple field datasets at differing times.

Year 3: Adaptation of the method to field data that we anticipate to be collected at the field site in Abu Dhabi. Tests on actual data if they exist. Tests using surrogate models of the field site that are jointly developed with Prof. Juanes. Begin to develop and evaluate methodology for interpretation of measurements of geophysical changes in terms of actual reservoir changes. This work will be done in collaboration with Prof. McLaughlin.

Year 4: Application of the method to field data. Technology transfer to Abu Dhabi.

4.3.2 Alarm System

4.3.2.1 State of the Art
Whether surface seismic, VSP or crosswell tomography methods are used for imaging of the reservoir, the associated data sets are expensive and time-consuming to collect. An efficient way of estimating whether or not the reservoir or cap rock has changed sufficiently to warrant additional collections of this sort of data is necessary to avoid incurring un-needed delays and costs. Some work has been done on developing these sorts of tools [*Zhou et al.,* 2010], but there has been little work done on the specific application to CO2 sequestration of methods for detecting and localizing small changes. This work builds upon ideas of so-called coda-wave interferometry in which two waveforms from identical experiments are correlated after scattering many times in the medium of interest to amplify the effects of small changes [*Poupinet et al.*, 1984; *Roberts et al.*, 1992; *Snieder et al.*,

2002]. Such waves can sample considerable portions of the reservoir allowing a small amount of data to be used to detect whether or not changes have occurred. In the mathematics community, work using the related concept of time reversal, in which a signal is recorded, time-reversed and sent back through the material of interest where it will focus, has been done [*Fink*, 1992].   How focused the signal will be depends on what part of the model the waves travel through and how much scattering is present in different regions of the model. By controlling what part of the recorded waveform is time-reversed, *Fouque and Poliannikov* [2006] show that the location of changes in scattering properties can be determined, at least in 1D idealized situations. There is evidence that in reservoirs with typical heterogeneities [*Lumley*, 2010], CO2 does not form a uniform infiltration zone but instead generates several layers that are expected to generate significant scattering [*Arts et al.*, 2004].   Even in homogeneous materials, when displacing water with CO2, we would expect significant small-scale structures to develop, such as viscous fingers and thin layers from gravity segregation [*Cinar et al.*, 2010; *Hesse et al.*, 2008; *Juanes and MacMinn*, 2008; *Juanes et al.*, 2010]. This makes CO2 sequestration an ideal target for interferometric techniques, such as those mentioned above, that exploit multiple-scattering to determine whether or not the location and distribution of CO2 changes over time. Significant changes could then result in the use of high-resolution techniques such as cross-well, VSP or surface seismics to further refine the understanding of where the changes occurred and precisely what has changed.

4.3.2.2 Proposed Work
We have begun work to extend the results of *Fouque and Poliannikov* [2006] so that they may be applied to more general situations such as those expected in CO2 sequestration [*Poliannikov and Malcolm*, 2010]. The basic idea of the method is to take a recorded signal, generated by an active source and measured at a single receiver, and mimic a time-reversal experiment by cross-correlating this signal with itself, i.e. we form

$$U_2 = u * u. \tag{4.3.1}$$

The autocorrelation, U_2, will have a peak around zero time. The shape of this peak will depend on both the source signature and the scattering properties of the medium, the latter of which can be described by a refocusing kernel, k. What we are interested in recovering is how this kernel changes during CO2 injection. To that end, we would monitor the spectrum of U_2 throughout the sequestration experiment at a set of permanently installed sources and receivers where data will be regularly collected. Without permanently installed receivers and repeated co-located sources we will not be able to test this methodology on field data sets, however, only a few locations would be essential and the stations could be the same as those used for micro-seismic monitoring.

Determining whether or not the medium has changed is only the first step, however, to be really useful a method must also be able to locate the change. *Fouque and Poliannikov* [2006] demonstrate that the change can be localized by looking at the spectrum of U_2 as a function of an expanding time-analysis window. In other words, as a function of T where

$$U_2^T = u(0:T) * u(0:T) \qquad (4.3.2)$$

Here $u(0:T)$ means the time history of the recorded trace taken from its origin time to time T. Analyzing the autocorrelation as a function of T, bounds the region where a measured change occurred. Looking at the spectrum of k, which is extracted (by deconvolving the source signature) from U_2, as a function of the window location, T, allows us to determine where the change is (from T) and whether the scatterers grow or shrink (from the dominant frequency of k). We will investigate the improvements possible by using multiple sets of sources and receivers, to reduce the bounds on the region of change.

We have tested the methodology on layered models, giving the results shown in Figure 4.3.1, from which we see that we can both locate and characterize changes in the statistical properties of the medium.

(a)   (b)
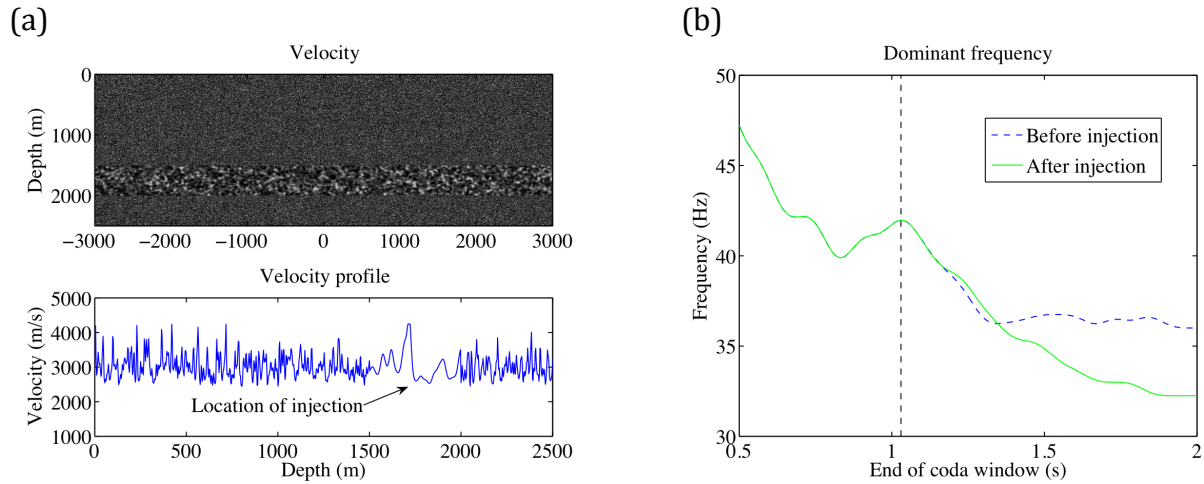
Figure 4.3.1. (a) Experimental setup. The top image is the velocity model used in these experiments, in the layer between 1500 and 2000 m an injection of CO2 is simulated by decreasing the scattering strength of the random perturbations from the mean velocity is increased. (b) Results of the coda-based alarm system. The change is located accurately and the difference before and after injection is clear; in addition, we are able to tell that there is less scattering before than after the simulated injection.

4.3.2.3 Detailed Work Plan
In this proposal, we will continue developing the method, focusing on making it robust enough to be applicable to field situations. This will proceed in several steps.

(1)   (Year 1) Work with multiple receivers in a 1D model to enable the monitoring of smaller changes than is possible with a single source/receiver pair. This will involve theoretical extensions, to ensure that the averaging converges to the correct model parameters when ensemble averaging over model parameters is replaced by averaging over source/receiver pairs.

(2)   (Year 1) Change the statistical properties of the medium so that they more closely resemble the layered Earth scenario. In other words, make the random perturbations longer in the lateral direction than they are in depth. This will involve the refinement of the theory beyond statistically homogeneous models.

(3)   (Year 2) Using one of the models developed in item 2 run a realistic flow simulation to determine the likely locations of CO2 in such a scenario. This will be a more realistic study, in particular if PI has available a realistic model of the reservoir, and will provide the basis for application to CO2 monitoring. We will keep the 'geology' fixed and monitor the CO2 location at different times in the flow simulation to see if we can track its movements.

(4)   (Year 2) Investigate the resolution to lateral changes in statistical properties.

(5)   (Year 3) Use the passive data recorded to see if we can adapt the technique to use only passive (noise) data. A first step would be to use seismic interferometry [*Larose et al.*, 2006; *Gouedard et al.*, 2008] to estimate the Green's functions and then apply the standard active source algorithm. Other options involve the study of the changes in this Green's function relative to its average to extract similar statistical properties from that data [*Brenguier et al.*, 2008a, 2008b]

(6)   (Year 3) Simulate a flow-leak, again in collaboration with Prof. Juanes.

(7)   (Year 4) Apply the technique to real data. This will involve significant progress in terms of the development of more robust techniques to the presence of noise and significant errors in the velocity model. It will also involve the extension of the theory from two layers to more general geologic structures.

4.4. Passive seismic (AM, MF, NT)

Until now, monitoring of CO2 sequestration has largely been done using active data (data using a man-made source). Using the array assembled for the micro-seismic work discussed in the following section, we propose to investigate how much of the active data can be replaced by passive data. We would propose using that array to passively listen for a significant time period (e.g. several days) frequently, beginning before and continuing throughout the injection. The obvious advantage of the passive approach is the reduction in cost associated with active sources; there may also be an advantage for repeatability because the need to generate identical sources at different times is removed. How much improvement is possible in the latter case depends on the stability over time of the passive sources. Passive sources in this region would be expect to come from a combination of teleseismic energy from seismicity in Iran, tidal noise and drilling/production noise from this and nearby fields. This diverse set of sources should give a good frequency range, resulting in accurately reconstructed Green's functions. (The reconstruction of Green's functions from passive data is discussed by both *Larose et al.* [2006] and *Gouedard et al.* [2008] and references therein.)

We would use these data, as soon as they are available, but anticipating in the third and fourth years, to investigate two aspects discussed briefly above. First, we would compare the correlation recovered Green's functions [*Larose et al.*, 2006; *Gouedard et al.*, 2008] to active source data. By assessing how similar these data sets are, with particular emphasis on regions of data that are most sensitive to change (estimated by the method of *Denli and Huang* [2010] for example), we would be able to determine whether future projects could achieve the same results with fewer active sources. The second aspect we would investigate, as mentioned above, is the combination of techniques such as those discussed by *Brenguier et al.* [2008a, 2008b] with our methods for localizing coda change to attempt to localize the changes, found by Brenguier's method, to determine leakage locations.

Detailed Work Plan

Year 1: Evaluate origin of seismic noise in Abu Dhabi using surface seismic data from existing stations.

Year 2: Evaluation of existing methods for detecting change using seismic noise and their applicability to the specific field selected for CO2 injection.

Year 3: Analysis of seismic data from the network of seismic stations that are deployed for microseismic monitoring to determine Green Functions between stations and comparison of results with predictions using known geology. Investigate the regions sampled by the Green Functions to determine their use in monitoring changes in the reservoir cause by CO2 injection.

Year 4: Summarize results.

4.5. Induced seismicity (NT, MF, BH)

Earthquakes occur when the shear stress on a potential rupture plane becomes high enough to exceed the failure stress, τ_f, given by

$$\tau_f = \mu(\sigma_n - p) + \tau_0, \qquad (4.5.1)$$

where µ is the coefficient of friction, σ_n is the normal stress on the plane, *p* is the pore fluid pressure, and τ_0 is the strength of the rock. Equation (4.5.1) shows that increasing the pore fluid pressure within a reservoir promotes failure by reducing the failure stress. In addition, the changes in volume associated with changing *p* change both the normal and shear stresses throughout the region. These changes can either promote failure or stability, depending on the relative sizes and signs of the changes in shear and normal stresses.

Induced seismicity has generally been observed to accompany fluid injections associated with Enhanced Oil Recovery (Zhang et al., 2009), geothermal energy development (Concha

et al. 2010), and storage of natural gas (Dosk and Haak, 2007). Seismicity has been reported to accompany the injection of CO2 (Zhou et al, 2010). A review of cases of induced seismicity associated with fluid injections and that type of information that can be gained by studying the seismicity is presented in Maxwell et al. (2010). As an example, Figure 4.5.1 shows the seismicity accompanying Enhanced Oil Recovery in a field in Oman. The figure shows a clear association between the locations of the mapped faults and the locations of the seismic events. Figure 4.5.2 shows the focal mechanisms determined for some of the induced seismic events. The focal mechanisms provide information about the sense of slip along the faults that can be used to constrain the *in situ* stress field and in geomechanical models. The locations of the events and their focal mechanisms provide information not only about faults that actively slip during injection but also provide indirect evidence about the locations of the injected fluids.
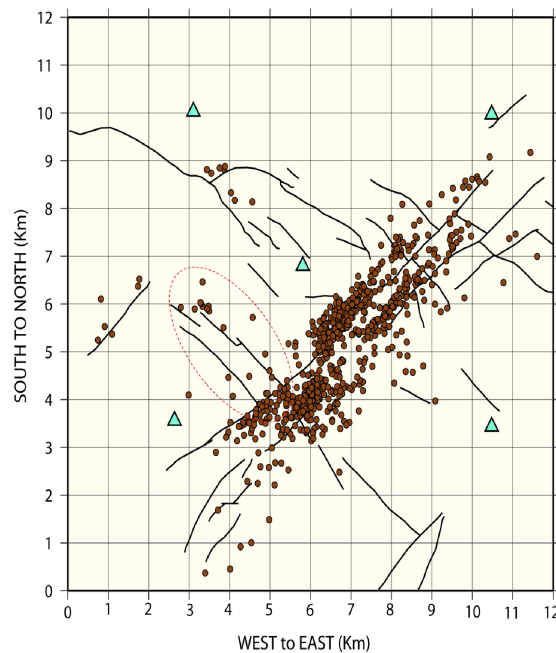
Figure 4.5.1. Locations of microseismic events accompanying Enhanced Oil Recovery in an oil field in Oman. The locations of over 1000 induced earthquakes are shown. Note that the majority of these earthquakes are in the proximity of the NE-SW fault. A group of induced earthquakes within the dashed circle may indicate the activation of a conjugate fault. The five observation stations are indicated with green triangles (from *Li et al.*, 2010).
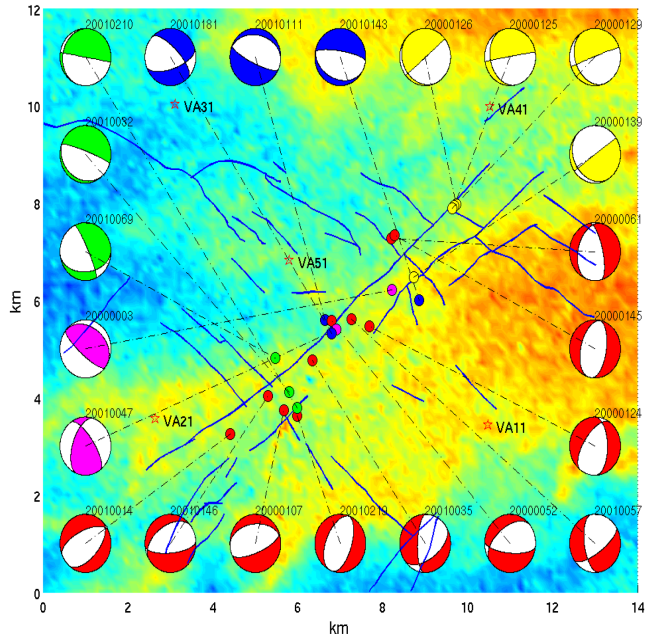
Figure 4.5.2. Focal mechanisms of 22 events that were studied in the Oman oil field. The color in the map indicates the local change in surface elevation with a maximum difference of about 10 m. Different focal mechanisms are grouped in several colors (from *Li et al.*, 2010).

Because of the magnitude of the direct effect of fluid pressure changes, induced seismicity is usually interpreted as providing information about the locations of flow paths in the reservoir. Methods for precise determination of the relative locations of induced seismic events allow for the identification of significant fluid-migration pathways (*Fehler et al.*, 2001). Whether induced by changes in fluid pressure or the accompanying changes in shear and normal stresses, focal mechanisms of the events can be estimated to provide constraints on reservoir stresses and possible changes of the stresses (*Li et al.*, 2010). This information can complement modeling of the surface deformation data and the ultimate construction of a geomechanical model. Velocity tomography using induced seismic data can be used to obtain information about reservoir structure and possible changes in structure associated with spatially-varying changes in fluid content within the reservoir (*Block et al.*, 1994; *Zhang and Thurber*, 2003; *Julien and Foulger*, 2009; *Concha et al.*, 2010). Velocity tomography along with temporal velocity tomography can be combined with determination of patterns in microearthquake locations, surface deformation measurements, and gravity measurements to construct a robust model of reservoir structure and changes in structure during production.

Determining the precise locations and focal mechanisms of induced earthquakes requires that a sensitive seismic network be installed in the vicinity of the reservoir. Higher frequencies can be better detected if the seismic stations are buried in the subsurface, preferably in boreholes. Higher frequencies will lead to sensitivity to smaller seismic events since smaller events are more dominated by higher frequencies than are larger events. In addition, the detection of higher frequencies on a subsurface network will lead to

better precision in the determined locations of the events, which will allow a better interpretation of the seismicity in terms of the geomechanical evolution of the reservoir and the preferential flow of CO2 along fractures or into specific regions within the reservoir.

Detailed Work Plan

Year 1: Study relevant induced seismicity data from Enhanced Oil Recovery and gas injection sites that are available from sites around the world. The goal will be to better understand the relation between induced seismicity and local geology and injection activities at the sites that can be used for estimating the level of induced seismicity to be expected at candidate CO2 storage sites.

Year 2. In collaboration with PI and ADCO, evaluate local seismicity in the UAE using recently-installed seismic stations. This will involve evaluating earthquakes having magnitude as low as 2-3, which are not hazardous but would provide information to interpret later observations of induced seismicity at candidate sites. Make plans for installing a seismic network at the most favored candidate site for CO2 injection to provide information about background seismicity.

Year 3. Design and advise on installation of a 6-station seismic network. Wherever possible, stations should be co-located with GPS sites that are planned. Begin collection and analysis of data recorded from teleseismic, regional and local seismicity to determine a velocity model that can be used to later locate events induced by CO2 injections. This model will also provide background information about the geological structure of the candidate reservoir.

Year 4. Complete analysis of data collected by 6-station network.

4.6 Geodetic Monitoring with InSAR and GPS (TH, BH, HG)

4.6.1 Summary of Recent InSAR Results
Because using geodetic observations to estimate reservoir properties is a rather new tool, we summarize recent work by Vasco and colleagues, who carried out inversions of geodetic data to estimate reservoir permeability variations at the In Salah, Algeria, gas field [*Vasco et al.,* 2008ab*,* 2010*; Rutqvist et al.,* 2009*; Onuma and Ohkawa,* 2009]. Uplift rates of up to 5 ± 1 mm/yr have been estimated over 3 injection wells (Figure 4.6.1a). This surface deformation accompanies injection of nearly one million tonnes/yr of CO_2 via 3 wells into a 20-m thick layer of sandstone at ~ 1850 m depth. About 40 InSAR scenes between 2003 and 2007 were analyzed to obtain temporal variations in the length of the line of sight (LOS) between the regional ground surface and the satellite [*Vasco et al.,* 2008b]. These scalar LOS changes, typically assumed to be dominated by vertical motions, were combined with the record of injection and flow models to estimate important reservoir parameters such as the variation in permeability within the reservoir.

Because these studies provide a concrete illustration of the concepts that we propose to extend and enhance, we highlight here some of the important results. Figure 4.6.1b shows the time derivative of pressure estimated via an inversion of the InSAR LOS changes in the reservoir surrounding well KB-501 305 days after injection began. (The thin line represents the horizontal part of the well where injection is occurring.)

Note that the image is not symmetric about the well, indicating that the permeability structure leads to flow into the region to the NW of the well at a rate higher than elsewhere. Using these pressure variations, flow trajectories can be calculated (Figure 4.6.1c) and the variability of permeability estimated (Figure 4.6.1d). Note that the region of inferred high permeability lies along the projection of a fault inferred from seismic imaging (dashed line). Thus InSAR observations can illuminate geologic structure and principal stress orientations. *Rutqvist et al.* [2009] used forward models to predict surface deformation near injection well KB501 for several scenarios of reservoir properties. They show that the surface deformation is sensitive to the permeability of the cap rock and to the presence of leaky fault zones, with rapid localized uplift over transmissive fractures.
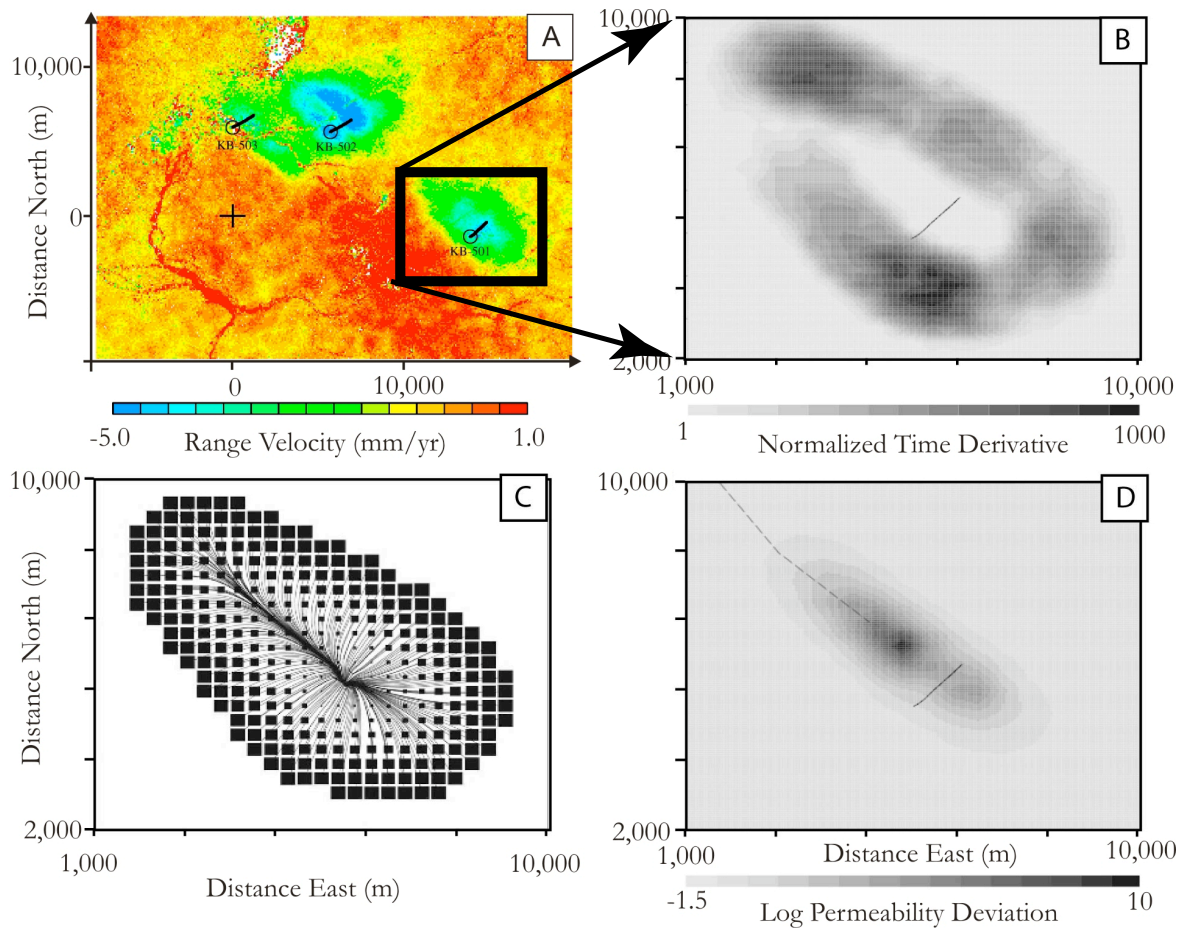

Figure 4.6.1: a) (from [*Vasco et al.*, 2010]) Rate of InSAR line-of-sight change at In Salah, Algeria. b) (from [*Vasco et al.*, 2008b]) Normalized time derivative of the pressure field in the region around well KB501 (outlined in rectangle), 305 days after beginning CO_2

injection, estimated from InSAR LOS changes. c) Trajectories (lines) and arrival times (squares) estimated from temporal evolution of the pressure field. d) Estimated logarithm of permeability multipliers. The region of high permeability follows a fault (dashed line) imaged seismically.

These studies conclude that there is evidence of interaction between preexisting fractures, increased pressure, and flow, yet they all assume that the surface deformation induced by the increased pressure can be characterized by an isotropic response. In a study of well KB-502, *Vasco et al.* [2010] carried out a kinematic inversion to estimate both isotropic changes in volume and the extent of opening of vertical fractures aligned with the geologic structure. They pointed out that the deformation of a fractured medium is different from that of an isotropic medium, and also that the effects of layered elastic structures are important. They found that the InSAR observations indicate substantial opening of fractures.

4.6.2 Advances Expected from Including 3-D Surface Deformation

This prior work demonstrates that InSAR observations of (scalar) changes in line-of-sight length can be used to estimate variations in permeability and monitor reservoir integrity. We propose an approach similar in concept, but with very significant improvements. First, we will measure 3-D vector surface deformation, not just scalar changes in LOS. Vector displacements are particularly sensitive to the opening of fractures that is occurring at In Salah. We will establish a network of ~50 GPS sites that will give high accuracy 3-D results well-resolved in time at specific sites. We will use InSAR observations from multiple viewing geometries to obtain 2-D vector displacements with continuous spatial sampling, but at coarser temporal sampling than provided by GPS.

Figure 4.6.2 illustrates the differences in 3-D surface deformation that would result from injecting fluid into an isotropic medium, versus into oriented cracks. The 3-D surface deformation for an isotropic source (equivalent to a sphere of radius 20 m) at a depth $d = 1$ km in an elastic halfspace is shown in Figure 4.6.2a. The horizontal displacements are oriented radially, with a maximum of 1.6 mm at 1.2 km = 1.2 d from the origin. The maximum vertical displacement is 3.8 mm. Fig. 4.6.2b shows the 3-D surface deformation caused by a vertical, NW-SE trending tensile dislocation of equal volume change at a depth d = 1 km. The region above the source subsides 1.2 mm; the maximum uplift of 2.1 mm occurs ~ 1 source depth away from the source. The horizontal displacements are oriented predominantly NE-SW away from the source, with a maximum value of 2.7 mm ~ 1.1 km SW and NE of the source. For the opening of a vertical fracture, the horizontal surface deformation typically exceeds the vertical surface deformation.
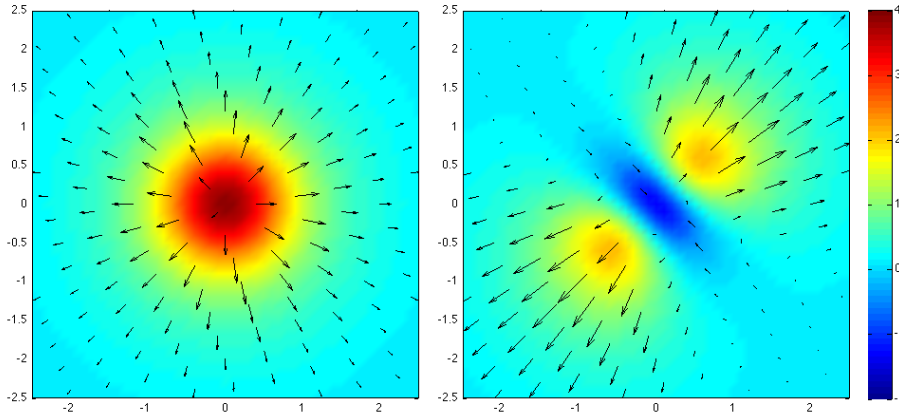
Figure 4.6.2: a) Horizontal (arrows) and vertical (color background, scale in mm) displacements resulting from the inflation of an isotropic source with volume increase 3 x 10^4 m^3 buried at a depth of 1 km. The region shown is 5,000 m in each horizontal direction. b) Horizontal and vertical displacements resulting from the inflation of a vertical tensile dislocation with the same volume and depth, striking NW-SE. The two panels are at the same scale; the maximum horizontal displacement plotted is 2.8 mm.

4.6.3 GPS Observations of Vector Surface Deformation from Natural Gas Production
We have been monitoring the deformations of a natural gas field in Oman for many years using GPS and InSAR. The experimental configuration is similar to what we propose would be used to monitor sequestration in Abu Dhabi. For the Oman field, we use five continuously operating receivers and 69 rover locations that are occupied in triplets using three GPS receivers to spatially densify the deformation measurements. The rover sites are occupied for about 24 hours each time they are observed. With three receivers, the network can be re-measured over a 23-day period. (The limited number of receivers used in this project was dictated by cost of receivers when the project was started in 2003.) The measurements in this network show the subsidence and central contraction of the field ex-pected from the withdrawal of natural gas. We also see temporal changes in the rates of both horizontal and vertical motions associated with changes in production rates. Figure 4.6.3 shows an example of results from a continuous GPS site near, but not at, the center of subsidence. The variations about the secular rates are correlated with changes in the pro-duction rates. In this figure, the root-mean-square (RMS) scatters of north, east and height residuals of 2.9, 1.2 and 14.9 mm, reflect the systematic variations due to changes in gas production. The short-term scatters of these coordinates are 0.5 mm in horizontal and 2.9 mm in vertical. These values are the noise levels in the GPS daily position determinations to be expected in the monitoring network recommended here. In the lower frame, we show the height residuals after removing a linear trend, along with the predicted temporal variations in height based on a model fit to the production. The RMS difference between the data and model is 5.4 mm, which is still above the GPS noise level, suggesting that additional modeling is justified.
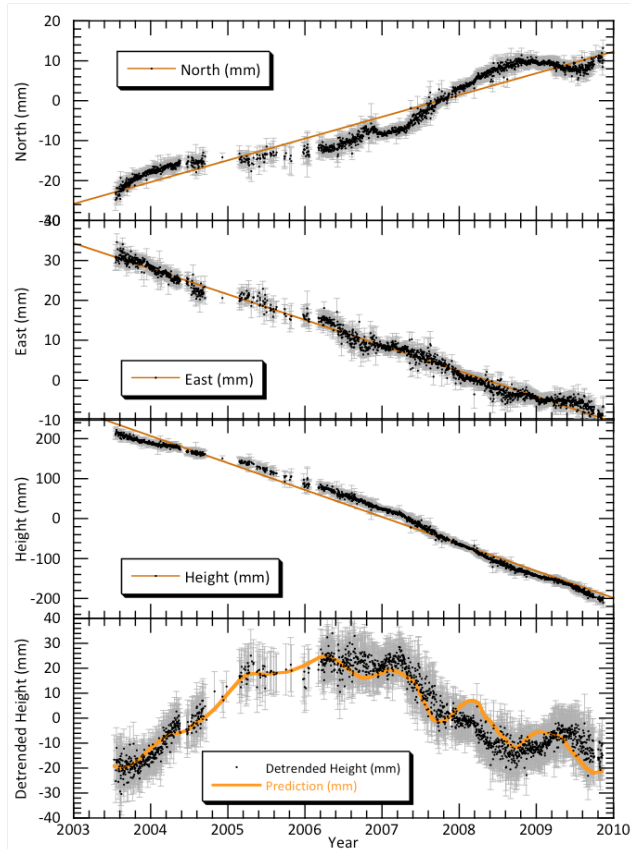
Figure 4.6.3: Top three frames: Daily evolution in the North, East, and Up components of displacement of a mark overlying a natural gas reservoir in Oman. Bottom frame: Height residuals after removing linear trends from the heights and production based prediction of height changes. MIT has been monitoring this reservoir since mid 2003. In addition to the secular motions, seasonal variations associated with varying production rates are visible. The gaps in the time series are due to early telemetry and receiver failures (resolved by early 2006).

4.6.4 Scaling of In Salah Results to Expected Signals in Abu Dhabi

The 3-D surface deformation associated with underground CO_2 storage can be estimated from published results at other sites. Deformation is inversely proportional to the square of the depth of injection, and proportional to the change in reservoir volume at depth, with a constant of proportionality that varies little between sites. Furthermore, the change in volume is proportional to the change in pore pressure, p, the thickness of the injection formation, and the Biot poroelastic expansion constant, $1/H = (\partial \varepsilon / \partial p)$ [*Domenico and Schwartz*, 1997]. For a region of volume, v, with dimensions $<<d$, the deformation scales as $pv/(Hd^2) = \delta v/d^2$. Note that the mass of gas injected or removed does not directly enter this calculation, but is indirectly accounted for by the change in pore-fluid pressure.

Surface deformation rates of approximately 5 mm/yr have been monitored at the In Salah site in Algeria where CO_2 has been continuously injected at depth of ~ 1850 m into a 20 m thick sandstone formation [*Vasco et al.,* 2008ab, 2010*; Rutqvist et al.,* 2009*; Onuma and Ohkawa,* 2009]. Rutqvist et al. [2009] estimated a pressure increase of ~ 3 MPa/yr over 3 years accompanying the CO_2 injection. Scaling of the rates at In Salah to the reservoirs that

would be measured in Abu Dhabi will depend on their depth, thickness, permeability, and rate of injection. As soon as we have estimates of these parameters, we will provide quantitative estimates. The depth at In Salah is likely an upper bound, and we expect higher rates of injection. Thus we are optimistic that deformation will be both measurable and diagnostic.

4.6.5   Geodetic Monitoring Work Plan

During the time interval covered by this proposal, we will focus on designing a robust geodetic monitoring program, including calibration of the expected system response and quantification of the delectability of the geodetic system. We recommend that two techniques be used to monitor the vector surface deformation associated with underground storage of CO_2. The most accurate is GPS (Figure 4.6.3). At this time, we envision a GPS network with $\sim$ 50 geodetic markers, comparable to our Oman network. In this network, 5 of the marks would be monitored continuously to provide excellent temporal coverage. The remaining $\sim$ 45 marks would be observed on an approximately weekly schedule using 10 roving receivers, providing a measurement at each mark $\sim$ monthly. This would give sufficient temporal coverage to resolve the signals such as those associated with CO_2 sequestration at In Salah [*Onuma and Ohkawa*, 2009].

Because the initiation of geologic sequestration follows soon after the end of this project, it is important to be ready to "hit the ground running" with the GPS component. During the third year of this project, we propose to acquire 10 GPS receivers, install a network, and begin measurements and analysis of the data acquired. In addition to providing pre-injection characterization, this will provide valuable experience in conditions unique to the field that will be chosen for sequestration. GPS receivers will be purchased by MIT because of their academic discount results in a cost 1/3 what would be incurred by an Abu Dhabi institution. Data analysis at MIT will be carried out by Professor T. A. Herring and the half-time geodetic researcher mentioned above. Field work will be supervised by Professor Hosni Ghedira of Masdar Institute and Karl Berteussen of Petroleum Institute. Professor Herring will assist in setting up a data analysis capability, as well as supervise the installation of the network. Professor Hager will take responsibility for the design of the network, based on the results of geomechanical models and visit the field with Professor Herring.

We also recommend monitoring the field with greater spatial coverage, but less complete temporal coverage, using InSAR. By combining changes in line-of-sight range from multiple look directions, we would be able to determine the pattern of surface deformation with unprecedented spatial resolution. Because of the orbital geometry, we will have little sensitivity to the north-south component of displacements. However, we will be able to determine 2-D vector displacements in the plane containing the two look vectors, with components that can be resolved into up-down and approximately east-west directions. Our models predict large differences in both up-down and east-west displacements for isotropic porosity versus porosity dominated by vertically oriented cracks for the fields we propose to monitor. Thus, being able to resolve this 2-D deformation should provide much more information than is available from a scalar change in range.

The first InSAR task is investigation of the accuracy of change detection that can be expected at the candidate fields using InSAR. This includes 1) investigation of whether DINSAR provides sufficient coherence to be useful quantitatively, as has been demonstrated for In Salah [*Onuma and Ohkawa*, 2009] and for our field in Oman; 2) determining if suitable targets exist for PSInSAR at sufficient spatial resolution, as is the case for In Salah [e.g., *Vasco et al.*, 2008ab] and our field in Oman; 3) determining the character of the atmospheric contribution to noise; and 4) characterizing sources of noise in the deformation field from near-surface sources such as aquifers.

We will begin by analyzing available existing InSAR acquisitions in the region to determine where sufficient coherence exists for interferometry. Three main space agencies will be approached for the archived SAR data: (1) the European Space Agency (ESA) for data acquired by the ERS1/2 (1992-2001) and ENVISAT (2002-present); (2) the Canadian Space Agency (CSA) for Radarsat1/2 data (1995-present); and the Japan Aerospace Exploration Agency (JAXA) for PALSAR data (2006-present). This task will be accomplished by the end of the first year. Assuming that the initial results are positive, we will request that images be taken each repeat pass over the candidate fields, for all available InSAR satellites, including the ESA platform (ENVISAT and ERS), RADARSAT, Terra SAR-X, Cosmo Sky-Med and ALOS-PALSAR. These acquisitions will take place uniformly distributed throughout the last 3 ½ years of the project, with analysis keeping pace with the acquisition.

A postdoctoral researcher at MIT will take the lead in the InSAR data analysis, in collaboration with Professor Herring. The researcher will devote full-time to the InSAR analysis over the first two years of the project. During the second two years, this geodetic researcher will spend half time on InSAR and half time on GPS. Masdar Institute will develop an InSAR analysis capability. The MIT analysis will be done using the ROI_PAC software package (http://www.openchannelfoundation.org/projects/ROI_PAC/). A second postdoctoral researcher, based at Masdar Institute, will allocate 50% of his time to the satellite data processing and InSAR data analysis, with special focus on X-band data (from Terra SAR and Cosmo Sky-Med satellites). The data analysis work at Masdar will be jointly supervised by Professors Ghedira (Masdar) and Herring (MIT). Masdar Institute will obtain a license for the SARscape software from ENVI/ITT. The scenes will be analyzed by both groups and the results compared.

4.6.5.1 Detailed Geodetic Tasks

The geodetic tasks are divided between InSAR and GPS.

1. Investigation of InSAR capability for measuring deformation in candidate fields

There are several tasks that will involve existing InSAR images:
   a) (Year 1) Investigate coverage of candidate fields by RADARSAT, ESA satellites, and ALOS-PALSAR and acquire those images that appear to be suitable for interferometry.
   b) (Year 1) Determine whether these acquisitions provide sufficient coherence for DInSAR analysis techniques to provide useful measurements of deformation.

c) (Year 1) Determine whether suitable targets exist for PSInSAR analysis at sufficient spatial resolution.
d) (Year 1) Compare InSAR analyses by MIT and Masdar Institute.

If the results of these tasks are positive, we will schedule frequent new acquisitions covering candidate fields from operational InSAR satellites and continue our analysis

e) (Year 1-4) Schedule acquisition of new scenes
f) (Year 1-4) Compare InSAR analyses by MIT and Masdar Institute.
g) (Year 1-4) Determine the character of the atmospheric contribution to the noise.
h) (Year 1-4) Characterize sources of noise in the pre-injection deformation field from near-surface sources such as aquifers.

2. Install GPS network at candidate field and begin measurements to gain experience in this field and characterize pre-injection deformation.
a) (Year 3) Purchase, test, and ship receivers to Masdar Institute.
b) (Year 3) Design network, based on most up to date understanding of the field.
c) (Year 3) Install network and train observers from Masdar Institute.
d) (Year 3-4) Colect and analyse GPS data to characterize pre-injection deformation field.
e) (Year 4) Compare deformation field estimates from GPS and InSAR.

4.7 Microgravity and Gravity Gradiometry (BH, TH)

The use of measurements of the gravitational effects of spatial and temporal variations in mass is becoming increasingly important as the result of recent technical innovations. Field capable instruments that measure absolute gravity with an accuracy < 5 μgal have recently been demonstrated [e.g., *Ferguson et al.*, 2008]. A new generation of gravity gradiometer has been developed that makes absolute measurements of the gravity gradient tensor to sub-Eötvös (1 E = 0.1 μgal/m) accuracy is also receiving attention. Each of these technologies shows promise for monitoring CO2 sequestration.

Pawlowski [1998] provides a succinct summary of the relative advantages of gravimetry and gravity gradiometry. Figure 4.7.1 compares the variations in gravity gradients (top two panels) and gravity (third panel) for the geologic cross section in the bottom panel. It seems apparent that there is more information in the gravity gradient, particularly at short wavelengths. However, this information comes at some cost. Conventional gravity surveying is highly developed, with instruments that are both more readily available and more robust. In addition, there are far more providers of gravity surveys than there are of gradiometer surveys. We provide here a description of both techniques. By the end of the project, we will provide a recommendation of which approach is preferred, taking into account cost, accuracy, and resolution.
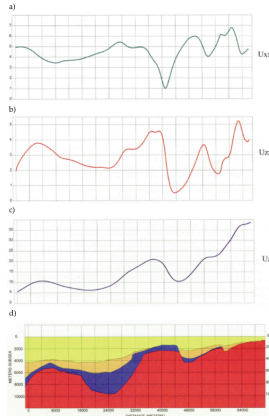
Figure 4.7.1. (from *Pawlowski* [1998]) Comparison of gradiometer data with conventional vertical gravity data for a simulated measurement at sea level for the geologic situation having the cross-section in the bottom panel (d). Shown above it are the gradiometer horizontal gravity gradient (a), the gradiometer vertical gravity gradient (b), and the conventional gravity anomaly (c). Density contrasts related to structuring within the sedimentary section (yellow, ocher, blue) and the igneous basement (red) cause the simulated gravity anomalies. The greater sharpness and separation of the gradiometer anomalies show the increased resolving power obtainable in principle with this technology.

4.7.1 4D Microgravity

Over the past decade, measurement and interpretations of temporal variations in gravity (often called "4D gravity") have improved to the point that they provide valuable information about reservoir processes. (A recent special section of *Geophysics*, edited by *Biegert et al.* [2008], provides a useful perspective on advances in this field.) Measurement of time varying of gravity provides new information, complementary to that provided by monitoring via time-lapse seismic and surface deformation. Gravity variations are directly sensitive to variations in density. Thus, although dissolved CO_2 is essentially invisible to seismic waves, the increased density results in variations in gravity. Similarly, surface deformation is sensitive to pressure, which, unlike density, is continuous across the front between CO_2 and water. Gravity by itself has low spatial resolution. This drawback can be substantially eliminated by including constraints from seismic imaging and surface deformation, as we propose in our data assimilation approach. 4D gravity observations are being carried out at Sleipner and In Salah [*Michael et al.,* 2010] and is recommended for best practice monitoring [e.g., *Chadwick et al.,* 2007].

In addition to providing important constraints on processes within the reservoir, monitoring gravity changes is an important tool for early warning. CO_2 escaping to shallow depth, with its low density and proximity to the surface, could result in a significant gravity signal.

Gravity variations can be measured either at the surface or within boreholes. Traditionally, relative gravity changes have been measured using spring-based gravimeters such as the Lacoste & Romberg model D or Scintrex CG-3M or CG-5 instruments. By designing observing scenarios that include multiple measurements at each site, gravity changes can be measured with an accuracy < 5 μgal [e.g., *Gettings et al.,* 2008]. Recently, field-capable absolute gravimeters, the Micro-g Lacoste A-10, have been developed that achieve this accuracy with simpler logistics [e.g., *Ferguson et al.,* 2008]. Sea-floor measurements can be carried out to the same high accuracy [e.g., *Alnes et al.*, 2008], but are expensive and slow. Measurements on land are much less costly and less cumbersome. Measurements at depth in a borehole provide the most resolution, but only at a few locations such as injection wells, production wells, and a handful of monitoring wells.

An estimate of gravity variations due to fluid movements can be obtained by approximating the distribution of injected material as a disk of radius r and thickness t with an effective density contrast $\Delta\rho\phi$. Here $\Delta\rho$ is the in situ density difference between the CO_2 and brine and ϕ is the porosity of the reservoir. The gravity anomaly measured on the axis of the disk a distance z above its top is:

$$\Delta g = 2\pi G \Delta \rho \varphi \left\{ t + \sqrt{z^2 + r^2} - \sqrt{z^2 + t^2 + r^2} \right\}, \tag{4.7.1.1}$$

where G is the universal gravitational constant For z, $t << r$, this reduces to the simple Bouguer correction, $2\pi\, G\Delta\rho\phi t$. For $t << z, r$, (4.7.1) reduces to a form that reduces the Bouguer correction in a way that is dependent on z/r:

$$\Delta g = 2\pi G \Delta \rho \varphi t \left\{ \left(1 + z^2/r^2 - (z/r)\sqrt{1 + z^2/r^2} \right) \Big/ \left(1 + z^2/r^2 \right) \right\}. \tag{4.7.1.2}$$

When $z/r = (1, 2)$, the Bouguer anomaly is reduced by a factor of $(0.3, 0.1)$, respectively. For $z/r >> 1$, this expression reduces to the point mass formula, $4\pi\, GM/z^2$, where M is the anomalous mass of the disk. All things being equal, microgravity monitoring of shallow reservoirs will be more informative than microgravity monitoring of deep reservoirs.

The above formula assumes that there is no change in elevation of the station between surveys, e.g., due to surface deformation. Changes in elevation lead to changes in gravity of 0.3 µg/mm (land) or 0.2 µg/mm (underwater). They should be measured, e.g., by precise GPS or InSAR (on land) or by pressure gauges (seafloor), and the effects removed from the gravity signal before interpretation.

Alnes et al. [2008] inverted seafloor measurements of 4D relative gravity at the Sleipner CO_2 sequestration site to constrain the in situ density of CO_2 to 640 – 770 kg/m^3. For Sleipner, $z \sim 1$ km, $t \sim 13$ m, $r \sim 700$ m, $\phi \sim 0.37$, and the maximum amplitude $\Delta g \sim$ -5 µgal. *Hare et al.* [2008] inverted 4D absolute gravity observations associated with a waterflood at Prudhoe Bay, AK. By tracking gravity variations in space and time, they inferred that the water flow was impeded by fault barriers, which were then breached to allow flooding of new compartments. Profiles of observations and models and model predictions are shown in Figure 4.7.1.1. (Note that the error from elevation changes and unmodeled near-surface hydrological variations are expected to be anomalously large in this environment.) For this reservoir, $z \sim 2.5$ km, $t \sim 100$ m, $r \sim 1300$ m, $\phi \sim 0.2$, and the maximum $\Delta g \sim 60$ µgal.
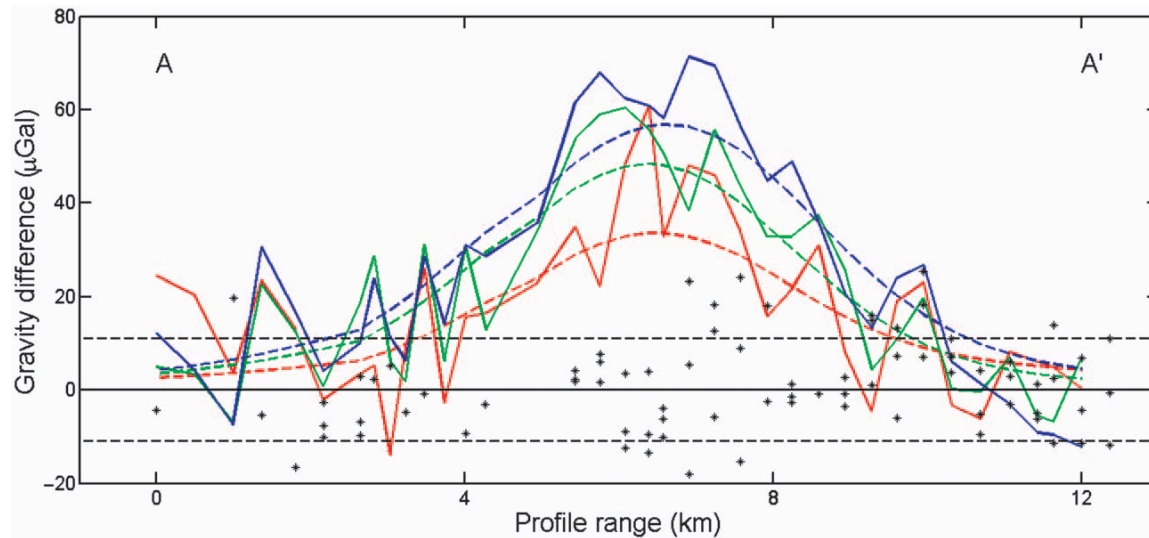
Figure 4.7.1.1 [from *Hare et al.*, 2008]. 4D gravity profiles for a line at Prudhoe Bay that has been monitored in eight gravity surveys since 1997. The dashed black lines are ±11 µGal or one standard deviation for the 4D gravity noise. Solid color lines represent 4D gravity and dashed color lines are theoretical gravity from models. The red curves represent epoch 2005–2003, the green curves are epoch 2006–2003, and the blue curves are epoch 2007–2003. Black dots represent 4D gravity noise (including gravimeter, height, and unmodeled hydrological effects) from preinjection measurements between 2000 and 2002.

Borehole Gravity

Borehole gravity measurements have the advantage that they can be positioned near the depth of the density anomaly, and measurements can be made both above and below the CO_2 plume, effectively doubling the Bouguer effect. Such measurements have been used both for detecting spatial changes in structure and for reservoir monitoring. A borehole gravity meter (BHGM) that is a miniature version of the LaCoste & Romberg land gravity meter is commercially available (see http://edcon-prj.com). Through the use of repeated measurements, the system can give data with a standard deviation of 3 mgal. For such measurements to provide meaningful time-lapse information, one must have the ability to position the instrument in the borehole to a location of better than 1 cm. This positioning may be obtained using collar locaters and locating the instrument relative to a collar. The instrument has a positioning capability that allows the sensor to be positioned within 1 mm of a desired location in a borehole. In addition, *Meyer* [2008] describes the use of differential gravity measurements in boreholes, where differential means simultaneous measurements of gravity at two locations. He refers to an interferometric borehole gravimeter that is capable of providing differential measurements as small as 1 mgal. He then investigates the use of this device for detecting fluid movement. He argues that a 1 mgal signal will be caused by displacement of a fluid front over a distance of 50 m at a distance of 200 m from the borehole.

Gasperikova and Hoverstein [2008] provide forward models of 4D gravity monitoring of example CO2 injection scenarios. Figure 4.7.1.2 shows their calculations of the predicted BHGM signals for a very small wedge (t = 100 m, $0 < r < 250$ m) representing only 20% CO_2 saturation of a layer with 20% porosity. The doubling of the signal across the layer is apparent, as is the falloff with distance away from the edge of the wedge.

Figure 4.7.2 [from *Gasperikova & Hoversten*, 2008]. a) CO_2 wedge of 250 m radius and density of 2260 kg/m³ representing 20% CO_2 saturation in 20% porosity inside a 100-m-thick sand layer with a density of 2285 kg/m³ at a depth of 1 km. The background density is 2160 kg/m³. b) Borehole-gravity response, µgal, of the model in a) as a function of distance from the edge of the wedge.
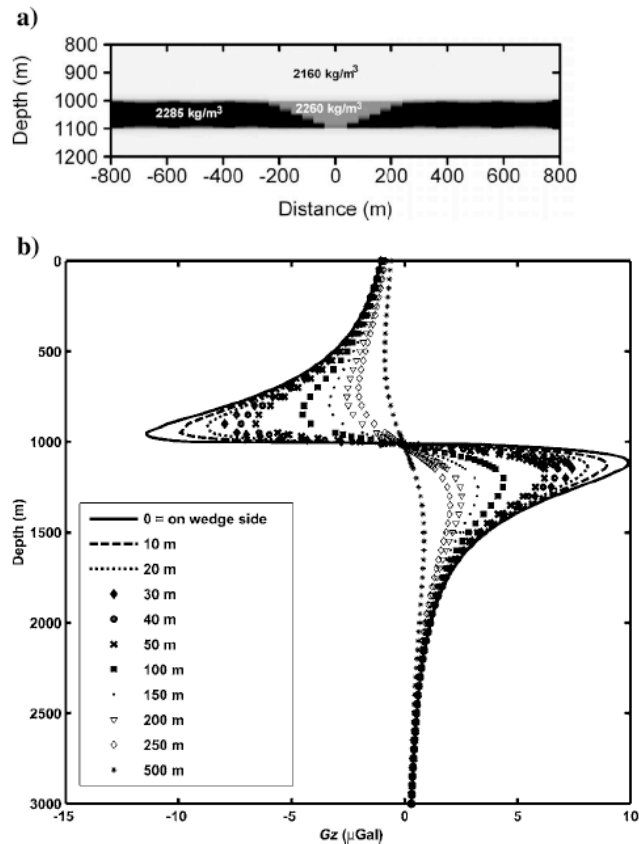
4.7.2 4D Time-lapse Gradiometry

Gravity gradiometry is a rapidly developing field, spurred by the desire to make sensitive measurements of density variations from airplanes for use in exploration for diamonds, minerals, and hydrocarbons. At present, the field is dominated by the Lockheed Martin GGI interferometer, which was developed for classified use in the navigation of nuclear submarines. The instrument uses two opposing pairs of accelerometers mounted on a rapidly spinning disk. The differences in acceleration measured by pairs of disks can be used to measure gravity gradients in the plane of the disk to extremely high accuracy. Three mutually orthogonal disks yield the five independent elements of the gravity gradient tensor [e.g., *Jekeli*, 2006]. Bell Geospace has both airborne and marine implementations of this instrument [http://www.bellgeo.com/tech/technology_system.html], providing measurements of the full gravity gradient tensor as a service. Examples of the signal expected for simple mass distributions are at [http://www.bellgeo.com/tech/technology_theory_of_FTG.html]. Equally accurate, but smaller and more robust systems, based on cold atom interferometry are on the horizon and may revolutionize the field [*Jekeli*, 2006].

4.7.3 Gravity work plan

Our overall goal is to propose a comprehensive strategy for monitoring the specific reservoirs under consideration. This includes evaluating the relative costs and merits of measuring perturbations in gravity using gravimeters or gravity gradiometers. We will do this by calculating the expected perturbations in gravity and gravity gradient for candidate

reservoirs and injection scenarios. One obvious consideration is the depth to the reservoir, d; for a given density contrast, $\Delta\rho$, scales as $\Delta\rho/d^2$, while the components of the gravity gradient tensor scale as $\Delta\rho/d^3$. This different dependence on d implies that gravity gradiometry is a relatively more effective tool for shallower reservoirs.

Accounting for all of the different sources of density contrast involved with sequestration of CO2 in a saline aquifer requires careful thought, as revealed by the following apparent paradox: Injection of CO2 into an aquifer adds mass to the system, which must result in an overall increase in gravity. Yet the intuitive expectation, verified for Sleipner, is that the lower density of CO2 (relative to the water displaced) should lead to a local decrease in gravity above the CO2 plume.

It is useful to think about at least 4 different sources of density variation with time and space associated with the injection of CO2 into an aquifer. The most obvious is the replacement of brine by CO2 in the pore space of the plume. The local average density variation from the injected CO2 depends on the pressure and temperature, the porosity, and the fraction of pore space in which the CO2 replaces the brine. Injecting the CO2 will increase the pore pressure, both in the CO2 plume and in the aquifer, depending quantitatively on the permeability and the flux of CO2 injected. This increased pore pressure indirectly affects the density distribution in several ways. First, the increased pressure compresses both the brine and the rock matrix, leading to an increase in density that can extend far beyond the CO2 plume itself, both in the reservoir and in the surrounding rock. Second, increasing the pore fluid pressure increases the porosity, leading to a decrease in average density of the reservoir region as high-density rock matrix is replaced by lower density brine and CO2. Third, increasing the pore fluid pressure increases the thickness of the aquifer, resulting in uplift of the overlying caprock and surface. This uplift leads to a perturbation to the original density field that must be considered in calculating the total gravitational effects of injection.

To summarize, the expected variations in gravity and gravity gradient depend strongly on the properties of the reservoir. Most important are the depth, d, the porosity, ϕ, the permeability, k, and the mass flux injected, Q. Also important are the compressibility of the brine, of the matrix, and of the cap rock and overburden. For a given Q, the pressure, p, scales as $Q/(k\,\rho_{CO2})$, where ρ_{CO2}, the density of the CO2 injected, is strongly dependent on d and temperature, T.

Useful estimates of these crucial parameters, along with models of pressure-induced changes in porosity, aquifer thickness, and deformation, should be available after the first year of the project. Thus, the gravity tasks will be carried out over the 2nd, 3rd, and 4th years of the project. These tasks will be carried out by a graduate student, with participation and supervision by Professor Hager, in collaboration with Professor Herring.

a) (year 2) Compute forward models of the spatial and temporal variations in gravity and gravity gradient for candidate reservoirs. These models will be tightly linked to the flow/geomechanical models (Section 2.1). Particular attention is required to identify all of

the different density contrasts and include them in a way that is consistent with the flow and geomechanics.

b) (years 3-4) Develop inverse models in order to address the resolution and variance operators for both gravity and gravity gradiometry for the candidate fields. This work will follow the procedure given by *Vasco* [1989], using a singular value decomposition of the gravity and gravity gradient kernels to obtain estimates of the model parameter resolution and model parameter variance for the two data types. These depend critically upon both the spatial discretization of the models and the distribution of measurements. A critical part of this task will be investigation of costs vs resolution of proposed observing scenarios, leading to an optimized observing scenario for the reservoir chosen.

c) (years 3-4) Investigate available instruments and potential collaborations for obtaining measurements of improved quality and lower cost. Professors Hager and Herring are involved in a collaboration with colleagues at Draper Laboratory to develop both improved gravimeters and gradiometers over the next several years. In addition, Professor Hager has made contact with researchers associated with the Lockheed Martin GGI, discussing the development of a more accurate, less expensive gradiometer designed for CCS applications. This project might lead to special opportunities to demonstrate the instrument in Abu Dhabi.

d) (year 4) Make and document a recommendation about whether to pursue measurements of gravity, gravity gradients, neither, or both for the monitoring phase.

4.8 Electrical Resistance Tomography (BH)

Because a formation with super-critical CO2 as the pore fluid has an electrical resistivity approximately five times that of a brine-saturated formation, electrical imaging techniques may provide valuable information about the migration of the CO2 plume, as well as changes in CO2 saturation. In particular, time-lapse Electrical Resistance Tomography (ERT) is being implemented at the SECARB Cranfield Site as a field test of this method [*Carrigan et al.*, 2009]. Although at present, this technology is not as mature as other monitoring techniques [e.g., *NETL*, 2009], it is important to keep abreast of developments over the next several years in order to provide a sound assessments of its costs, technical maturity, and potential benefits.

High resolution mapping of subsurface electrical properties has been used to characterize and monitor fluid migration in the subsurface for hydrological systems with much smaller resistivity changes than CO2 provides [e.g., *Daily et al.,* 1992, 1998; *Binley et al.*, 1996]. Thus, in theory, ERT is capable of providing useful images of plume location. However, CO2 sequestration requires measurements be made at much greater depth than these hydrological studies, partially offsetting the advantages of the large contrast in resistance [e.g., *Carrigan et al.,* 2009]. Challenges include working in deep boreholes at elevated temperature and pressure and corrosive brines; the necessity of keeping the interior of the borehole clear for other monitoring measurements, necessitating an annular casing of the

well, the long runs of the cables, which lead to impedance and mechanical integrity issues. And once the system is cemented in, it is impossible to repair.

The measurements needed to estimate the resistivity structure is acquired by using an array of electrodes, typically distributed along two or more fiberglass-cased boreholes. For each measurement, four electrodes are used to minimize the effects of contact resistance and polarization at the interface between the electrodes and the formation. A known current is injected between two of the electrodes and the voltage is measured between the other two electrodes, with the resistance between the electrode pairs related to the current and voltage via Ohm's law. The measurements are repeated for all independent combinations of electrodes.[*Daily et al.,* 2003], [*Ramirez at al.,* 2003]. Even with a data set containing hundreds of measurements, their inversion is typically under constrained. The nonuniqueness is typically dealt with via smoothness constraints or assumptions about the geometric form of the resistivity anomaly. ERT is best used in conjunction with other observations such as seismics and surface deformation [e.g., *Carrigan et al.,* 2009].

Detailed Work Plan
Work on this task will comprise a continuous low-level effort during the first 3 years, followed by a more intense effort in the final year, culminating in documentation of recommendations. Professor Hager will take responsibility for these tasks.

a) (Years 1-3) Extend our literature search on field results to date.
b) (Years 1-3) Assure that the joint data inversion and data assimilation in 4.1 is developed to include consideration of ERT measurements.
c) (Year 4) Address formally the resolving power of ERT in the context of other monitoring measurements.
d) (Year 4) Provide a cost-benefit analysis of these (possibly expensive) measurements

4.9 Geochemical and Surface Monitoring (NT, MS)

4.9.1 Isotopic Characterization of CO_2 for Monitoring (NT)

CO_2 is a ubiquitous compound that is in the atmosphere, water and soil. CO_2 concentrations change both spatially and temporally. The causes of changes could be natural and/or due to human activity (e.g. increased vehicular traffic). An important aspect of monitoring is to determine whether any change in surface concentration is due to possible leakage from the sequestered CO_2. This determination requires "foolproof" tracers that would work in a CO_2 rich environment.

The geochemical tracers we recommend are cluster isotopes - long chains made of different isotopes of carbon and oxygen. A sampling of such isotopes is given in Table 4.9.1. These compounds are formed during the combustion process. They contain the "DNA" signatures of every batch of CO_2 produced. The concentrations of a subset of these isotopes in the atmosphere are extremely low, as shown in Table 4.9.1. Because of the low background they are extremely sensitive to small changes.

For monitoring with isotopic tracers, the isotopic signature of the CO_2 being injected is determined. Then, periodically or whenever an escape is suspected, air and soil samples are tested to determine whether they contain any CO_2 bearing the isotopic signatures of the injected CO_2.

Table 4.9.1: Multiple 'isotopologues' or 'clumped isotopes'

Isotopologue	Mass	Abundance	
$^{16}O^{12}C^{16}O$	44	98.40%	
$^{16}O^{13}C^{16}O$	45	1.10%	
$^{17}O^{12}C^{16}O$	45	730	ppm
$^{18}O^{12}C^{16}O$	46	0.40%	
$^{17}O^{13}C^{16}O$	46	8.19	ppm
$^{17}O^{12}C^{17}O$	46	135	ppb
$^{18}O^{13}C^{16}O$	47	45	ppm
$^{17}O^{12}C^{18}O$	47	1.5	ppm
$^{17}O^{13}C^{17}O$	47	1.5	ppb
$^{18}O^{12}C^{18}O$	48	4.1	ppm
$^{17}O^{13}C^{18}O$	48	16.7	ppb
$^{18}O^{13}C^{18}O$	49	46	ppb

Detailed Work Plan
The use of clumped isotopes is a relatively new development among geochemical tracers. The tasks listed below are planned for testing the efficacy of this approach for CO_2 leak monitoring.

1. (Year 1) Undertake a comprehensive review of geochemical tracers and the use of clumped isotopes.

2. (Year 2) Determine the background level of clumped isotopes in the candidate sequestration sites by analyzing collected air and soil samples.

3. (Year 3) Determine the isotopic signatures of CO_2 emitted from plants that are the likely sources for the CO_2 to be sequestered.

4. (Year 4) Develop a protocol to be used for the sampling and monitoring during the actual sequestration.

4.9.2 Diode Laser Absorption Sensors for Continuous CO2 Surface Monitoring (MS, NT)

In addition to the proposed wide spectrum of sub-surface CO2 monitoring techniques and the geo-mechanical studies for cap-rock integrity that will instruct on an eventual fracture

which will result in early CO2 leaks to the surface, we propose here the development of a measurement method for continuous CO2 detection across the surface of the geological storage formation. The monitored surface of the storage reservoir can be 10's to 100's of km2 and the use of numerous fixed and/or mobile gas analysis detectors to continuously monitor the CO2 concentration across such surfaces is not conceivable. However laser beams that can travel several kilometers in practically no time without losing their coherence can scan large surface areas and detect the concentration and location of any chemical species provided the right laser wavelength, detection scheme, and inversion techniques are selected. Thus, the work proposed here aims at developing diode laser absorption techniques for continuous CO2 surface leak detection.

Laser based methods (such as laser-Raman scattering radar) for the remote detection of atmospheric pollutants have been studied and used since the early seventies (Hildal and Byer 1971, Inaba and Kobayasi 1972). Although these early techniques are still in use today for vertical distribution tropospheric and stratospheric gas detection they are not adopted for ground surface scanning and detection. In addition, these systems are bulky and very expensive. IR Diode laser based techniques, on the other hand, which were developed in the 80's and 90's of the last century found broad use in industrial and environmental detection applications, especially due to their reduced size and cost (see e.g. Mark Allen 1998, Webber et al 2000, and Philip Martin 2002). During the 80's and early 90's Infra Red (IR) laser absorption spectroscopy had been mainly restricted to laboratory experiments on chemical kinetics and especially as related to combustion and plasma processes (see Sassi 1999). But since the late nineties there has been a rapid expansion towards its use in more applied areas such as atmospheric and pollution monitoring as well as process monitoring and control. These advances have largely benefited from improvements in laser technology and associated electro-optics deriving from applications in the telecommunications and consumer electronics industries. In addition, there has been an increased interest in direct species and parameter measurements in the atmosphere and in the environment in general.

In laser absorption measurement the narrow band laser beam is wavelength tuned across a much broader molecular absorption line and the change in the detected-transmitted laser power is measured (see figure 1 below). At known temperature and pressure, among other experimental parameters, this power change is proportional to the absorbing species concentration along the path length of the laser beam. Spatially resolved absolute concentrations can be obtained using tomograpghical inversion methods. The technique can be used to monitor one or several species at the same time with quite high spatial and temporal resolutions. In addition to their wide spread use and low cost IR diode lasers can be used with fiber optic technology and inexpensive spectrometry components to build a large emitter/sensor network that can scan and monitor a specific chemical species over very large areas. Lately the technique has been used for in situ sensing of atmospheric CO2 with laser diodes emitting near 2.05 micrometers in laboratory experiments and a compact version of it has been adopted for European campaign of atmospheric measurements (see Zeninari et al 2004). The field has even seen the development of measuring field-scale isotopic CO2 with tunable diode laser absorption spectroscopy for stable isotope studies of ecosystem-atmosphere CO2 exchange (see Bowling et al 2003).
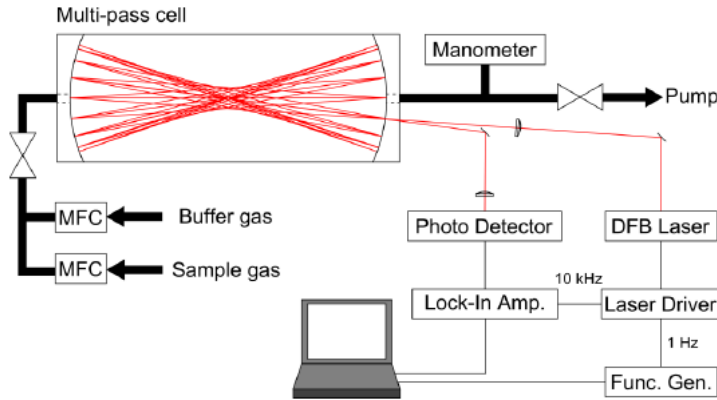
Figure 4.9.1: Conventional laboratory diode laser absorption apparatus for species detection (from Asakawa et al. 2010)

Our own work on laser diagnostics techniques (see Sassi 1999) and the commercial availability of IR diode lasers in addition to all the emission and detection optical components make us confident of developing an optimal network of diode laser absorption sensors for continuous CO_2 leak detection over sub-surface storage reservoirs. We will start by developing the technique in the laboratory and use multiple laser beam reflection schemes to simulate the covered large reservoir area (Figure 4.9.2).
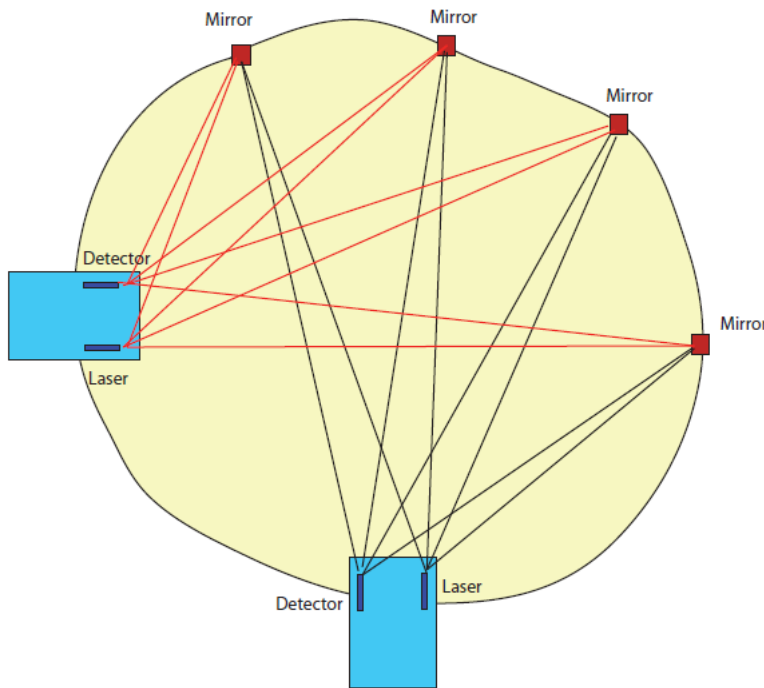
Figure 4.9.2. Schematic of the deployment of the technology in the field.

We will also develop software that includes tomographical inversion methods to recover the spatial location and the absolute concentration of a CO_2 point source. This will take us at least three years. Once the technique is harnessed we will collaborate with ADCO and Masdar Carbon to implement it on site for large-scale injection of CO_2.

5. Education and Knowledge Transfer (RJ, BH)

References

References for Section 2.1

Armero F. (1999). Formulation and finite element implementation of a multiplicative model of coupled poro-plasticity at finite strains under fully saturated conditions. Comput Methods Appl Mech Eng 171: 205–241.

Armero F. and Simo J.C. (1992). A new unconditionally stable fractional step method for non-linear coupled thermomechanical problems. Int J Numer Methods Eng 35: 737–766.

Barton, C. A., M. D. Zoback, and D. Moos (1995), Fluid flow along potentially active faults in crystalline rock, Geology, 23, 683-686.

Dean R.H., Gai S., Stone C.M., and Minkoff S.E. (2006). A comparison of techniques for coupling porous flow and geomechanics. SPE J 11(1): 132–140.

Ferronato M., Gambolati G., Teatini, C.J.P. (2008). Numerical modelling of regional faults in land subsidence prediction above gas/oil reservoirs. Int J Numer Anal Meth Geomech 32(6): 633–657.

Fredrich J.T., Arguello J.G., Deitrick G.L., and de Rouffignac E.P. (2000). Geomechanical modeling of reservoir compaction, surface subsidence, and casing damage at the Belridge diatomite field. SPE Res Eval Eng 3(4): 348–359.

Jean L., Mainguy M., Masson R., and Vidal-Gilbert S. (2007). Accelerating the convergence of coupled geomechanical-reservoir simulations. Int J Numer Anal Meth Geomech 31: 1163–1181.

Jha B. and Juanes R. (2007). A locally conservative finite element framework for the simulation of coupled flow and reservoir geomechanics. Acta Geotechnica 2: 139–153.

Kim J., Tchelepi H.A., and Juanes R. (2009). Stability, accuracy and efficiency of sequential methods for coupled flow and geomechanics. SPE Res Simul Sym (SPE 119084), The Woodlands, Texas, 2–4 February.

Lewis R.W. and Schrefler B.A. (1998). The finite element method in the static and dynamic deformation and consolidation of porous media. Chichester, England: Wiley, 2nd edition.

Lewis R.W. and Sukirman Y. (1993). Finite element modelling of three-phase flow in deforming saturated oil reservoirs. Int J Numer Anal Meth Geomech 17: 577–598.

Mainguy M. and Longuemare P. (2002). Coupling fluid flow and rock mechanics: formulations of the partial coupling between reservoir and geomechanics simulators. Oil Gas Sci Tech 57: 355–367.

Morris, J. P., Y. Hao, W. Foxall, and W. McNab (2010), A Study of Injection-Induced Mechanical Deformation at the In Salah CO2 Storage Project, 44th US Rock Mechanics Symposium, ARMA 10-307.

Rice, J., and M. P. Cleary (1976), Some basic stress diffusion solutions for fluid-saturated elastic porous media with compressible constituents, Rev. Geophys. Space Phys., 14, 227-214.

Settari A. and Mourits F. (1998). A coupled reservoir and geomechanical simulation system. SPE J 3: 219–226.

Settari A. and Walters D.A. (2001). Advances in coupled geomechanical and reservoir modeling with applications to reservoir compaction. SPE J 6(3): 334–342.
Thomas L.K., Chin L.Y., Pierson R.G., and Sylte J.E. (2003). Coupled geomechanics and reservoir simulation. SPE J 8(4): 350–358.

Tran D., Nghiem L., and Buchanan L. (2005). Improved iterative coupling of geomechanics with reservoir simulation. SPE Res Simul Sym (SPE 93244), Houston, 31 Jan.-2 Feb.

Tran D., Settari A., and Nghiem L. (2004). New iterative coupling between a reservoir simulator and a geomechanics module. SPE J 9(3): 362–369.

References for Section 2.2

Backers, T., et al. (2005), Tensile fracture propagation and acoustic emission activity in sandstone: The effect of loading rate, *International Journal of Rock Mechanics and Mining Sciences*, *42*(7-8), 1094-1101.

Baud, P., et al. (2000), Dilatancy, compaction, and failure mode in Solnhofen limestone, *Journal of Geophysical Research-Solid Earth*, *105*(B8), 19289-19303.

Baud, P., et al. (2006), Shear-enhanced compaction and strain localization: Inelastic deformation and constitutive modeling of four porous sandstones, *J. Geophys. Res.*, *111*, B12401, doi:12410.11029/12005JB004101.

Bernabe, Y., et al. (2006), A note on the oscillating flow method for measuring rock permeability, *International Journal of Rock Mechanics and Mining Sciences*, *43*(2), 311-316.

Bernabé, Y., et al. (2003), Permeability-porosity relationships in rocks subjected to various evolution processes, *Pure Appl. Geophysics*, *160*(5-6), 937-960.

Bernabé, Y., et al. (2006), A note on the oscillating flow method for measuring rock permeability, *Int. J. Rock Mech. Mining Sci.*, *43* 311-316.

Boitnott, G. N. (1997), Use of complex pore pressure transients to measure permeability of rocks, *SPE - Society of Petroleum Engineers of AIME*, *1997*, 37-45.

Cox, S. F. (2002), Fluid flow in mid- to deep crustal shear systems: Experimental constraints, observations on exhumed high fluid flux shear systems, and implications for seismogenic processes, *Earth Planets Space*, *54*(11), 1121-1125.

Druckenmiller, M. L., and M. M. Maroto-Valer (2005), Carbon sequestration using brine of adjusted pH to form mineral carbonates, *Fuel Processing Technology*, *86*(14-15), 1599-1614.

Egermann, P., et al. (2005), An experimental investigation of reaction-transport phenomena during CO2 injection, in *14th. SPE Middle East Oil & Gas Show and Conference*, edited, p. SPE paper 93674, Bahrain.

Elsworth, D., and H. Yasuhara (2006), Short-timescale chemo-mechanical effects and their influence on the transport properties of fractured rock, *Pure and Applied Geophysics*, *163*(10), 2051-2070.

Emberley, S., et al. (2004), Geochemical monitoring of fluid-rock interaction and CO2 storage at the Weyburn CO2-injection enhanced oil recovery site, Saskatchewan, Canada, *Energy*, *29*(9-10), 1393-1401.

Faulkner, D. R., and E. H. Rutter (1998), The gas permeability of clay-bearing fault gouge at 20 degrees C, *Geolog. Soc. Special Publications*, *147*, 147-156.

Faulkner, D. R., and E. H. Rutter (2000), Comparisons of water and argon permeability in natural clay- bearing fault gouge under high pressure at 20 degrees C, *J. Geophys. Res. - Sol. Earth*, *105*(B7), 16415-16426.

Faulkner, D. R., et al. (2002), The effect of temperature and the nature of the pore fluid on the permeability of phyllosilicate-rich fault gouge, *Eos, Transactions, Amer. Geophysical Union*, *83*(47, Suppl.), F1371.

Fischer, G. J., and M. S. Paterson (1989), Dilatancy During Rock Deformation at High-Temperatures and Pressures, *J. Geophys. Res. - Sol. Earth Planets*, *94*(B12), 17607-17617.

Fischer, G. J., and M. S. Paterson (1992), Measurement of permeability and storage capacity in rocks during deformation at high temperature and pressure, in *Fault Mech. transport properties rocks*, edited by B. Evans and T.-F. Wong, pp. 213-252, Academic Press, San Diego, CA.

Fortin, J., et al. (2009), Acoustic Emissions Monitoring during Inelastic Deformation of Porous Sandstone: Comparison of Three Modes of Deformation, *Pure and Applied Geophysics*, *166*(5-7), 823-841.

Hall, S. A. (2009), *When geophysics met geomechanics: Imaging of geomechanical properties and processes using elastic waves*, 147-175 pp.

Karner, S. L., et al. (2003), Subcritical compaction and yielding of granular quartz sand, *Tectonophysics*, *377*(3-4), 357-381.

Karner, S. L., et al. (2008), Hydrothermal deformation of granular quartz sand, *J. Geophys. Res.*, *113*, B05404, doi:05410.01029/02006JB004710.

Kranz, R. L., and J. D. Blacic (1984), Permeability changes during time-dependent deformationof silicate rock, *Geophys. Res. Lett.*, *9*, 1-4.

Kranz, R. L., et al. (1990), Hydraulic diffusivity measurements on laboratory rock samples using an oscillating pore pressure method, *Int. J. Rock Mech. Min. Sci.*, *27*, 517-526.

Lei, X. L., and Z. Q. Xue (2009), Ultrasonic velocity and attenuation during CO2 injection into water-saturated porous sandstone: Measurements using difference seismic tomography, *Physics of the Earth and Planetary Interiors*, *176*(3-4), 224-234.

Liteanu, E., and C. J. Spiers (2009), Influence of pore fluid salt content on compaction creep of calcite aggregates in the presence of supercritical CO2, *Chemical Geology*, *265*(1-2), 134-147.

Lockner, D. A., et al. (1991), Quasi-static fault growth and shear fracture energy in granite, *Nature*, *350*(6313), 39-42.

Milsch, H., et al. (2003), Reaction-induced fluid flow in synthetic quartz-bearing marbles, *Contributions to Mineralogy and Petrology*, *146*(3), 286-296.

Min, K.-B., et al. (2009), Chemically and mechanically mediated influences on the transport and mechanical characteristics of rock fractures, *International Journal of Rock Mechanics and Mining Sciences*, *46*(1), 80-89.

Mok, U., et al. (2002), Permeability, porosity and pore geometry of chemically altered porous silica glass, *Journal of Geophysical Research*, *107*(B1).

Ngwenya, B. T., et al. (2001), A constitutive law for low-temperature creep of water-saturated sandstones, *J. Geophys. Res. - Sol. Earth*, *106*(B10), 21811-21826.

Ngwenya, B. T., et al. (2003), Permeability evolution during progressive development of deformation bands in porous sandstones, *J. Geophys. Res. - Sol. Earth*, *108*(B7), 2485, doi:2410.1029/2001JB000463.

Ojala, I. O., et al. (2004), Loading rate dependence of permeability evolution in porous aeolian sandstones, *Journal of Geophysical Research*, *109*(B1).

Pokrovsky, O. S., et al. (2009), Effect of organic and inorganic ligands on calcite and magnesite dissolution rates at 60 degrees C and 30 atm pCO(2), *Chemical Geology*, *265*(1-2), 33-43.

Polak, A., et al. (2004), Spontaneous switching of permeability changes in a limestone fracture with net dissolution, *Water Resources Research*, *40*(3).

Schubnel, A., et al. (2005), Damage and recovery of calcite rocks deformed in the cataclastic regime, *Geological Society Special Publications*, *245*, 203-221.

Shukla, R., et al. (2010), A review of studies on CO2 sequestration and caprock integrity, *Fuel*, *In Press, Uncorrected Proof*.

Song, I., et al. (2004), One-dimensional fluid diffusion induced by constant-rate flow injection: Theoretical analysis and application to the determination of fluid permeability and specific storage of a cored rock sample, *Journal of Geophysical Research-Solid Earth*, *109*(B5).

Song, I., and J. Renner (2006a), Experimental investigation into the scale dependence of fluid transport in heterogeneous rocks, *Pure and Applied Geophysics*, *163*(10), 2103-2123.

Song, I., and J. Renner (2006b), Linear pressurization method for determining hydraulic permeability and specific storage of a rock sample, *Geophysical Journal International*, *164*(3), 685-696.

Song, I., and J. Renner (2007), Analysis of oscillatory fluid flow through rock samples, *Geophysical Journal International*, *170*(1), 195-204.

Song, I., and J. Renner (2008), Hydromechanical properties of Fontainebleau sandstone: Experimental determination and micromechanical modeling, *Journal of Geophysical Research-Solid Earth*, *113*(B9).

Stanchits, S., et al. (2009), Initiation and Propagation of Compaction Bands in Dry and Wet Bentheim Sandstone, *Pure and Applied Geophysics*, *166*(5-7), 843-868.

Stanchits, S. A., et al. (2003), Anisotropic changes in P-wave velocity and attenuation during deformation and fluid infiltration of granite, *Bulletin of the Seismological Society of America*, *93*(4), 1803-1822.

Streit, E. E., and R. R. Hillis (2004), Estimating fault stability and sustainable fluid pressures for underground storage of CO2 in porous rock, *Energy*, *29*(9-10), 1445-1456.

Wei, Z., et al. (2010), Micromechanics of cataclastic pore collapse in limestone, *Journal of Geophysical Research-Solid Earth*, *115*, -.

Wong, T. F., and P. Baud (2009), Grain Crushing, Pore Collapse and Strain Localization in Porous Sandstone, *Mechanics of Natural Solids*, 239-254
297.

Xiao, X., and B. Evans (2003), Shear enhanced compaction during nonlinear viscous creep of porous calcite-quartz aggregates, *Earth Planet. Sci. Lett.*, *216*(4), 725-740.

Xiao, X., et al. (2003), Deformation mechanisms and failure modes in Solnhofen limestone, paper presented at Soil Rock America, Proc. 39th U.S. Rock Mech. Symposium, Cambridge, Mass.

Xiao, X.-h., et al. (2006), Permeability evolution during non-linear viscous creep of calcite rocks, *Pure Appl. Geophys.*, *163*, 2071-2102, doi:2010.1007/s0024-2006-2115-2071.

Xu, L. L., et al. (2009), The effect of dissolved magnesium on creep of calcite II: transition from diffusion creep to dislocation creep, *Contributions to Mineralogy and Petrology*, *157*(3), 339-358.

Yasuhara, H., et al. (2006), Spontaneous switching between permeability enhancement and degradation in fractures in carbonate: Lumped parameter representation of mechanically- and chemically-mediated dissolution, *Transport in Porous Media*, *65*(3), 385-409.

Zevenhoven, R., et al. (2006), Chemical fixation of CO2 in carbonates: Routes to valuable products and long-term storage, *Catalysis Today*, *115*(1-4), 73-79.

Zhang, S., et al. (1994a), Porosity and permeability evolution during hot isostatic pressin of calcite aggregates, *J. Geophys. Res.*, *99*, 341-352.

Zhang, S., et al. (1994b), The influence of room temperature deformation on porosity and permeability in calcite aggregates, *J. Geophys. Res. - Sol. Earth*, *99*, 15761-15775.

Zhang, S., et al. (2000), Reaction-enhanced permeability during decarbonation of calcite + quartz -> wollastonite + carbon dioxide, *Geology*, *28*(10), 911-914.

Zhu, W., et al. (2009), Failure mechanisms and permeability evolution of solnhofen limestone at elevated temperature, *in preparation*.

References for Section 3 (capacity estimates and risk assessment at the basin scale)

S. Bachu, D. Bonijoly, J. Bradshaw, R. Burruss, S. Holloway, N. P. Christensen, and O. M. Mathiassen (2007). CO2 storage capacity estimation: methodology and gaps. *Int. J. Greenhouse Gas Control*, 1:430-443.

S. Bachu, W. D. Gunther, and E. H. Perkins (1994). Aquifer disposal of CO2: Hydrodynamic and mineral trapping. *Energy Conv. Manag.*, 35(4):269-279.

G. I. Barenblatt (1996). *Scaling, Self-Similarity, and Intermediate Asymptotics.* Cambridge Texts in Applied Mathematics. Cambridge University Press.

DOE-NETL (2007). National Energy Technology Laboratory Department of Energy. Carbon Sequestration Atlas of the United States and Canada. http://www.netl.doe.gov/technologies/carbon seq/refshelf/atlas/.

J. Ennis-King and L. Paterson (2005). Role of convective mixing in the long-term storage of carbon dioxide in deep saline formations. *Soc. Pet. Eng. J.*, 10(3):349-356.

M. Flett, R. Gurton, and I. Taggart (2004). The function of gas-water relative permeability hysteresis in the sequestration of carbon dioxide in saline formations. In *SPE Asia Pacific Oil and Gas Conference and Exhibition*, Perth, Australia, October 18-20, 2004 (SPE 88485).

G. Garven (1995). Continental scale groundwater flow and geologic processes. *Annu. Rev. Earth Planet. Sci.*, 89:89-117.

G. Garven and R. A. Freeze (1984a). Theoretical analysis of the role of groundwater flow in the genesis of stratabound ore deposits. 1. Mathematical and numerical model. *Am. J. Sci.*, 284(10):1085-1124.

G. Garven and R. A. Freeze (1984b). Theoretical analysis of the role of groundwater flow in the genesis of stratabound ore deposits. 2. Quantitative results. *Am. J. Sci.*, 284(10):1125-1174.

W. D. Gunter, B. Wiwchar, and E. H. Perkins (1997). Aquifer disposal of CO_2-rich greenhouse gases: Extension of the time scale of experiment for CO_2-sequestering reactions by geochemical modeling. *Miner. Pet.*, 59(1-2):121-140.

M. A. Hesse, F. M. Orr, Jr., and H. A. Tchelepi (2008). Gravity currents with residual trapping. *J. Fluid Mech.*, 611:35-60.

M. A. Hesse, H. A. Tchelepi, B. J. Cantwel, and F. M. Orr, Jr. (2007). Gravity currents in horizontal porous layers: transition from early to late self-similarity. *J. Fluid Mech.*, 577:363-383.

H. E. Huppert and A. W. Woods. Gravity-driven flows in porous media. *J. Fluid Mech.*, 292:55-69.

IPCC (2005). *Special Report on Carbon Dioxide Capture and Storage,* B. Metz, O. Davidson, H. de Coninck, M. Loos and L. Meyer (eds.). Cambridge University Press.

IPCC (2007). *Climate Change 2007: Synthesis Report*. IPCC, Geneva, Switzerland, 2007.

R. Juanes and C. W. MacMinn (2008). Upscaling of capillary trapping under gravity override: Application to CO_2 sequestration in aquifers. In *SPE/DOE Symposium on Improved Oil Recovery*, Tulsa, OK, April 19-23, 2008 (SPE 113496).

R. Juanes, C. W. MacMinn, and M. L. Szulczewski (2010). The footprint of the CO_2 plume during carbon dioxide storage in saline aquifers: storage efficiency for capillary trapping at the basin scale. *Transp. Porous Media*, 82(1):19-30.

R. Juanes, E. J. Spiteri, F. M. Orr, Jr., and M. J. Blunt (2006). Impact of relative permeability hysteresis on geological CO_2 storage. *Water Resour. Res.*, 42:W12418.

I. N. Kochina, N. N. Mikhailov, and M. V. Filinov. Groundwater mound damping. *Int. J. Eng. Sci.*, 21:413-421.

A. Kumar, R. Ozah, M. Noh, G. A. Pope, S. Bryant, K. Sepehrnoori, and L. W. Lake (2005). Reservoir simulation of CO_2 storage in deep saline aquifers. *Soc. Pet. Eng. J.*, 10(3):336-348.

S. Lyle, H. E. Huppert, M. Hallworth, M. Bickle, and A. Chadwick (2005). Axisymmetric gravity currents in a porous medium. *J. Fluid Mech.*, 543:293-302.

MIT (2007). *The Future of Coal – An Interdisciplinary MIT Study*. MIT Press.

S. Mo, P. Zweigel, E. Lindeberg, and I. Akervoll (2005). Effect of geologic parameters on CO_2 storage in deep saline aquifers. In *14th Europec Biennial Conference*, Madrid, Spain, June 13-16, 2005 (SPE 93952).

J. M. Nordbotten, M. A. Celia, and S. Bachu (2005). Analytical solution for CO_2 plume evolution during injection. *Transp. Porous Media*, 58(3):339-360.

J. M. Nordbotten, D. Kavetski, M. A. Celia, and S. Bachu (2009). Model for CO_2 leakage including multiple geological layers and multiple leaky wells. *Environ. Sci. Technol.*, 43(3):743-749.

A. Riaz, M. Hesse, H. A. Tchelepi, and F. M. Orr, Jr (2006). Onset of convection in a gravitationally unstable, diffusive boundary layer in porous media. *J. Fluid Mech.*, 548:87-111.

M. L. Szulczewski and R. Juanes (2009). A simple but rigorous model for calculating CO_2 storage capacity in deep saline aquifers at the basin scale. *Energy Procedia* (Proc. GHGT-9), 1(1):3307-3314, doi:10.1016/j.egyproc.2009.02.117.

D. Vella and H. E. Huppert (2006). Gravity currents in a porous medium at an inclined plane. *J. Fluid Mech.*, 555:353-362.

References for Section 4.1 (data assimilation)

Moore, S. and D. McLaughlin, Design of field experiments to determine the ecological effects of petroleum in intertidal ecosystems", *Water Research*, 12(12), 1091-1099, 1978.

Graham, W. and D. McLaughlin, stochastic analysis of nonstationary subsurface solute transport, 2. Conditional moments, *Water Resources Research*, 25(11), 2331-2355, 1989.

McLaughlin, D., L.B. Reid, S.G. Li, J. Hyman, A stochastic method for characterizing groundwater contamination, *Ground Water*, 31(2), 237-249, 1993.

McLaughlin, D., An integrated approach to hydrologic data assimilation: interpolation, smoothing, and forecasting, *Advances in Water Resources*, 25(8-12), 1275-1286, 2002.

McLaughlin, D., A probabilistic perspective on nonlinear model inversion and data assimilation, Subsurface Hydrology: Data Integration for Properties and Processes Geophysical Monograph Series 171, American Geophysical Union, 10.1029/171GM17, 2007.

Jafarpour B., D. McLaughlin, History matching with an ensemble Kalman filter and discrete cosine parameterization, *Computational Geosciences*, 12(2), 227-244, 2008.

Jafarpour, B. and D. McLaughlin, Estimating reservoir permeabilities with the ensemble Kalman filter: importance of ensemble design, *Jour. Soc. Petr. Engr.*, 14 (2), 374-388, SPE-108941-PA, 2009.

Jafarpour, B. and D. McLaughlin, Reservoir characterization with the discrete cosine transform, *Jour. Soc. Petr. Engr.*, 14(1), 182-201, SPE-106453-PA, 2009

Arulampalam, M. S., A tutorial on particle filters for online non-linear/nongaussian Bayesian tracking, *IEEE Trans. Signal Proc.*,50(2), 174–188, 2002.

Evensen, G., The Ensemble Kalman Filter: theoretical formulation and practical implementation, *Ocean Dynamics*, 53(4), 343–367, 2003.

Evensen, G., Sampling strategies and square root analysis schemes for the ensemble Kalman filter, *Ocean Dynamics*, 54(6), 539–560, 2004.

Jazwinski, A. H., *Stochastic Processes and Filtering Theory*, Academic, San Diego, CA, 376 pp., 1970.

Box, G.E.P. and Tiao, G.C. (1973) *Bayesian Inference in Statistical Analysis*, Wiley, ISBN 0-471-57428-7.

Steuer, R.E. (1986). *Multiple Criteria Optimization: Theory, Computations, and Application*. New York: John Wiley & Sons, Inc.

Zhou, Y., D. McLaughlin, and D. Entekhabi, Assessing the performance of the ensemble Kalman filter for land surface data assimilation, *Mon. Weather Rev.*, 134 (8), 2128–2142, 2006.

References for Section 4.2 (pressure monitoring)

Ringrose,P., M. Atbi, D. Mason, M. Espinassous, Ø. Myhrer, M. Iding, A. Mathieson, and I. Wright (2009), Plume development around well KB-502 at the In Salah CO2 storage site, *first break, 27*, 85-89.

References for Sections 4.3 and 4.4 (active and passive seismic)

R. Arts, O. Eiken, A. Chadwick, P. Zweigel, L. van der Meer, B. Zinszner (2004), Monitoring of CO2 injected at Sleipner using time-lapse seismic data, *Energy*, 29, 1383-1392.

Brenguier, F. et al. (2008), Postseismic relaxation along the San Andreas fault in the Parkfield area investigated with continuous seismological observations. *Science, 321, 1478*.

Brenguier, F. et al. (2008b) Towards forecasting volcanic eruptions using seismic noise. *Nature Geoscience, 1, 126*.

Byerley, G. et al. (2009), 4D Seismic Monitoring Applied to SAGD Operations at Surmont, Alberta, Canada, *SEG Expanded Abstracts 28*, 3959.

Cheng, A., (2008). Measurements of the earth at the scale of logs, crosswells and VSPs, in *Earth Heterogeneity and scattering effects of seismic waves, H. Sato and M. Fehler ed., Advances in Geophysics Volume 50, Elsevier, 2008*.

Concha, D., M. Fehler, and H. Zhang (2010). Imaging the Soultz enhanced geothermal reservoir using double-difference tomography and microseismic data from the 1993 hydraulic stimulationexperiment, in preparation.

Denli, H. and Huang, L., (2009), Double-difference elastic wavefrom tomography in the time domain, *SEG Expanded Abstracts 28,* 2302.

Denli, H. and Huang, L., (2010), Elastic-wave Sensitivty Propagation, *Geophysics, 75, T83.*

Fink, M., (1992), Time Reversal of Ultrasonic Fields -Part I: Basic Principles, *IEEE Transactions on Ultrasonics, Ferroelectrics, and frequency control,39, 555.*

Fehler, M. L. Huang, R. Wu, and X. Xie, Seismic image resolution: numerical investigation of role of migration imaging operator, expanded abstract for presentation at the 2005 annual meeting of the Soc. Expl. Geophysicists, Houston, 2005.

Fouque, J.-P., and Poliannikov O.V., (2006), Time-reversal detection in one-dimensional random media. *Inverse Problems.*

Gassmann, F. (1951) Über die Elastizität poroser Medien, Vierteljahrsschrift der Naturforschenden Gesellschaft in Zürich, **96**, 1-23.

Gouedard et al., (2008), Cross-correlation of random fields: mathematical approach and applications, *Geophysical Prospecting*, *56*, *375*.

Larose, E. et al., (2006), Correlation of random wavefields: An interdisciplinary review, *Geophysics 71 (4), SI11*.

Li, J., H. Zhang, S. Kuleli, and M. Toksoz (2009). Focal mechanism determination using high-frequency, full waveform inversion, SEG, Expanded Abstracts, 28 , no. 1, 2312-2316

Lumley, D. et al. (2003), 4D Seismic Data Processing Issues and Examples, *SEG Expanded Abstracts, 22*, 1394.

Lumley, D. (2010), 4D Seismic Monitoring of CO2 Sequestration, *The Leading Edge 29 (150)*.

Poupinet, G., Ellsworth, W.L., Frechet, J., (1984), Monitoring velocity variations in the crust using earthquake doublets: an application to the Calaveras Fault, California. *J. Geophy. Res. 89*, 5719–5731.

Prange, M. W. Bailey, B.Couet, H. Djikpesse, M. Armstrong, A. Galli, D Wilkinson (2008). Valuing future information under uncertainty using polynomial chaos, *Decision Analysis* **5**, 140-156.

Roberts, P.M., Phillips, W.S., Fehler, M.C., (1992) Development of the active doublet method for measuring small velocity and attenuation changes in solids. *J. Acoust. Soc. Am. 91*, 3291–3302.

Snieder, R., et al., (2002). Coda wave interferometry for estimating nonlinear behavior in seismic velocity. *Science 295*, 2253–2255.

Wu, R., X. Xie, M. Fehler, and L. Huang (2005) Spatial resolution of seismic imaging, expanded abstract for presentation at the 2005 annual meeting of the Soc. Expl. Geophysicists, Houston.

Zhang, H., and Thurber, C. H., (2003), Double-Difference Tomography: The Method and Its Application to the Hayward Fault, California, *Bull. Seism. Soc. Am,* 93, 1875-1889.

Zhou, R., L. Huang, J. Rutledge, M. Fehler, T. Daley, and E. Majer (2010). Coda-wave interferometry of time-lapse VSP data for monitoring geological carbon sequestration, *International Journal of Greenhouse Gas Control*, **4**, 679-686.

References for Section 4.5 (induced seismicity)

Block, L., C. Cheng, M. Fehler, and W.S. Phillips, Seismic imaging of the velocity structure in the vicinity of a hydrofrac in a geothermal reservoir, *Geophysics* **59**, 102- 112, 1994.

Dost, B., and H. W. Haak (2007). Natural and induced seismicity, in Th.E. Wong, D.A.J. Batjes, and J. de Jager, eds., *Geology of the Netherlands*, Royal Netherlands Academy of Arts and Sciences, 223-229.

Fehler, M. A. Jupe, and H. Asanuma, More than Cloud: new techniques for characterizing reservoir structure using induced seismicity, The Leading Edge, **20**, 324-328, 2001.

Li, J., H. Zhang, S. Kuleli, and N. Toksoz, Focal mechanism determination using high frequency waveform matching and its application to small magnitude induced earthquakes, *Geophys. J. Int.*, in press.

Julian, B. and G. Foulger, Time-dependent seismic tomography of geothermal systems (expanded abstract), Stanford Geothermal Workshop, paper #36, available at http://pangea.stanford.edu/ERE/pdf/IGAstandard/SGW/2009/2009program.htm, 2009.

Maxwell, S., J. Rutledge, R. Jones, and M. Fehler (2010). Petroleum reservoir characterization using Downhole microseismic monitoring, *Geophysics*, in press.

Zhang, H., S. Sarkar, M. Toksoz, S. Kuleli, and F. Al-Kindy (2009). Passive seismic tomography using induced seismicity at a petroleum field in Oman, *Geophysics* **74**, WCB57-WCB69, 2009.

Zhou, R., L. Huang, and J. Rutledge, Microseismic event location for monitoring CO2 injection using double-difference tomograpgy, *The Leading Edge*, 208 – 214, Feb. 2010.

References for Section 4.6 (geodesy)

Domenico, P.A. and F.W. Schwartz (1997), *Physical & Chemical Hydrology*. New York: John Wiley & Sons.

Rutqvist, J., D. Vasco, and L. Myer (2009), *Coupled reservoir-geomechanical analysis of CO2 injection at In Salah, Algeria.* Energy Procedia, **1**(1), 1847-1854.

Onuma, T. and S. Ohkawa, Detection of surface deformation related with CO2 injection by DInSAR at In Salah (2009), Algeria, *Energy Procedia*, **1**, 2177–2184.

Vasco, D., A. Ferretti, and F. Novali (2008a), Estimating permeability from quasi-static deformation: Temporal variations and arrival-time inversion. *Geophysics*, **73**: p. O37-O52.

Vasco, D., A. Ferretti, and F. Novali (2008b), Reservoir monitoring and characterization using satellite geodetic data: Interferometric Synthetic Aperture Radar observations from the Krechba field, Algeria*. Geophysics*, **73**: p. P.WA113–WA122.

Vasco, D. W., A. Rucci, A. Ferretti, F. Novali, R. C. Bissell, P. S. Ringrose, A. S. Mathieson, and I. W. Wright (2010), Satellite-based measurements of surface deformation reveal fluid flow associated with the geological storage of carbon dioxide, *Geophys. Res. Lett., 37*, L03303, doi:10.1029/2009GL041544.

References for Section 4.7 (gravity)

Alnes, H., O. Eiken, and T. Stenvold (2008), Monitoring gas production and CO_2 injection at the Sleipner field using time-lapse gravimetry, *Geophysics*, *73*, WA155-WA161.

http://www.bellgeo.com/tech/technology_system.html

Biegert, E., J. Ferguson, and X. Li (2008), Special Section: 4D gravity monitoring — Introduction, *Geophysics*, *73*, WA1-WA2.

Casten, U, and U. Haussmann (1990), Improvement of observation accuracy of the LaCoste-Romberg (Model D) gravity meter by supplementary installation of electronic feedback, Geophysical Prospecting, **38**, 5, 489-498.

Chadwick, A., Arts, R., Bernstone, C., May, F., Thibeau, S., Zweigel, P. (Eds.) (2007), Best Practice for the Storage of CO2 in Saline Aquifers—Observations and Guidelines from the SACS and CO2STORE Projects. British Geological Survey, Nottingham, 267 pp.

Ferguson, J. F., F. J. Klopping, T. Chen, J. E. Seibert, J. L. Hare, and J. L. Brady (2008), The 4D microgravity method for waterflood surveillance: Part 3 — 4D absolute microgravity surveys at Prudhoe Bay, Alaska, *Geophysics*, *73*, WA163-WA171.

Gasperikova, E., and G. M. Hoversten (2008), Gravity monitoring of CO_2 movement during sequestration: Model studies, *Geophysics*, *73*, WA105-WA112.

Gettings, P., D. S. Chapman1, and R. Allis (2008), Techniques, analysis, and noise in a Salt Lake Valley 4D gravity experiment, *Geophysics*, *73*, WA71-WA82.

Hare, J. L., J. F. Ferguson, and J. L. Brady (2008), The 4D microgravity method for waterflood surveillance: Part IV — Modeling and interpretation of early epoch 4D gravity surveys at Prudhoe Bay, Alaska, *Geophysics*, *73*, WA173-WA180.

Jekeli, C. (2006), Airborne gradiometry error analysis, *Surv. Geophys., 27*, 257-275.

Meyer, T. (2008), Monitoring water front advances with down-hole gravity sensors, abstract, SEG Annual Meeting.

Michael, K., A. Golab, V. Shulakova, J. Ennis-King, G. Allinson, S. Sharma, T. Aiken (2010), Geological storage of CO2 in saline aquifers—A review of the experience from existing storage operations, *Int. J. Greenhouse Gas Control, 4*, 659-667.

Vasco, D.W. (1989), Resolution and variance operators of gravity and gravity gradiometry, *Geophysics*, *54*, 889-899.

References for Section 4.8 (Electrical Resistance Tomography)

Binley, A., S. Henry-Poulter, and B. Shaw (1996), Examination Of Solute Transport In An Undisturbed Soil Column Using Electrical Resistance Tomography, *Water Resources Res.*, 32(4), 763-69.

Carrigan, C.R., A. L. Ramirez, R. L. Newmark, R. Aines, S. J. Friedmann (2009), Application Of ERT For Tracking CO2 Plume Growth And Movement At The SECARB Cranfield Site, 8th Annual Conference on Carbon Capture & Sequestration Pittsburgh, PA, United States.

Daily, W., A. Ramirez, D. LaBrecque, and J. Nitao (1992), Electrical Resistivity Tomography Of Vadose Water Movement, *Water Resources Research*, 28(5), 1429-1442.

Daily, W.D., A. Ramirez, and R. Johnson (1998), Electrical Impedance Tomography Of A Perchloroethelyne Release, *J. Envir. and Eng. Geophysics*, 2(3), 189-201.

Daily, W. D., A. Ramirez, A. Binley and D. LaBrecque (2003), Electrical resistance tomography – Theory and practice, Lawrence Livermore National Laboratory UCRL-JC-144936, *SEG Special Publication- Near-Surface Geophysics*.

NETL (National Energy Technology Laboratory) (2009), *Best Practices for Monitoring, Verification, and Accounting of CO2 Stored in Deep Geologic Formations,* DOE/NETL-311/081508.

Ramirez, A. L., R. L. Newmark, and W. D. Daily (2003), Monitoring Carbon Dioxide Floods Using Electrical Resistance Tomography (ERT): Sensitivity Studies, *Journal Envir. Eng. Geophys.*, 8(3), 187-208.

III. MILESTONES AND PROJECT TIMELINE

Suggested dates for this Phase of the project: Jan 1, 2011 – Dec 31, 2014

	Year 1	Year 2	Year 3	Year 4
Task 1 - Site characterization				
1. Compile data	■			
2. Discuss merits of each site	■			
3. Delineate reservoir arquitecture	■			
4. Make recommendations for additional data	■	■	■	
5. Rank potential target formations	■	■	■	
Task 2 - Geomechanical processes and caprock integrity				
Subtask 2.1 - Development of coupled computational models of flow and geomechanics				
1. Initial assessment of caprock integrity	■	■		
2. Theoretical and computational developments				
a. Extend fixed stress-split to multiphase	■			
b. Develop framework for flow along faults		■	■	
c. Develop framework for fault poromech.		■	■	
3. Computer code implementation				
a. Implement single-phase flow in Pylith	■			
b. Incorporate realistic material behavior				
c. Investigate scenarios of fault slip				
d. Implement coupled multiphase poromech.			■	
e. Enhance GPRS with flow through faults			■	■
f. Implement coupled GPRS-Pylith code			■	■
4. Application to Abu Dhabi reservoirs				
a. Gather data	■			
b. Integrate different sources of data				
c. Evaluate scenarios of fault slip				
d. Simulate test cases of fault slip	■	■	■	
e. Apply GPRS-Pylith code to selected aquifers				■
Subtask 2.2 - Laboratory studies of geomechanics and mineral trapping				
1. Design, acquire and install equipment	■			
2. Collect samples, prepare initial specimens	■			
3. Chemical and structural analysis of initial specimens	■			
4. Design and test protocols for fluid preparation	■			
5. Calibrate equipment	■			
6. Triaxial tests on 1 cm samples	■	■		
7. Triaxial perm. and resistivity tests 5 cm samples		■		
8. Triaxial testing, with CO2+brine		■	■	
9. Measure kinetics of fluid/rock reactions		■	■	
10. Triaxial, perm. and resis. tests with multiphase fluids		■	■	
11. Acoustic tomography and resistivity imaging		■	■	
12. Analyze acoustic data; tomography		■	■	
13. Analyze mechanical and chemical data	■	■	■	■
14. Chemical and microstructural analysis of specimens	■	■	■	
Task 3 - Capacity estimates and risk assessment of basin-scale CO2 injection				
1. Develop mathematical models of CO2 migration				
a. Pressure evolution	■			
b. Capillary trapping	■			
c. Dissolution trapping	■	■	■	
d. Caprock failure and leakage	■	■	■	
2. Apply mathematical models to selected reservoirs in UAE				
a. Flow models		■	■	

   b. Mechanical models
3. Estimate CO2 storage capacity and injectivity
  a. First estimate from flow models
  b. Revised estimate from leakage models
4. Develop risk assessment methodologies
  a. Sensitivity analysis to model parameters
  b. Probability distributions for selected parameters
  c. Uncertainty analysis
  d. Estimates of risk of CO2 leakage
5. Comparison of analytical models with reservoir simulation models
  a. Flow models
  b. Mechanical models

Task 4 - Comprehensive monitoring program
Subtask 4.1 - Data assimilation and monitoring design
1. Assess monitoring needs
2. Develop and test data assimilation procedures
3. Develop monitoring design procedures
4. Evaluate and screen proposed sensing technologies
5. Technology transfer

Subtask 4.2 - Pressure variations in wells
1. Extend literature search
2. Collect information about existing wells
3. Include well information in data assimilation
4. Address resolution of well data
5. Provide cost-benefit analysis of these measurements

Subtask 4.3 - Active seismic
1. Develop the double-difference elastic tomography
2. Initial tests on synthetic data
3. Minimize influence of acquisition at different times
4. Adapt method to data available
5. Apply method to synthetic models of CO2 migration
6. Develop method to interpret CO2 saturation changes
7. Apply the method to field data from CO2 pilots

Subtask 4.4 - Passive seismic
1. Evaluate origin of seismic noise from existing stations
2. Evaluate applicability of existing methods for detecting change
3. Analysis of seismic data from monitoring network
4. Determine Green functions between stations
5. Apply Green functions to determine changes

Subtask 4.5 - Induced seismicity
1. Study induced seismicity from EOR world-wide
2. Evaluate local seismicity in UAE
3. Plan the details of seismic network installation
4. Collect and analyze data from seismic network
5. Determine velocity model to later locate events

Subtask 4.6 - Geodetic monitoring with InSAR and GPS
1. Investigation of InSAR capability for measuring deformation in candidate fields
  a. Investigate coverage and acquire images
  b. Determine whether coherent is sufficient
  c. Investigate spatial resolution of PSInSAR
  d. Compare InSAR analyses from MIT and Masdar
  e. Schedule acquisition of new scenes

f. Compare InSAR analyses by MIT and Masdar
g. Determine atmospheric contribution to the noise
h. Characterize sources of noise
2. Install GPS network at candidate field
  a. Purchase, test and ship receivers
  b. Design network
  c. Install network and train observers in Abu Dhabi
  d. Collect and analyze GPS data
  e. Compare deformation from GPS and InSAR
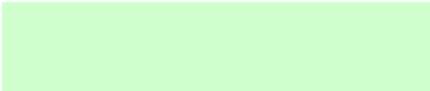
Subtask 4.7 - Microgravity and gravity gradiometry
1. Compute forward models of gravity variations
2. Develop inverse models; investigate cost vs. resolution
3. Investigate available instrumentation for improved quality
4. Make and document recommendation
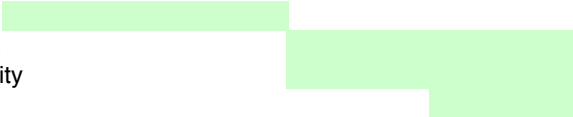
Subtask 4.8 - Electrical resistance tomography
1. Literature search on field results
2. Incorporate ERT measurements on data assimilation
3. Investigate resolving power of ERT
4. Provide a cost-benefit analysis

Subtask 4.9 - Geochemical and surface monitoring
1. Isotopic characterization of CO2
  a. Review geochemical tracers and clumped isotopes
  b. Determine background level of clumped isotopes
  c. Determine isotopic signatures of anthropogenic CO2
  d. Develop protocol for sampling and monitoring
2. Diode laser absorption sensors for continuous CO2 surface monitoring
  a.

Task 5 - Education and knowledge transfer
1. Reporting (quarterly progress reports, annual reports)
2. Annual two-day conference and business meeting
3. CCS short course at MIT
4. Visits from PI and Masdar researchers to MIT
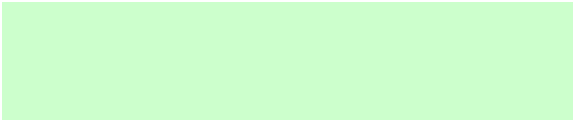
APPENDIX. BRIEF BIOSKETCH OF KEY PERSONNEL

Bradford H. Hager
Bradford H. Hager is Cecil and Ida Green Professor of Earth Sciences at MIT. He earned his Ph.D. from Harvard University in 1978 and was a professor at Caltech's Seismological Laboratory before joining MIT in 1989. His research interests include the relationship between space-geodetic observations of surface deformation, earthquakes, and dynamical processes in Earth's interior. He has expertise on tectonic earthquakes in regional fault systems, as well as deformation and earthquakes induced by reservoir production. Hager was the Chair of the Southern California Earthquake Center Fault Systems Working Group, 2001 – 2006, then member of the Executive Committee, Computational Infrastructure for Geodynamics, 2006 – 2008, instrumental in the development of the PyLith finite element code. He was also a member of the Executive Committee of the National Research Council's Decadal Survey by the Committee on Earth Science and Applications from Space, recommending that NASA fly the DESDynI InSAR/LIDAR mission. Hager is currently co-chair of NASA's DESDynI Science Study Group, responsible for earthquake, hydrocarbon, and carbon sequestration applications.

Ruben Juanes
Ruben Juanes is the ARCO Associate Professor in Energy Studies, in the Department of Civil and Environmental Engineering at MIT. Prior to joining the MIT faculty in 2006, he was Acting Assistant Professor at Stanford University (2003-2005), and Assistant Professor at UT Austin (2006). He leads a research group in the area of multiphase flow in porous media, with application to energy-driven problems: oil and gas recovery, methane hydrates, and geological carbon sequestration. He is the author of over 40 peer-reviewed journal publications and over 50 conference papers. In addition to his graduate and undergraduate teaching at MIT, he is the director of the MIT short course "Carbon Capture and Storage: Science, Technology and Policy." He has been a plenary speaker at several conferences, including the 2006 Gordon Research Conference (GRC) on Flow and Transport in Permeable Media, and the 2010 GRC on Natural Gas Hydrates. He was the recipient of the inaugural US Department of Energy Early Career Award. He holds MS and PhD Degrees from the University of California at Berkeley.

Alison Malcolm
Alison Malcolm is an Assistant Professor of Geophysics at MIT. She earned her Ph.D. from The Colorado School of Mines in 2005 and joined the MIT faculty in 2008. Her research interests include seismic reflection imaging and inversion with a particular emphasis on mathematical aspects of different techniques. She is also involved in projects dealing with several aspects of nonlinearity in imaging. Her work finds application in locating and characterizing oil reservoirs, imaging of geothermal reservoirs, as well as CO2 sequestration. She is currently the secretary of the Society for Industrial and Applied Mathematics Activity Group on Imaging Science.

<u>Dennis B. McLaughlin</u>
Dennis B. McLaughlin is H.M. King Bhumibol Professor of Water Resource Systems at MIT. He served as a consultant working on estimation, control, and water resource topics for 15

years before returning to academia to earn his Ph.D in Civil Engineering from Princeton University in 1983. His research interests include environmental data assimilation and monitoring, remote sensing for environmental applications, and water resource systems. He teaches classes in environmental modeling and optimization and has lectured extensively on applications of data assimilation concepts in hydrology, meteorology, and petroleum engineering. McLaughlin is a Fellow of the American Geophysical Union and a member of the American Meteorological Society. He has served as deputy editor of Water Resources Research and on a number of professional journal editorial boards. He has also been a member of national committees concerned with performance assessments of high level nuclear waste disposal at the WIPP site near Carlsbad, New Mexico and with site characterization and remedial design for the Hanford radioactive waste disposal site near Richland, Washington. He has served as a visiting scientist at TNO in the Netherlands, ETH in Zurich, Switzerland, CSIRO in Perth, Australia, and at Balliol College, Oxford University.